

Determination of the strong coupling constant α_s from transverse energy–energy correlations in multijet events at $\sqrt{s}=8$ TeV using the ATLAS detector

Aaboud, M.; Newman, Paul; ATLAS Collaboration

DOI:

[10.1140/epjc/s10052-017-5442-0](https://doi.org/10.1140/epjc/s10052-017-5442-0)

License:

Creative Commons: Attribution (CC BY)

Document Version

Publisher's PDF, also known as Version of record

Citation for published version (Harvard):

Aaboud, M, Newman, P & ATLAS Collaboration 2017, 'Determination of the strong coupling constant α_s from transverse energy–energy correlations in multijet events at $\sqrt{s}=8$ TeV using the ATLAS detector', *European Physical Journal C*, vol. 77, 872. <https://doi.org/10.1140/epjc/s10052-017-5442-0>

[Link to publication on Research at Birmingham portal](#)

General rights

Unless a licence is specified above, all rights (including copyright and moral rights) in this document are retained by the authors and/or the copyright holders. The express permission of the copyright holder must be obtained for any use of this material other than for purposes permitted by law.

- Users may freely distribute the URL that is used to identify this publication.
- Users may download and/or print one copy of the publication from the University of Birmingham research portal for the purpose of private study or non-commercial research.
- User may use extracts from the document in line with the concept of 'fair dealing' under the Copyright, Designs and Patents Act 1988 (?)
- Users may not further distribute the material nor use it for the purposes of commercial gain.

Where a licence is displayed above, please note the terms and conditions of the licence govern your use of this document.

When citing, please reference the published version.

Take down policy

While the University of Birmingham exercises care and attention in making items available there are rare occasions when an item has been uploaded in error or has been deemed to be commercially or otherwise sensitive.

If you believe that this is the case for this document, please contact UBIRA@lists.bham.ac.uk providing details and we will remove access to the work immediately and investigate.

Determination of the strong coupling constant α_s from transverse energy–energy correlations in multijet events at $\sqrt{s} = 8$ TeV using the ATLAS detector

ATLAS Collaboration^{*}

CERN, 1211 Geneva 23, Switzerland

Received: 11 July 2017 / Accepted: 4 December 2017 / Published online: 15 December 2017
 © CERN for the benefit of the ATLAS collaboration 2017. This article is an open access publication

Abstract Measurements of transverse energy–energy correlations and their associated asymmetries in multi-jet events using the ATLAS detector at the LHC are presented. The data used correspond to $\sqrt{s} = 8$ TeV proton–proton collisions with an integrated luminosity of 20.2 fb^{-1} . The results are presented in bins of the scalar sum of the transverse momenta of the two leading jets, unfolded to the particle level and compared to the predictions from Monte Carlo simulations. A comparison with next-to-leading-order perturbative QCD is also performed, showing excellent agreement within the uncertainties. From this comparison, the value of the strong coupling constant is extracted for different energy regimes, thus testing the running of $\alpha_s(\mu)$ predicted in QCD up to scales over 1 TeV. A global fit to the transverse energy–energy correlation distributions yields $\alpha_s(m_Z) = 0.1162 \pm 0.0011$ (exp.) $^{+0.0084}_{-0.0070}$ (theo.), while a global fit to the asymmetry distributions yields a value of $\alpha_s(m_Z) = 0.1196 \pm 0.0013$ (exp.) $^{+0.0075}_{-0.0045}$ (theo.).

Contents

1	Introduction	1
2	ATLAS detector	2
3	Monte Carlo simulation	2
4	Data sample and jet calibration	3
5	Results at the detector level	4
6	Correction to particle level	5
7	Systematic uncertainties	5
8	Experimental results	6
9	Theoretical predictions	6
9.1	Non-perturbative corrections	9
9.2	Theoretical uncertainties	9
10	Comparison of theoretical predictions and experimental results	10

11	Determination of α_s and test of asymptotic freedom	10
11.1	Fits to individual TEEC functions	13
11.2	Global TEEC fit	14
11.3	Fits to individual ATEEC functions	16
11.4	Global ATEEC fit	16
12	Conclusion	16
	Appendix	17
	References	19

1 Introduction

Experimental studies of the energy dependence of event shape variables have proved very useful in precision tests of quantum chromodynamics (QCD). Event shape variables have been measured in e^+e^- experiments from PETRA–PEP [1–3] to LEP–SLC [4–7] energies, at the ep collider HERA [8–12] as well as in hadron colliders from Tevatron [13] to LHC energies [14, 15].

Most event shape variables are based on the determination of the thrust’s principal axis [16] or the sphericity tensor [17]. A notable exception is given by the energy–energy correlations (EEC), originally proposed by Basham et al. [18], and measurements [19–31] of these have significantly improved the precision tests of perturbative QCD (pQCD). The EEC is defined as the energy-weighted angular distribution of hadron pairs produced in e^+e^- annihilation and, by construction, the EEC as well as its associated asymmetry (AEEC) are infrared safe. The second-order corrections to these functions were found to be significantly smaller [32–35] than for other event shape variables such as thrust.

The transverse energy–energy correlation (TEEC) and its associated asymmetry (ATEEC) were proposed as the appropriate generalisation to hadron colliders in Ref. [36], where leading-order (LO) predictions were also presented. As a jet-based quantity, it makes use of the jet transverse energy

^{*} e-mail: atlas.publications@cern.ch

$E_T = E \sin \theta$ since the energy alone is not Lorentz-invariant under longitudinal boosts along the beam direction. Here θ refers to the polar angle of the jet axis, while E is the jet energy.¹ The next-to-leading-order (NLO) corrections were obtained recently [37] by using the NLOJET++ program [38,39]. They are found to be of moderate size so that the TEEC and ATEEC functions are well suited for precision tests of QCD, including a precise determination of the strong coupling constant α_s . The TEEC is defined as [40]

$$\frac{1}{\sigma} \frac{d\Sigma}{d\cos\phi} \equiv \frac{1}{\sigma} \sum_{ij} \int \frac{d\sigma}{dx_{Ti} dx_{Tj} d\cos\phi} x_{Ti} x_{Tj} dx_{Ti} dx_{Tj} \\ = \frac{1}{N} \sum_{A=1}^N \sum_{ij} \frac{E_{Ti}^A E_{Tj}^A}{\left(\sum_k E_{Tk}^A\right)^2} \delta(\cos\phi - \cos\phi_{ij}), \quad (1)$$

where the last expression is valid for a sample of N hard-scattering multi-jet events, labelled by the index A , and the indices i and j run over all jets in a given event. Here, x_{Ti} is the fraction of transverse energy of jet i with respect to the total transverse energy, i.e. $x_{Ti} = E_{Ti} / \sum_k E_{Tk}$, ϕ_{ij} is the angle in the transverse plane between jet i and jet j and $\delta(x)$ is the Dirac delta function, which ensures $\phi = \phi_{ij}$.

The associated asymmetry ATEEC is then defined as the difference between the forward ($\cos\phi > 0$) and the backward ($\cos\phi < 0$) parts of the TEEC, i.e.

$$\frac{1}{\sigma} \frac{d\Sigma^{\text{asym}}}{d\cos\phi} \equiv \frac{1}{\sigma} \frac{d\Sigma}{d\cos\phi} \Big|_{\phi} - \frac{1}{\sigma} \frac{d\Sigma}{d\cos\phi} \Big|_{\pi-\phi}.$$

Recently, the ATLAS Collaboration presented a measurement of the TEEC and ATEEC [41], where these observables were used for a determination of the strong coupling constant $\alpha_s(m_Z)$ at an energy regime of $\langle Q \rangle = 305$ GeV. This paper extends the previous measurement to higher energy scales up to values close to 1 TeV. The analysis consists in the measurement of the TEEC and ATEEC distributions in different energy regimes, determining $\alpha_s(m_Z)$ in each of them, and using these determinations to test the running of α_s predicted by the QCD β -function. Precise knowledge of the running of α_s is not only important as a precision test of QCD at large scales but also as a test for new physics, as the existence of new coloured fermions would imply modifications to the β -function [42,43].

¹ ATLAS uses a right-handed coordinate system with its origin at the nominal interaction point (IP) in the centre of the detector and the z -axis along the beam pipe. The x -axis points from the IP to the centre of the LHC ring, and the y -axis points upward. Cylindrical coordinates (r, φ) are used in the transverse plane, φ being the azimuthal angle around the beam pipe. The pseudorapidity is defined in terms of the polar angle θ as $\eta = -\ln \tan(\theta/2)$.

2 ATLAS detector

The ATLAS detector [44] is a multipurpose particle physics detector with a forward-backward symmetric cylindrical geometry and a solid angle coverage of almost 4π .

The inner tracking system covers the pseudorapidity range $|\eta| < 2.5$. It consists of a silicon pixel detector, a silicon microstrip detector and, for $|\eta| < 2.0$, a transition radiation tracker. It is surrounded by a thin superconducting solenoid providing a 2 T magnetic field along the beam direction. A high-granularity liquid-argon sampling electromagnetic calorimeter covers the region $|\eta| < 3.2$. A steel/scintillator tile hadronic calorimeter provides coverage in the range $|\eta| < 1.7$. The endcap and forward regions, spanning $1.5 < |\eta| < 4.9$, are instrumented with liquid-argon calorimeters for electromagnetic and hadronic measurements. The muon spectrometer surrounds the calorimeters. It consists of three large air-core superconducting toroid systems and separate trigger and high-precision tracking chambers providing accurate muon tracking for $|\eta| < 2.7$.

The trigger system [45] has three consecutive levels: level 1, level 2 and the event filter. The level 1 triggers are hardware-based and use coarse detector information to identify regions of interest, whereas the level 2 triggers are software-based and perform a fast online data reconstruction. Finally, the event filter uses reconstruction algorithms similar to the offline versions with the full detector granularity.

3 Monte Carlo simulation

Multi-jet production in pp collisions is described by the convolution of the production cross-sections for parton-parton scattering with the parton distribution functions (PDFs). Monte Carlo (MC) event generators differ in the approximations used to calculate the underlying short-distance QCD processes, in the way parton showers are built to take into account higher-order effects and in the fragmentation scheme responsible for long-distance effects. PYTHIA and HERWIG++ event generators were used for the description of multi-jet production in pp collisions. These event generators differ in the modelling of the parton shower, hadronisation and underlying event. PYTHIA uses p_T -ordered parton showers, in which the p_T of the emitted parton is decreased in each step, while for the angle-ordered parton showers in HERWIG++, the relevant scale is related to the angle between the emitted and the incoming parton. The generated events were processed with the ATLAS full detector simulation [46] based on GEANT4 [47].

The baseline MC samples were generated using PYTHIA 8.160 [48] with the matrix elements for the underlying $2 \rightarrow 2$ processes calculated at LO using the CT10 LO PDFs [49] and matched to p_T -ordered parton showers. A set of tuned

parameters called the AU2CT10 tune [50] was used to model the underlying event (UE). The hadronisation follows the Lund string model [51].

A different set of samples were generated with HERWIG++ 2.5.2 [52], using the LO CTEQ6L1 PDFs [53] and the CTEQ6L1-UE-EE-3 tune for the underlying event [54]. HERWIG++ uses angle-ordered parton showers, a cluster hadronisation scheme and the underlying-event parameterisation is given by JIMMY [55].

Additional samples are generated using SHERPA 1.4.5 [56], which calculates matrix elements for $2 \rightarrow N$ processes at LO, which are then convolved with the CT10 LO PDFs, and uses the CKKW [57] method for the parton shower matching. These samples were generated with up to three hard-scattering partons in the final state.

In order to compensate for the steeply falling p_T spectrum, MC samples are generated in seven intervals of the leading-jet transverse momentum. Each of these samples contain of the order of 6×10^6 events for PYTHIA8 and 1.4×10^6 events for HERWIG++ and SHERPA.

All MC simulated samples described above are subject to a reweighting algorithm in order to match the average number of pp interactions per bunch-crossing observed in the data. The average number of interactions per bunch-crossing amounts to $\langle \mu \rangle = 20.4$ in data, and to $\langle \mu \rangle = 22.0$ in the MC simulation.

4 Data sample and jet calibration

The data used were recorded in 2012 at $\sqrt{s} = 8$ TeV and collected using a single-jet trigger. It requires at least one jet, reconstructed with the anti- k_t algorithm [58] with radius parameter $R = 0.4$ as implemented in FASTJET [59]. The jet transverse energy measured by the trigger system is required to be greater than 360 GeV at the trigger level. This trigger is fully efficient for values of the scalar sum of the calibrated transverse momenta of the two leading jets, $p_{T1} + p_{T2}$, denoted hereafter by H_{T2} , above 730 GeV. This is the lowest unprescaled trigger for the 2012 data-taking period, and the integrated luminosity of the full data sample is 20.2 fb^{-1} .

Events are required to have at least one vertex, with two or more associated tracks with transverse momentum $p_T > 400$ MeV. The vertex maximising $\sum p_T^2$, where the sum is performed over tracks, is chosen as the primary vertex.

In the analysis, jets are reconstructed with the same algorithm as used in the trigger, the anti- k_t algorithm with radius parameter $R = 0.4$. The input objects to the jet algorithm are topological clusters of energy deposits in the calorimeters [60]. The baseline calibration for these clusters corrects their energy using local hadronic calibration [61, 62]. The four-momentum of an uncalibrated jet is defined as the sum

Table 1 Summary of the H_{T2} bins used in the analysis. The table shows the number of events falling into each energy bin together with the value of the scale Q at which the coupling constant α_s is measured

H_{T2} range [GeV]	Number of events	$\langle Q \rangle = \langle H_{T2} \rangle / 2$ [GeV]
[800, 850]	1 809 497	412
[850, 900]	1 240 059	437
[900, 1000]	1 465 814	472
[1000, 1100]	745 898	522
[1100, 1400]	740 563	604
[1400, 5000]	192 204	810

of the four-momenta of its constituent clusters, which are considered massless. Thus, the resulting jets are massive. However, the effect of this mass is marginal for jets in the kinematic range considered in this paper, as the difference between transverse energy and transverse momentum is at the per-mille level for these jets.

The jet calibration procedure includes energy corrections for multiple pp interactions in the same or neighbouring bunch crossings, known as “pile-up”, as well as angular corrections to ensure that the jet originates from the primary vertex. Effects due to energy losses in inactive material, shower leakage, the magnetic field, as well as inefficiencies in energy clustering and jet reconstruction, are taken into account. This is done using an MC-based correction, in bins of η and p_T , derived from the relation of the reconstructed jet energy to the energy of the corresponding particle-level jet, not including muons or non-interacting particles. In a final step, an in situ calibration corrects for residual differences in the jet response between the MC simulation and the data using p_T -balance techniques for dijet, γ +jet, Z+jet and multi-jet final states. The total jet energy scale (JES) uncertainty is given by a set of independent sources, correlated in p_T . The uncertainty in the p_T value of individual jets due to the JES increases from (1–4)% for $|\eta| < 1.8$ to 5% for $1.8 < |\eta| < 4.5$ [63].

The selected jets must fulfill $p_T > 100$ GeV and $|\eta| < 2.5$. The two leading jets are further required to fulfil $H_{T2} > 800$ GeV. In addition, jets are required to satisfy quality criteria that reject beam-induced backgrounds (jet cleaning) [64].

The number of selected events in data is 6.2×10^6 , with an average jet multiplicity $\langle N_{\text{jet}} \rangle = 2.3$. In order to study the dependence of the TEEC and ATEEC on the energy scale, and thus the running of the strong coupling, the data are further binned in H_{T2} . The binning is chosen as a compromise between reaching the highest available energy scales while keeping a sufficient statistical precision in the TEEC distributions, and thus in the determination of α_s . Table 1 summarises this choice, as well as the number of events in each energy bin and the average value of the chosen scale $Q = H_{T2}/2$, obtained from detector-level data.

5 Results at the detector level

The data sample described in Sect. 4 is used to measure the TEEC and ATEEC functions. In order to study the kinematical dependence of such observables, and thus the running of the strong coupling with the energy scale involved in the hard

process, the binning introduced in Table 1 is used. Figure 1 compares the TEEC and ATEEC distributions, measured in two of these bins, with the MC predictions from PYTHIA8, HERWIG++ and SHERPA.

The TEEC distributions show two peaks in the regions close to the kinematical endpoints $\cos\phi = \pm 1$. The first

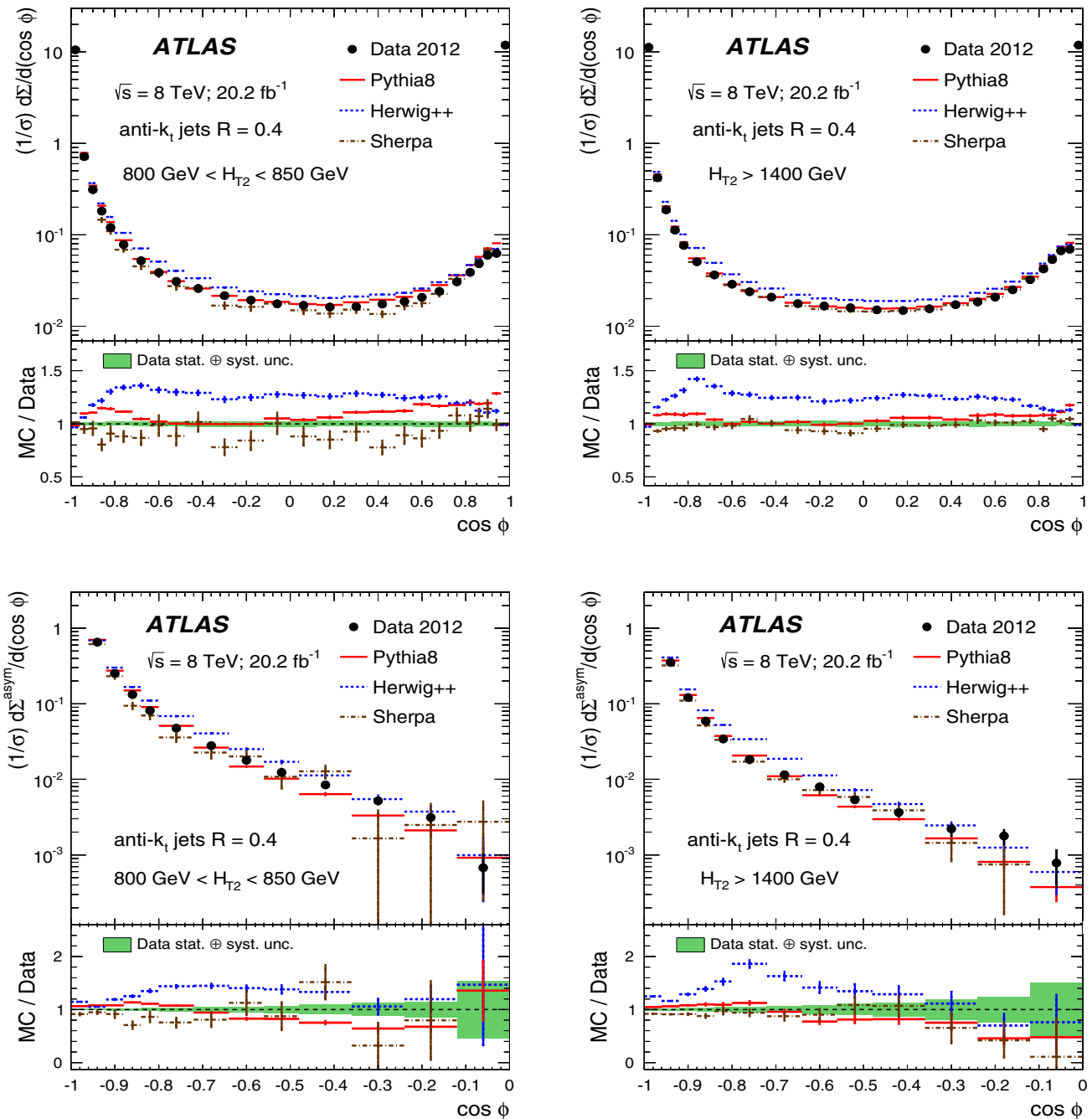


Fig. 1 Detector-level distributions for the TEEC (top) and ATEEC functions (bottom) for the first and the last H_{T2} intervals chosen in this analysis, together with MC predictions from PYTHIA8, HERWIG++ and SHERPA. The total uncertainty, including statistical and detector

experimental sources, i.e. those not related to unfolding corrections, is also indicated using an error bar for the distributions and a green-shaded band for the ratios. The systematic uncertainties are discussed in Sect. 7

one, at $\cos\phi = -1$ is due to the back-to-back configuration in two-jet events, which dominate the sample, while the second peak at $\cos\phi = +1$ is due to the self-correlations of one jet with itself. These self-correlations are included in Eq. (1) and are necessary for the correct normalisation of the TEEC functions. The central regions of the TEEC distributions shown in Fig. 1 are dominated by gluon radiation, which is decorrelated from the main event axis as predicted by QCD and measured in Refs. [65,66].

Among the MC predictions considered here, PYTHIA8 and SHERPA are the ones which fit the data best, while HERWIG++ shows significant discrepancies with the data.

6 Correction to particle level

In order to allow comparison with particle-level MC predictions, as well as NLO theoretical predictions, the detector-level distributions presented in Sect. 5 need to be corrected for detector effects. Particle-level jets are reconstructed in the MC samples using the anti- k_t algorithm with $R = 0.4$, applied to final-state particles with an average lifetime $\tau > 10^{-11}$ s, including muons and neutrinos. The kinematical requirements for particle-level jets are the same as for the definition of TEEC/ATEEC at the detector level.

In the data, an unfolding procedure is used which relies on an iterative Bayesian unfolding method [67] as implemented in the ROOUNFOLD program [68]. The method makes use of a transfer matrix for each distribution, which takes into account any inefficiencies in the detector, as well as its finite resolution. The PYTHIA8 MC sample is used to determine the transfer matrices from the particle-level to detector-level TEEC distributions. Pairs of jets not entering the transfer matrices are accounted for using inefficiency correction factors.

The excellent azimuthal resolution of the ATLAS detector, together with the reduction of the energy scale and resolution effects by the weighting procedure involved in the definition of the TEEC function, are reflected in the fact that the transfer matrices have very small off-diagonal terms (smaller than 10%), leading to very small migrations between bins.

The statistical uncertainty is propagated through the unfolding procedure by using pseudo-experiments. A set of 10^3 replicas is considered for each measured distribution by applying a Poisson-distributed fluctuation around the nominal measured distribution. Each of these replicas is unfolded using a fluctuated version of the transfer matrix, which produces the corresponding set of 10^3 replicas of the unfolded spectra. The statistical uncertainty is defined as the standard deviation of all replicas.

7 Systematic uncertainties

The dominant sources are those associated with the MC model used in the unfolding procedure and the JES uncertainty in the jet calibration procedure.

- **Jet Energy Scale:** The uncertainty in the jet calibration procedure [63] is propagated to the TEEC by varying each jet energy and transverse momentum by one standard deviation of each of the 67 nuisance parameters of the JES uncertainty, which depend on both the jet transverse momentum and pseudorapidity. The total JES uncertainty is evaluated as the sum in quadrature of all nuisance parameters, and amounts to 2%.
- **Jet Energy Resolution:** The effect on the TEEC function of the jet energy resolution uncertainty [69] is estimated by smearing the energy and transverse momentum by a smearing factor depending on both p_T and η . This amounts to approximately 1% in the TEEC distributions.
- **Monte Carlo modelling:** The modelling uncertainty is estimated by performing the unfolding procedure described in Sect. 6 with different MC approaches. The difference between the unfolded distributions using PYTHIA and HERWIG++ defines the envelope of the uncertainty. This was cross-checked using the difference between PYTHIA and SHERPA, leading to similar results. This is the dominant experimental uncertainty for this measurement, being always below 5% for the TEEC distributions, and being larger for low H_{T2} .
- **Unfolding:** The mismodelling of the data made by the MC simulation is accounted for as an additional source of uncertainty. This is assessed by reweighting the transfer matrices so that the level of agreement between the detector-level projection and the data is enhanced. The modified detector-level distributions are then unfolded using the method described in Sect. 6. The difference between the modified particle-level distribution and the nominal one is then taken as the uncertainty. This uncertainty is smaller than 0.5% for the full $\cos\phi$ range for all bins in H_{T2} . The impact of this uncertainty on the TEEC function is below 1%.
- **Jet Angular Resolution:** The uncertainty in the jet angular resolution is propagated to the TEEC measurements by smearing the azimuthal coordinate ϕ of each jet by 10% of the resolution in the MC simulation. This is motivated by the track-to-cluster matching studies done in Ref. [65]. This impacts the TEEC measurement at the level of 0.5%.

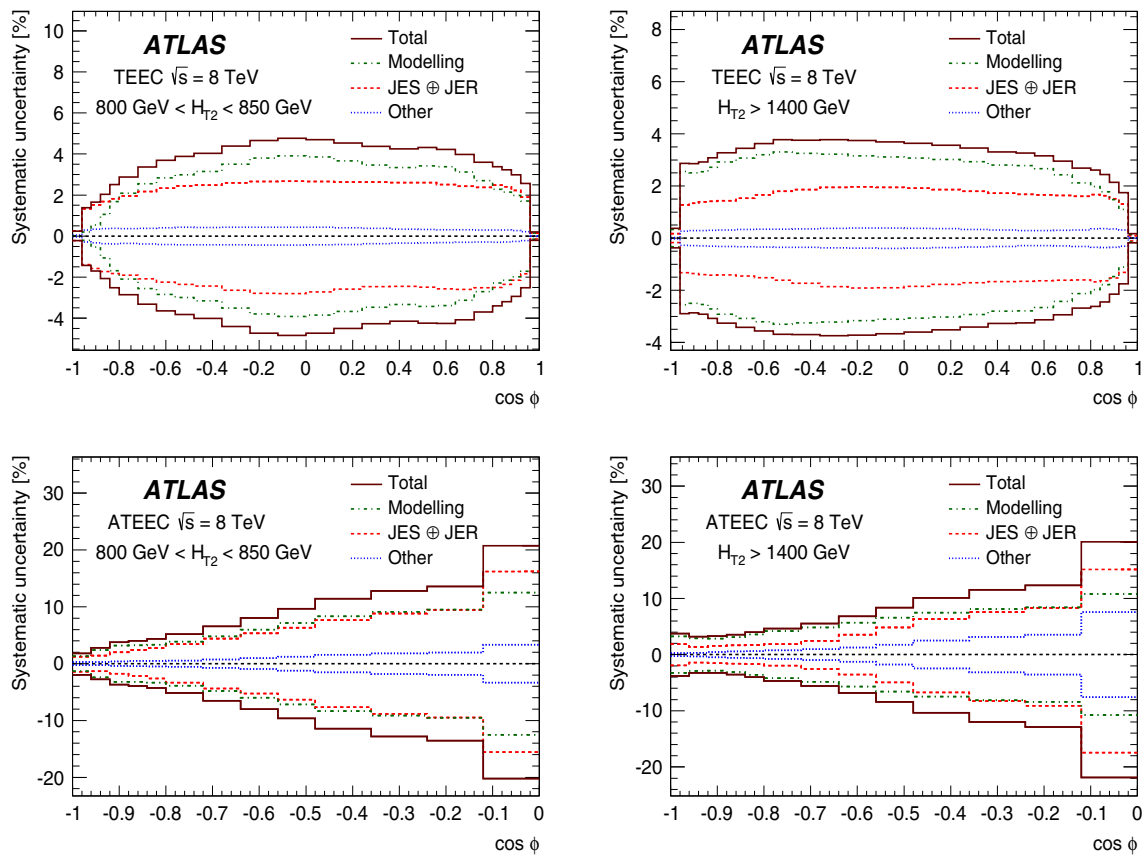


Fig. 2 Systematic uncertainties in the measured TEEC (top) and ATEEC distributions (bottom) for the first and the last bins in H_{T2} . The total uncertainty is below 5% in all bins of the TEEC distributions

- **Jet cleaning:** The modelling of the efficiency of the jet-cleaning cuts is considered as an additional source of experimental uncertainty. This is studied by tightening the jet cleaning-requirements in both data and MC simulation, and considering the double ratio between them. The differences are below 0.5%.

In order to mitigate statistical fluctuations, the resulting systematic uncertainties are smoothed using a Gaussian kernel algorithm. The impact of these systematic uncertainties is summarised in Fig. 2, where the relative errors are shown for the TEEC and ATEEC distributions for each H_{T2} bin considered.

8 Experimental results

The results of the unfolding are compared with particle-level MC predictions, including the estimated systematic uncertainties. Figure 3 shows this comparison for the TEEC, while the ATEEC results are shown in Fig. 4. The level of agreement seen here between data and MC simulation is similar to

that at detector level. PYTHIA and SHERPA broadly describe the data, while the HERWIG++ description is disfavoured.

9 Theoretical predictions

The theoretical predictions for the TEEC and ATEEC functions are calculated using perturbative QCD at NLO as implemented in NLOJET++ [38,39]. Typically $\mathcal{O}(10^{10})$ events are generated for the calculation. The partonic cross-sections, $\hat{\sigma}$, are convolved with the NNLO PDF sets from MMHT 2014 [70], CT14 [71], NNPDF 3.0 [72] and HERAPDF 2.0 [73] using the LHAPDF6 package [74]. The value of $\alpha_s(m_Z)$ used in the partonic matrix-element calculation is chosen to be the same as that of the PDF. At leading order in α_s , the TEEC function defined in Eq. (1) can be expressed as

$$\frac{1}{\sigma} \frac{d\Sigma}{d\phi} = \frac{\Sigma_{a_i, b_i} f_{a_1/p}(x_1) f_{a_2/p}(x_2) \otimes \hat{\Sigma}^{a_1 a_2 \rightarrow b_1 b_2 b_3}}{\Sigma_{a_i, b_i} f_{a_1/p}(x_1) f_{a_2/p}(x_2) \otimes \hat{\sigma}^{a_1 a_2 \rightarrow b_1 b_2}}, \quad (2)$$

where $\hat{\Sigma}^{a_1 a_2 \rightarrow b_1 b_2 b_3}$ is the partonic cross-section weighted by the fractions of transverse energy of the outgoing partons,

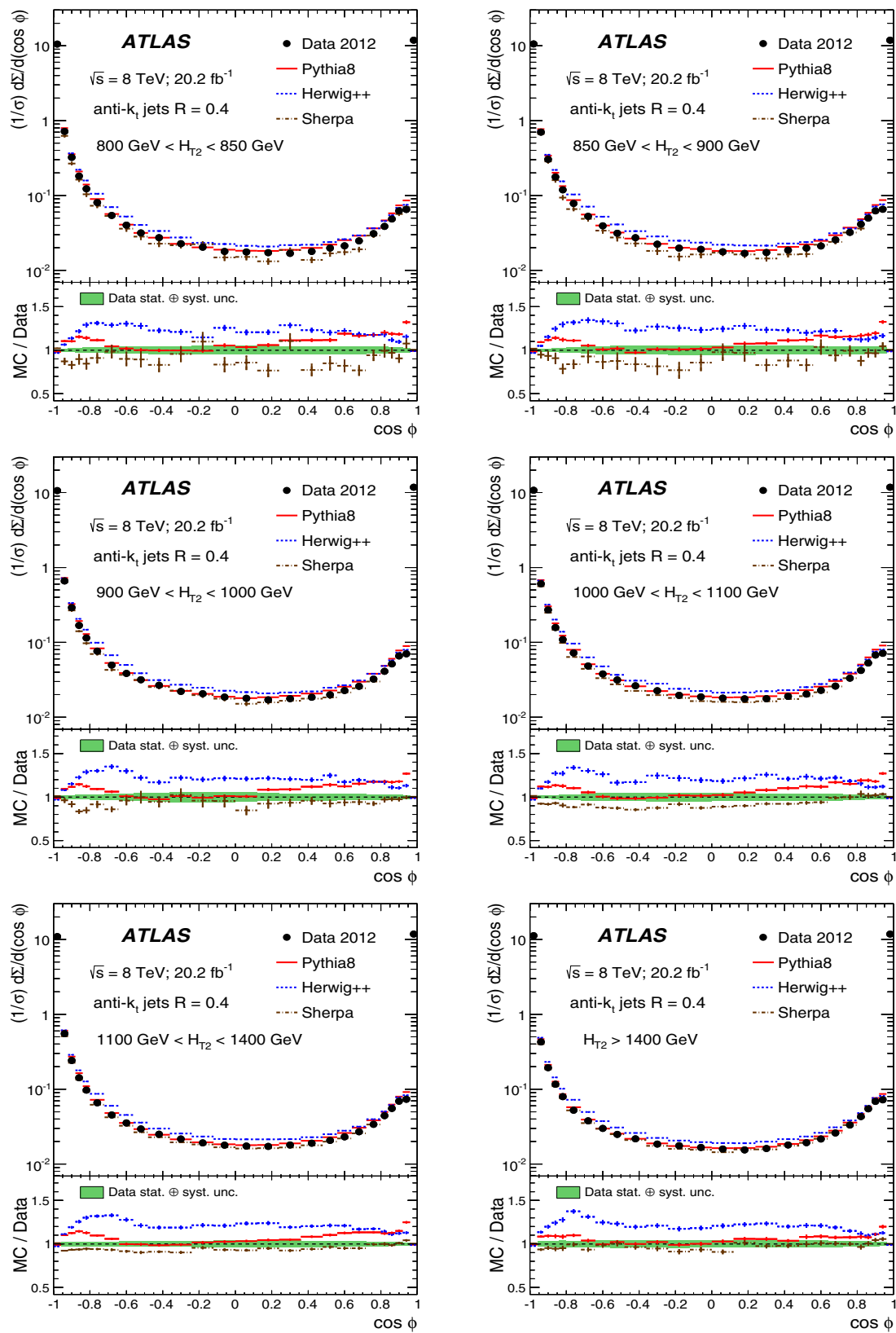


Fig. 3 Particle-level distributions for the TEEC functions in each of the H_{T2} intervals chosen in this analysis, together with MC predictions from PYTHIA8, HERWIG++ and SHERPA. The total uncertainty, includ-

ing statistical and other experimental sources is also indicated using an error bar for the distributions and a green-shaded band for the ratios

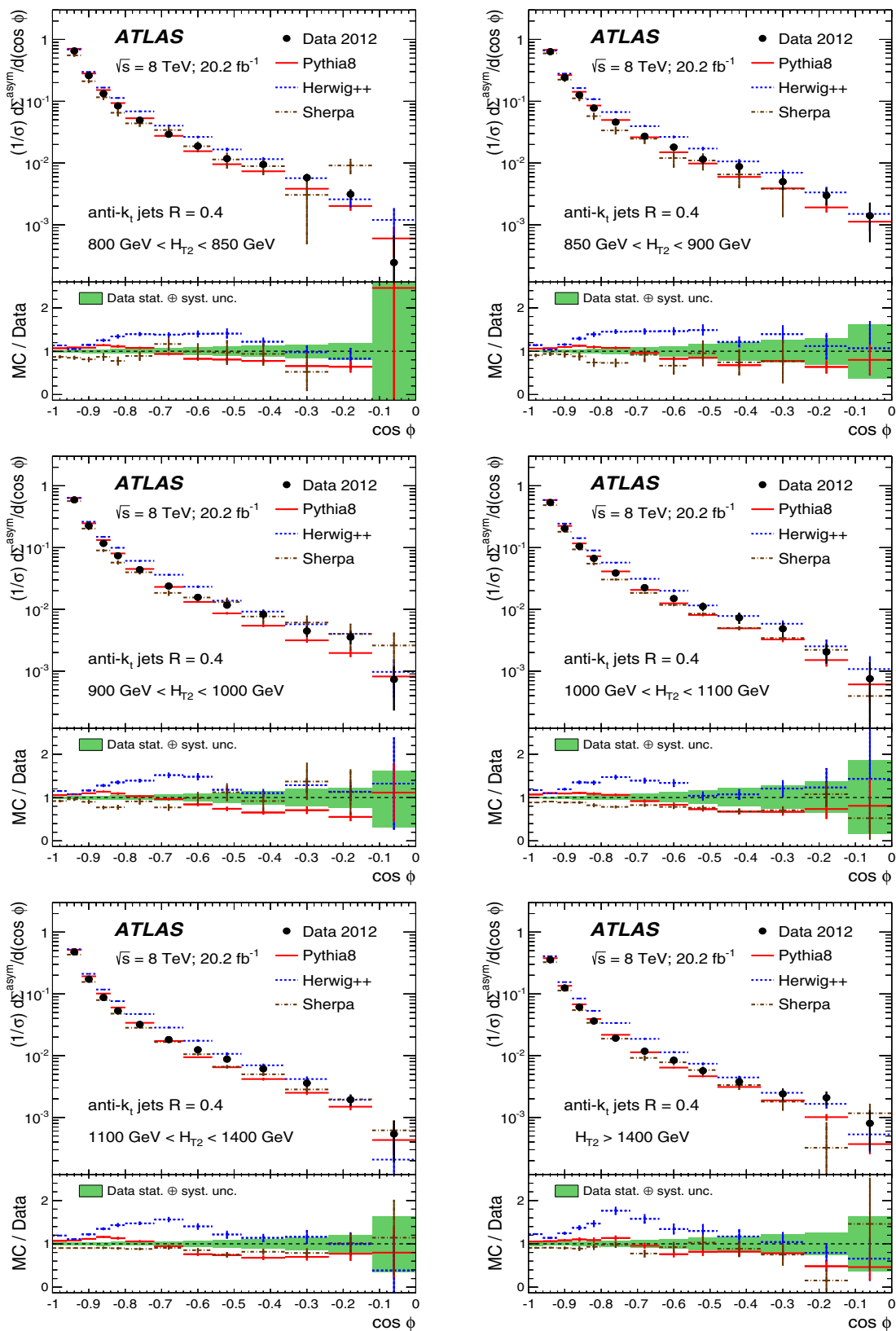


Fig. 4 Particle-level distributions for the ATEEC functions in each of the H_{T2} intervals chosen in this analysis, together with MC predictions from PYTHIA8, HERWIG++ and SHERPA. The total uncertainty, includ-

ing statistical and other experimental sources is also indicated using an error bar for the distributions and a green-shaded band for the ratios

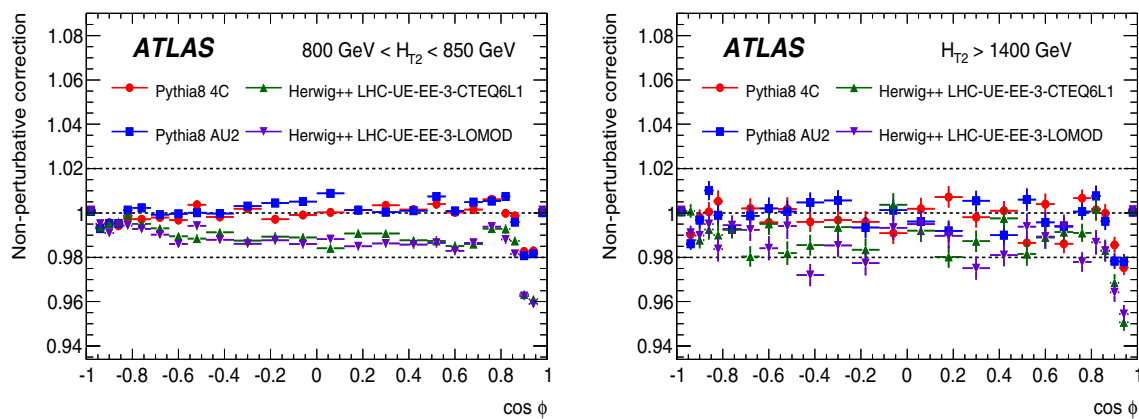


Fig. 5 Non-perturbative correction factors for TEEC in the first and last bins of H_{T2} as a function of $\cos \phi$

$x_{T1}x_{Tj}$ as in Eq. (1); x_i ($i = 1, 2$) are the fractional longitudinal momenta carried by the initial-state partons, $f_{a1/p}(x_1)$ and $f_{a2/p}(x_2)$ are the PDFs and \otimes denotes a convolution over x_1, x_2 .

At $\mathcal{O}(\alpha_s^4)$, the numerator in Eq. (2) entails calculations of the $2 \rightarrow 3$ partonic subprocesses at NLO accuracy, and the $2 \rightarrow 4$ partonic subprocesses at LO. In order to avoid the double collinear singularities appearing in the latter, the angular range is restricted to $|\cos \phi| \leq 0.92$. This avoids calculating the two-loop virtual corrections to the $2 \rightarrow 2$ subprocesses. Thus, with the azimuthal angle cut, the denominator in Eq. (2) includes the $2 \rightarrow 2$ and $2 \rightarrow 3$ subprocesses up to and including the $\mathcal{O}(\alpha_s^3)$ corrections.

The nominal renormalisation and factorisation scales are defined as a function of the transverse momenta of the two leading jets as follows [75]

$$\mu_R = \frac{p_{T1} + p_{T2}}{2}; \quad \mu_F = \frac{p_{T1} + p_{T2}}{4}.$$

This choice eases the comparison with the previous measurement at $\sqrt{s} = 7$ TeV [41], where the renormalisation scale was the same. The relevant scale for the perturbative calculation is the renormalisation scale, as variations of the factorisation scale lead to small variations of the physical observable. The scale choice for the NLO pQCD templates used to extract α_s as well as for the presentation of the measurement is not uniquely defined. The nominal scale choice, $H_{T2}/2$, used in this paper is based on previous publications [41, 76]. However, it should be noted that other scale choices, which explicitly take into account the kinematics of the third jet, are also viable options and can be considered in future measurements.

The following comments are in order. The NLOJET++ calculations are performed in the limit of massless quarks. PDFs are based on the $n_f = 5$ scheme. There is therefore a residual uncertainty due to the mass of the top

quark. This is expected to be small since at LHC energies $\sigma_{t\bar{t}} \ll \sigma_{\text{QCD}}$. The correct treatment of top quark mass effects in the initial as well as in final state is not yet available.

9.1 Non-perturbative corrections

The pQCD predictions obtained using NLOJET++ are generated at the parton level only. In order to compare these predictions with the data, one needs to correct for non-perturbative (NP) effects, namely hadronisation and the underlying event. Here, doing this relies on bin-by-bin correction factors calculated as the ratio of the MC predictions for TEEC distributions with hadronisation and UE turned on to those with hadronisation and UE turned off. These factors, which are calculated using several MC models, are used to correct the pQCD prediction to the particle level by multiplying each bin of the theoretical distributions. Figure 5 shows the distributions of the factors for the TEEC as a function of $\cos \phi$ and for two bins in the energy scale H_{T2} . They were calculated using several models, namely PYTHIA8 with the AU2 [77] and 4C tunes [78] and HERWIG++ with the LHC-UE-EE-3-CTEQ6L1 and LHC-UE-EE-3-LOMOD tunes [54]. From these four possibilities, PYTHIA8 with the AU2 tune is used for the nominal corrections.

9.2 Theoretical uncertainties

The theoretical uncertainties are divided into three classes: those corresponding to the renormalisation and factorisation scale variations, the ones corresponding to the PDF eigenvectors, and the ones for the non-perturbative corrections.

- The theoretical uncertainty due to the choice of renormalisation and factorisation scales is defined as the envelope of all the variations of the TEEC and ATEEC distributions obtained by varying up and down the scales

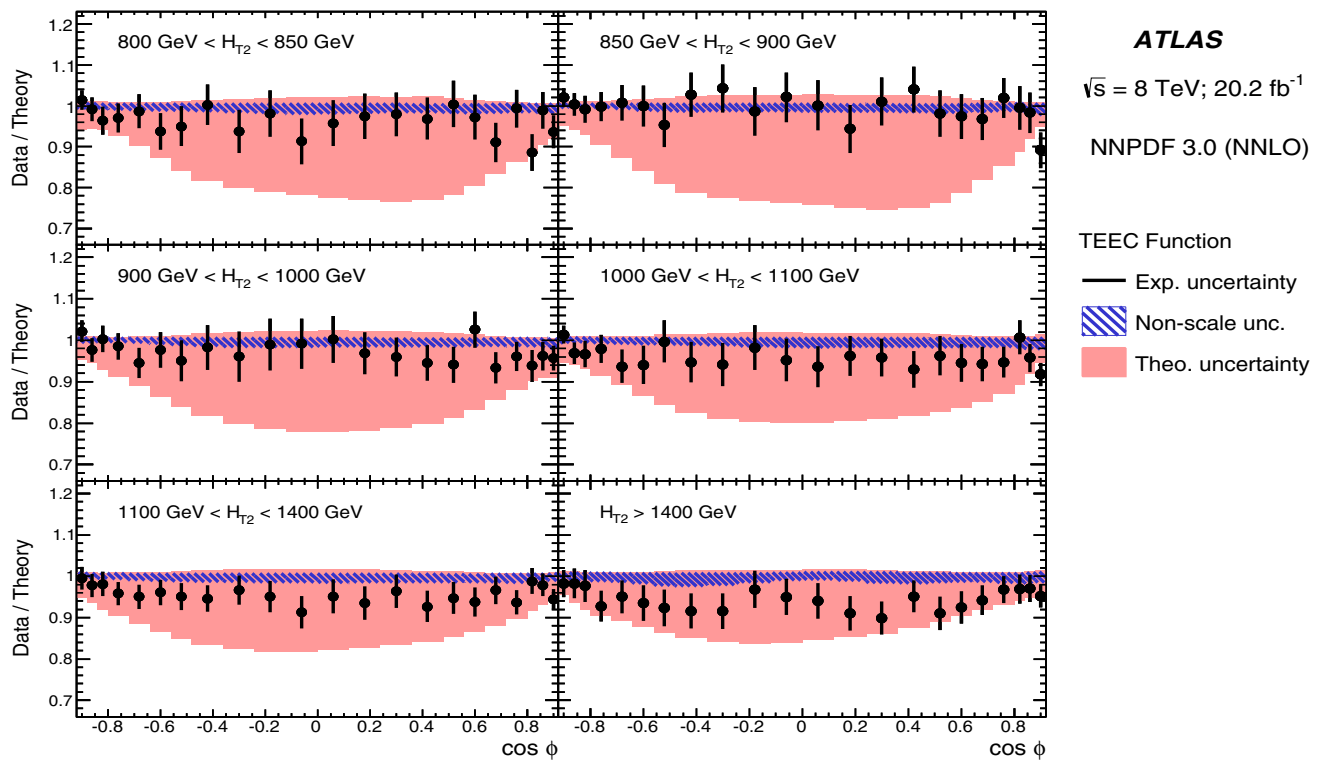


Fig. 6 Ratios of the TEEC data in each H_{T2} bin to the NLO pQCD predictions obtained using the NNPDF 3.0 parton distribution functions, and corrected for non-perturbative effects

μ_R, μ_F by a factor of two, excluding those configurations in which both scales are varied in opposite directions. This is the dominant theoretical uncertainty in this measurement, which can reach 20% in the central region of the TEEC distributions.

- The parton distribution functions are varied following the set of eigenvectors/replicas provided by each PDF group [70–73]. The propagation of the corresponding uncertainty to the TEEC and ATEEC is done following the recommendations for each particular set of distribution functions. The size of this uncertainty is around 1% for each TEEC bin.
- The uncertainty in the non-perturbative corrections is estimated as the envelope of all models used for the calculation of the correction factors in Fig. 5. This uncertainty is around 1% for each of the TEEC bins considered in the NLO predictions, i.e. those with $|\cos \phi| \leq 0.92$.
- The uncertainty due to α_s is also considered for the comparison of the data with the theoretical predictions. This is estimated by varying α_s by the uncertainty in its value for each PDF set, as indicated in Refs. [70–73].

The total theoretical uncertainty is obtained by adding these four theoretical uncertainties in quadrature. The total uncertainty can reach 20% for the central part of the TEEC, due to the large value of the scale uncertainty in this region.

10 Comparison of theoretical predictions and experimental results

The unfolded data obtained in Sect. 8 are compared to the pQCD predictions, once corrected for non-perturbative effects. Figures 6 and 7 show the ratios of the data to the theoretical predictions for the TEEC and ATEEC functions, respectively. The theoretical predictions were calculated, as a function of $\cos \phi$ and for each of the H_{T2} bins considered, using the NNPDF 3.0 PDFs with $\alpha_s(m_Z) = 0.1180$.

From the comparisons in Figs. 6 and 7, one can conclude that perturbative QCD correctly describes the data within the experimental and theoretical uncertainties.

11 Determination of α_s and test of asymptotic freedom

From the comparisons made in the previous section, one can determine the strong coupling constant at the scale given by the pole mass of the Z boson, $\alpha_s(m_Z)$, by considering the following χ^2 function

$$\chi^2(\alpha_s, \vec{\lambda}) = \sum_{\text{bins}} \frac{(x_i - F_i(\alpha_s, \vec{\lambda}))^2}{\Delta x_i^2 + \Delta \xi_i^2} + \sum_k \lambda_k^2, \quad (3)$$

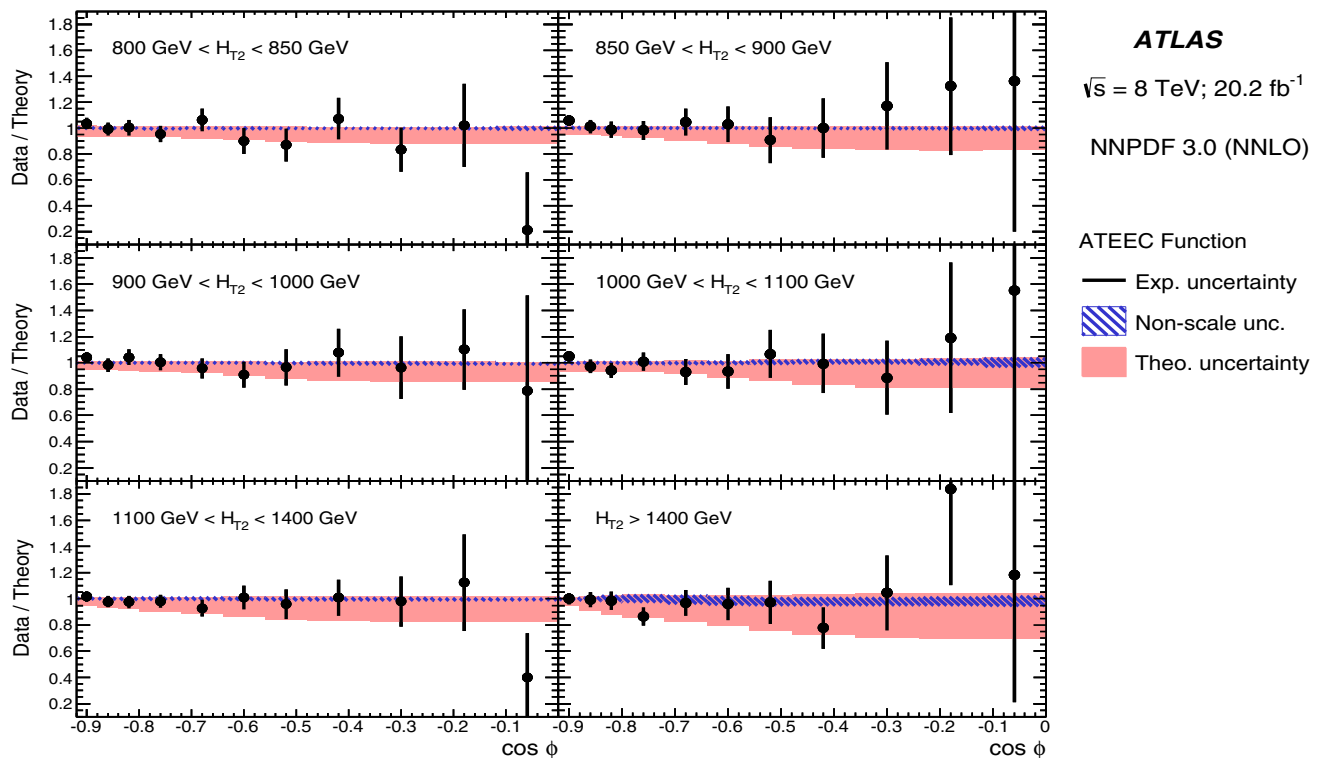


Fig. 7 Ratios of the ATEEC data in each H_{T2} bin to the NLO pQCD predictions obtained using the NNPDF 3.0 parton distribution functions, and corrected for non-perturbative effects

Table 2 Values of the strong coupling constant at the Z boson mass scale, $\alpha_s(m_Z)$ obtained from fits to the TEEC function for each H_{T2} interval using the NNPDF 3.0 parton distribution functions. The values of the average scale $\langle Q \rangle$ for each energy bin are shown in the first

column, while the values of the χ^2 function at the minimum are shown in the third column. The uncertainty referred to as NP is the one related to the non-perturbative corrections

$\langle Q \rangle$ (GeV)	$\alpha_s(m_Z)$ value (NNPDF 3.0)	χ^2/N_{dof}
412	0.1171 ± 0.0021 (exp.) $^{+0.0081}_{-0.0022}$ (scale) ± 0.0013 (PDF) ± 0.0001 (NP)	24.3/21
437	0.1178 ± 0.0017 (exp.) $^{+0.0073}_{-0.0017}$ (scale) ± 0.0014 (PDF) ± 0.0002 (NP)	28.3/21
472	0.1177 ± 0.0017 (exp.) $^{+0.0079}_{-0.0023}$ (scale) ± 0.0015 (PDF) ± 0.0001 (NP)	27.7/21
522	0.1163 ± 0.0017 (exp.) $^{+0.0067}_{-0.0016}$ (scale) ± 0.0016 (PDF) ± 0.0001 (NP)	22.8/21
604	0.1181 ± 0.0017 (exp.) $^{+0.0082}_{-0.0022}$ (scale) ± 0.0017 (PDF) ± 0.0005 (NP)	24.3/21
810	0.1186 ± 0.0023 (exp.) $^{+0.0085}_{-0.0035}$ (scale) ± 0.0020 (PDF) ± 0.0004 (NP)	23.7/21

where the theoretical predictions are varied according to

$$F_i(\alpha_s, \vec{\lambda}) = \psi_i(\alpha_s) \left(1 + \sum_k \lambda_k \sigma_k^{(i)} \right). \quad (4)$$

In Eqs. (3) and (4), α_s stands for $\alpha_s(m_Z)$; x_i is the value of the i -th point of the distribution as measured in data, while Δx_i is its statistical uncertainty. The statistical uncertainty in the theoretical predictions is also included as $\Delta \xi_i$, while $\sigma_k^{(i)}$ is the relative value of the k -th source of systematic uncertainty in bin i .

This technique takes into account the correlations between the different sources of systematic uncertainty discussed in Sect. 7 by introducing the nuisance parameters $\{\lambda_k\}$, one for each source of experimental uncertainty. Thus, the minimum of the χ^2 function defined in Eq. (3) is found in a 74-dimensional space, in which 73 correspond to nuisance parameters $\{\lambda_i\}$ and one to $\alpha_s(m_Z)$.

The method also requires an analytical expression for the dependence of the fitted observable on the strong coupling constant, which is given by $\psi_i(\alpha_s)$ for bin i . For each PDF set, the corresponding $\alpha_s(m_Z)$ variation range is considered and the theoretical prediction is obtained for each value of

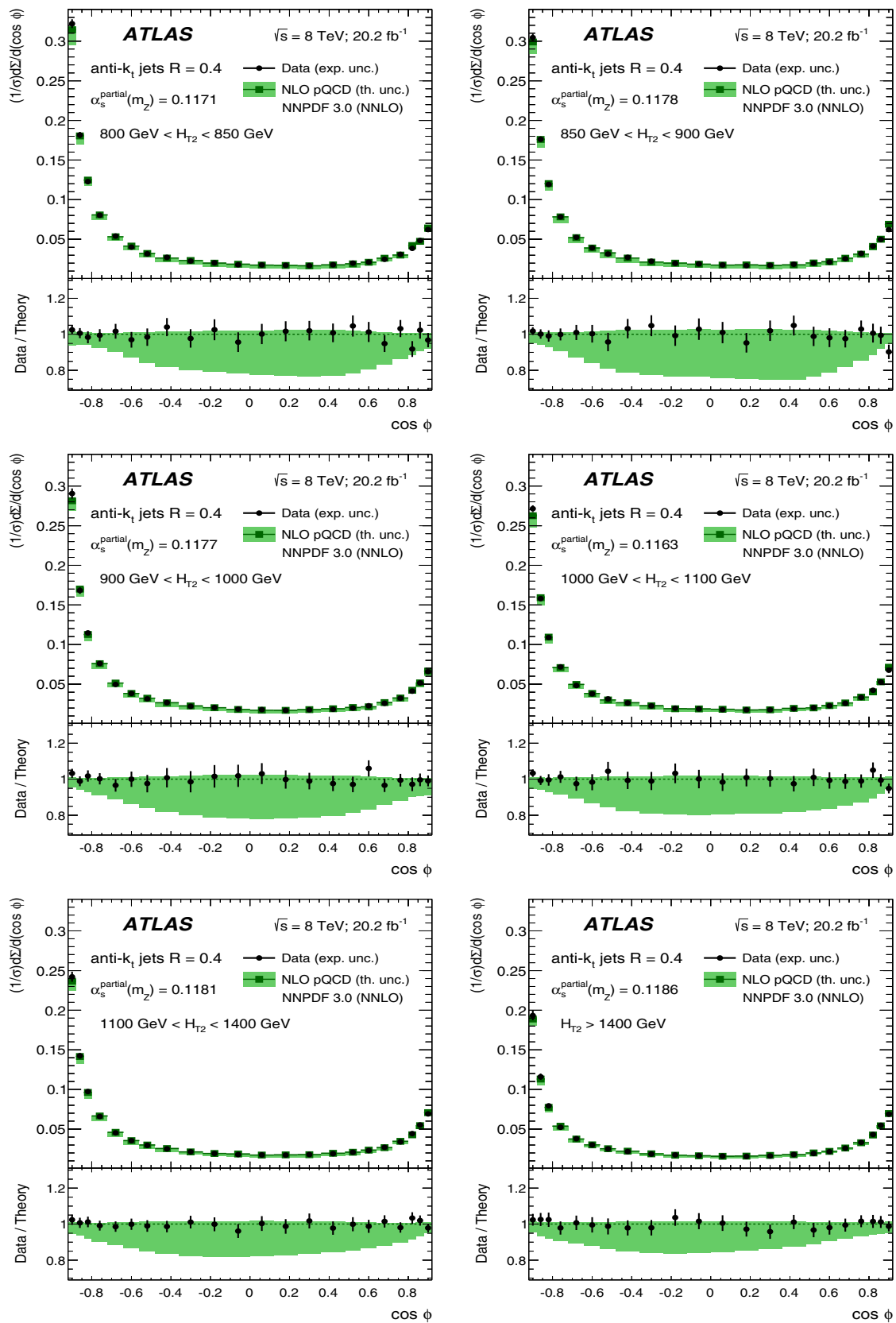


Fig. 8 Comparison of the TEEC data and the theoretical predictions after the fit. The value of $\alpha_s(m_Z)$ used in this comparison is fitted independently for each energy bin

Table 3 Values of the strong coupling constant at the measurement scales, $\alpha_s(Q^2)$ obtained from fits to the TEEC function for each H_{T2} interval using the NNPDF 3.0 parton distribution functions. The uncertainty referred to as NP is the one related to the non-perturbative corrections

$\langle Q \rangle$ (GeV)	$\alpha_s(Q^2)$ value (NNPDF 3.0)
412	0.0966 ± 0.0014 (exp.) $^{+0.0054}_{-0.0015}$ (scale) ± 0.0009 (PDF) ± 0.0001 (NP)
437	0.0964 ± 0.0012 (exp.) $^{+0.0048}_{-0.0011}$ (scale) ± 0.0009 (PDF) ± 0.0002 (NP)
472	0.0955 ± 0.0011 (exp.) $^{+0.0051}_{-0.0015}$ (scale) ± 0.0009 (PDF) ± 0.0001 (NP)
522	0.0936 ± 0.0011 (exp.) $^{+0.0043}_{-0.0010}$ (scale) ± 0.0010 (PDF) ± 0.0001 (NP)
604	0.0933 ± 0.0011 (exp.) $^{+0.0050}_{-0.0014}$ (scale) ± 0.0011 (PDF) ± 0.0003 (NP)
810	0.0907 ± 0.0013 (exp.) $^{+0.0049}_{-0.0020}$ (scale) ± 0.0011 (PDF) ± 0.0002 (NP)

Table 4 The results for α_s from fits to the TEEC using different PDFs. The uncertainty referred to as NP is the one related to the non-perturbative corrections. The uncertainty labelled as ‘mod’ corresponds to the HERAPDF modelling and parameterisation uncertainty

PDF	$\alpha_s(m_Z)$ value	χ^2/N_{dof}
MMHT 2014	0.1151 ± 0.0008 (exp.) $^{+0.0064}_{-0.0047}$ (scale) ± 0.0012 (PDF) ± 0.0002 (NP)	173/131
CT14	0.1165 ± 0.0010 (exp.) $^{+0.0067}_{-0.0061}$ (scale) ± 0.0016 (PDF) ± 0.0003 (NP)	161/131
NNPDF 3.0	0.1162 ± 0.0011 (exp.) $^{+0.0076}_{-0.0061}$ (scale) ± 0.0018 (PDF) ± 0.0003 (NP)	174/131
HERAPDF 2.0	0.1177 ± 0.0008 (exp.) $^{+0.0064}_{-0.0040}$ (scale) ± 0.0005 (PDF) ± 0.0002 (NP) $^{+0.0008}_{-0.0007}$ (mod)	169/131

$\alpha_s(m_Z)$. The functions $\psi_i(\alpha_s)$ are then obtained by fitting the values of the TEEC (ATEEC) in each $(H_{T2}, \cos \phi)$ bin to a second-order polynomial. For both the TEEC and ATEEC functions, the fits to extract $\alpha_s(m_Z)$ are repeated separately for each H_{T2} interval, thus determining a value of $\alpha_s(m_Z)$ for each energy bin. The theoretical uncertainties are determined by shifting the theory distributions by each of the uncertainties separately, recalculating the functions $\psi_i(\alpha_s)$ and determining a new value of $\alpha_s(m_Z)$. The uncertainty is determined by taking the difference between this value and the nominal one.

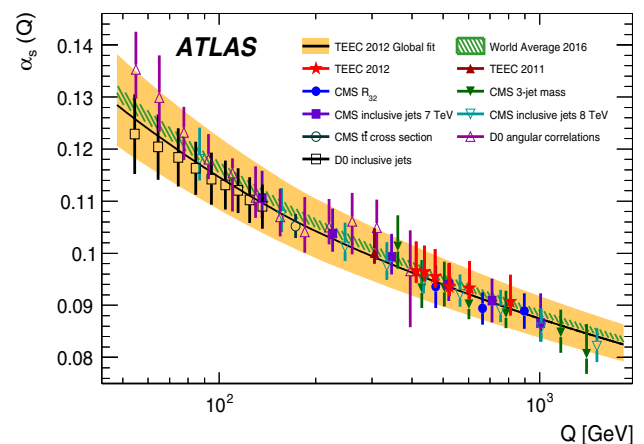
Each of the obtained values of $\alpha_s(m_Z)$ is then evolved to the corresponding measured scale using the NLO solution to the renormalisation group equation (RGE), given by

$$\alpha_s(Q^2) = \frac{1}{\beta_0 \log x} \left[1 - \frac{\beta_1}{\beta_0^2} \frac{\log(\log x)}{\log x} \right]; \quad x = \frac{Q^2}{\Lambda^2}, \quad (5)$$

where the coefficients β_0 and β_1 are given by

$$\beta_0 = \frac{1}{4\pi} \left(11 - \frac{2}{3}n_f \right); \quad \beta_1 = \frac{1}{(4\pi)^2} \left(102 - \frac{38}{3}n_f \right),$$

and Λ is the QCD scale, determined in each case from the fitted value of $\alpha_s(m_Z)$. Here, n_f is the number of active flavours at the scale Q , i.e. the number of quarks with mass $m < Q$. Therefore, $n_f = 6$ in the six bins considered in Table 1. When evolving $\alpha_s(m_Z)$ to $\alpha_s(Q)$, the proper transition rules for $n_f = 5$ to $n_f = 6$ are applied so that $\alpha_s(Q)$ is a continuous function across quark thresholds. Finally, the results are combined by performing a global fit, where all bins are merged together.

**Fig. 9** Comparison of the values of $\alpha_s(Q)$ obtained from fits to the TEEC functions at the energy scales given by $\langle H_{T2} \rangle/2$ (red star points) with the uncertainty band from the global fit (orange full band) and the 2016 world average (green hatched band). Determinations from other experiments are also shown as data points. The error bars, as well as the orange full band, include all experimental and theoretical sources of uncertainty. The strong coupling constant is assumed to run according to the two-loop solution of the RGE

11.1 Fits to individual TEEC functions

The values of $\alpha_s(m_Z)$ obtained from fits to the TEEC function in each H_{T2} bin are summarised in Table 2. The theoretical predictions used for this extraction use NNPDF 3.0 as the nominal PDF set.

The values summarised in Table 2 are in good agreement with the 2016 world average value [79], as well as with previous measurements, in particular with previous extractions using LHC data [41, 76, 80–84]. The values of the χ^2 indicate

Table 5 Values of the strong coupling constant at the Z boson mass scale, $\alpha_s(m_Z)$ obtained from fits to the ATEEC function for each H_{T2} interval using the NNPDF 3.0 parton distribution functions. The values of the average scale $\langle Q \rangle$ for each energy bin are shown in the first

column, while the values of the χ^2 function at the minimum are shown in the third column. The uncertainty referred to as NP is the one related to the non-perturbative corrections

$\langle Q \rangle$ (GeV)	$\alpha_s(m_Z)$ value (NNPDF 3.0)	χ^2/N_{dof}
412	0.1209 ± 0.0036 (exp.) $^{+0.0085}_{-0.0031}$ (scale) ± 0.0013 (PDF) ± 0.0004 (NP)	10.6/10
437	0.1211 ± 0.0026 (exp.) $^{+0.0064}_{-0.0014}$ (scale) ± 0.0015 (PDF) ± 0.0010 (NP)	6.8/10
472	0.1203 ± 0.0028 (exp.) $^{+0.0060}_{-0.0013}$ (scale) ± 0.0016 (PDF) ± 0.0002 (NP)	8.8/10
522	0.1196 ± 0.0025 (exp.) $^{+0.0054}_{-0.0010}$ (scale) ± 0.0017 (PDF) ± 0.0004 (NP)	10.9/10
604	0.1176 ± 0.0031 (exp.) $^{+0.0058}_{-0.0008}$ (scale) ± 0.0020 (PDF) ± 0.0005 (NP)	6.4/10
810	0.1172 ± 0.0037 (exp.) $^{+0.0053}_{-0.0009}$ (scale) ± 0.0022 (PDF) ± 0.0001 (NP)	9.8/10

Table 6 Values of the strong coupling constant at the measurement scales, $\alpha_s(Q^2)$ obtained from fits to the ATEEC function for each H_{T2} interval using the NNPDF 3.0 parton distribution functions. The uncertainty referred to as NP is the one related to the non-perturbative corrections

$\langle Q \rangle$ (GeV)	$\alpha_s(Q^2)$ value (NNPDF 3.0)
412	0.0992 ± 0.0024 (exp.) $^{+0.0056}_{-0.0020}$ (scale) ± 0.0009 (PDF) ± 0.0002 (NP)
437	0.0986 ± 0.0017 (exp.) $^{+0.0041}_{-0.0009}$ (scale) ± 0.0010 (PDF) ± 0.0007 (NP)
472	0.0973 ± 0.0018 (exp.) $^{+0.0038}_{-0.0008}$ (scale) ± 0.0010 (PDF) ± 0.0001 (NP)
522	0.0957 ± 0.0016 (exp.) $^{+0.0034}_{-0.0006}$ (scale) ± 0.0011 (PDF) ± 0.0003 (NP)
604	0.0930 ± 0.0019 (exp.) $^{+0.0035}_{-0.0005}$ (scale) ± 0.0012 (PDF) ± 0.0003 (NP)
810	0.0899 ± 0.0021 (exp.) $^{+0.0031}_{-0.0005}$ (scale) ± 0.0013 (PDF) ± 0.0001 (NP)

that agreement between the data and the theoretical predictions is good. The nuisance parameters for the TEEC fits are generally compatible with zero. One remarkable exception is the nuisance parameter associated to the modelling uncertainty, which deviates by half standard deviation with a very small error bar. This is an indication that these data can be used to further tune MC event generators which model multi-jet production.

Figure 8 compares the data with the theoretical predictions after the fit, i.e. where the fitted values of $\alpha_s(m_Z)$ and the nuisance parameters are already constrained. Table 3 shows the values of α_s evolved from m_Z to the corresponding scale Q using Eq. (5). The appendix includes tables in which the values of $\alpha_s(m_Z)$ obtained from the TEEC fits are extrapolated to different values of Q , given by the averages of kinematical quantities other than $H_{T2}/2$.

11.2 Global TEEC fit

The combination of the previous results is done by considering all the H_{T2} bins into a single, global fit. The result obtained using the NNPDF 3.0 PDF set has the largest PDF uncertainty and thus, in order to be conservative, it is the one quoted as the final value of $\alpha_s(m_Z)$.

The impact of the correlations of the JES uncertainties on the result is studied by considering two additional correlation scenarios, one with stronger and one with weaker correlation

assumptions [63]. From the envelope of these results, an additional uncertainty of 0.0007 is assigned in order to cover this difference.

The results for $\alpha_s(m_Z)$ are summarised in Table 4 for each of the four PDF sets investigated in this analysis

As a result of considering all the data, the experimental uncertainties are reduced with respect to the partial fits. Also, it should be noted that the values of α_s extracted with different PDF sets show good agreement with each other within the PDF uncertainties, and are compatible with the latest world average value $\alpha_s(m_Z) = 0.1181 \pm 0.0011$ [79].

The final result for the TEEC fit is

$$\alpha_s(m_Z) = 0.1162 \pm 0.0011 \text{ (exp.) } ^{+0.0076}_{-0.0061} \text{ (scale)} \\ \pm 0.0018 \text{ (PDF)} \pm 0.0003 \text{ (NP)}.$$

A comparison of the results for α_s from the global and partial fits is shown in Fig. 9. In this figure, the results from previous experiments [41, 76, 80–83, 85, 86] are also shown, together with the world average band [79]. Agreement between this result and the ones from other experiments is very good, even though the experimental uncertainties in this analysis are smaller than in previous measurements in hadron colliders.

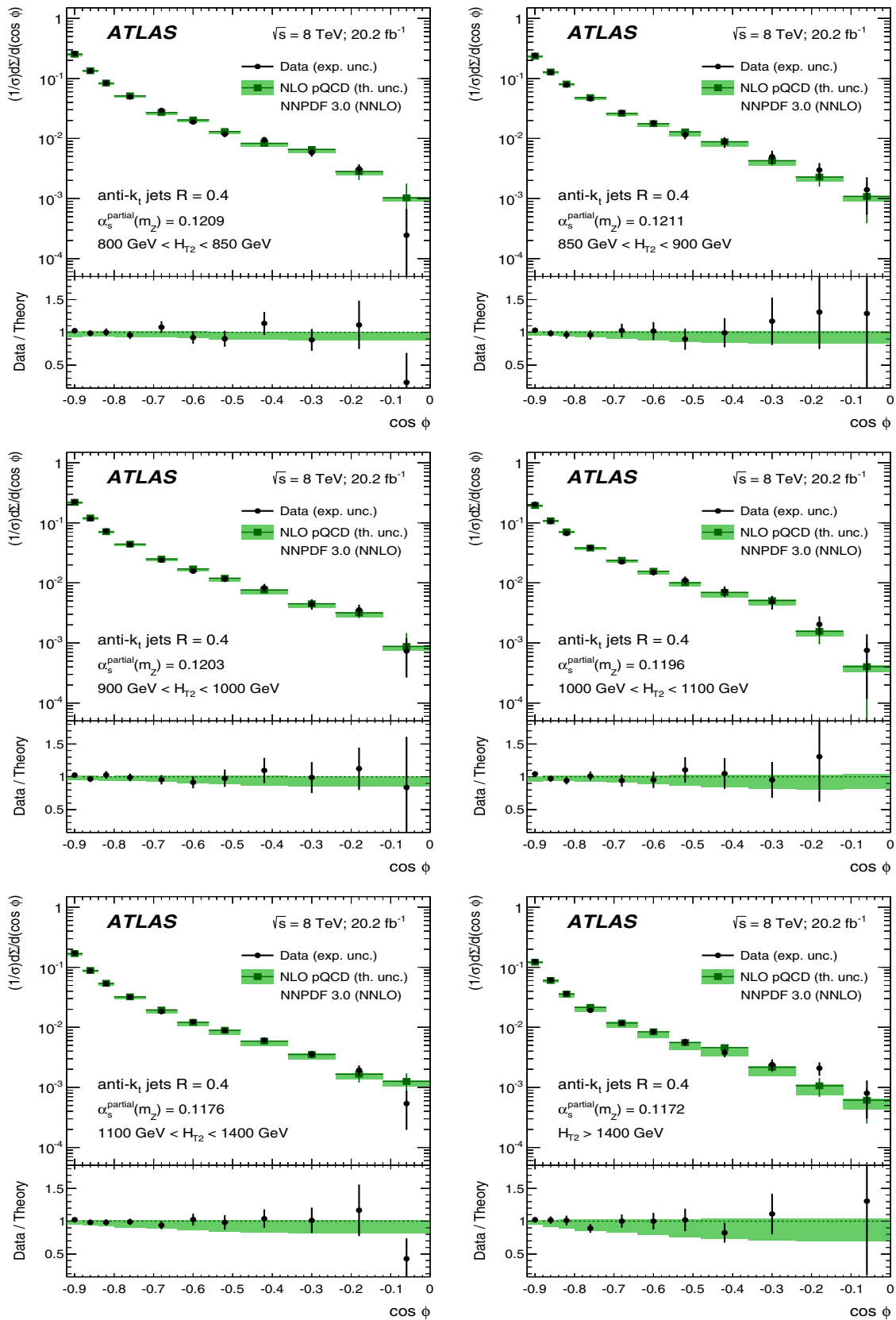


Fig. 10 Comparison of the ATEEC data and the theoretical predictions after the fit. The value of $\alpha_s(m_Z)$ used in this comparison is fitted independently for each energy bin

Table 7 The results for α_s from fits to the ATEEC using different PDFs. The uncertainty referred to as NP is the one related to the non-perturbative corrections. The uncertainty labelled as ‘mod’ corresponds to the HERAPDF modelling and parameterisation uncertainty

PDF	$\alpha_s(m_Z)$ value	χ^2/N_{dof}
MMHT 2014	0.1185 ± 0.0012 (exp.) $^{+0.0047}_{-0.0010}$ (scale) ± 0.0010 (PDF) ± 0.0004 (NP)	57.0/65
CT14	0.1203 ± 0.0013 (exp.) $^{+0.0053}_{-0.0014}$ (scale) ± 0.0015 (PDF) ± 0.0004 (NP)	55.4/65
NNPDF 3.0	0.1196 ± 0.0013 (exp.) $^{+0.0061}_{-0.0013}$ (scale) ± 0.0017 (PDF) ± 0.0004 (NP)	60.3/65
HERAPDF 2.0	0.1206 ± 0.0012 (exp.) $^{+0.0050}_{-0.0014}$ (scale) ± 0.0005 (PDF) ± 0.0002 (NP) ± 0.0007 (mod)	54.2/65

11.3 Fits to individual ATEEC functions

The values of α_s extracted from the fits to the measured ATEEC functions are summarised in Table 5, together with the values of the χ^2 functions at the minima.

The values extracted from the ATEEC show smaller scale uncertainties than their counterpart values from TEEC. This is understood to be due to the fact that the scale dependence is mitigated for the ATEEC distributions because, for the TEEC, this dependence shows some azimuthal symmetry. Also, it is important to note that the values of the χ^2 indicate excellent compatibility between the data and the theoretical predictions. Good agreement, within the scale uncertainty, is also observed between these values and the ones extracted from fits to the TEEC, as well as among themselves and with the current world average. The nuisance parameters are compatible with zero within one standard deviation.

As before, the values of $\alpha_s(Q^2)$ at the scales of the measurement are obtained by evolving the values in Table 5 using Eq. (5). The results are given in Table 6. As in the TEEC case, Fig. 10 compares the data with the theoretical predictions after the fit. The appendix includes tables in which the values of $\alpha_s(m_Z)$ obtained from the ATEEC fits are extrapolated to different values of Q , given by the averages of kinematic quantities other than $H_{T2}/2$.

11.4 Global ATEEC fit

As before, the global value of $\alpha_s(m_Z)$ is obtained from the combined fit of the ATEEC data in the six bins of H_{T2} . Again, the NNPDF 3.0 PDF set is used for the final result as it provides the most conservative choice. Also, as in the TEEC case, two additional correlation scenarios have been considered for the JES uncertainty. An additional uncertainty of 0.0003 is assigned in order to cover the differences.

The results are summarised in Table 7 for the four sets of PDFs considered in the theoretical predictions.

The values shown in Table 7 are in good agreement with the values in Table 4, obtained from fits to the TEEC functions. Also, it is important to note that the scale uncertainty

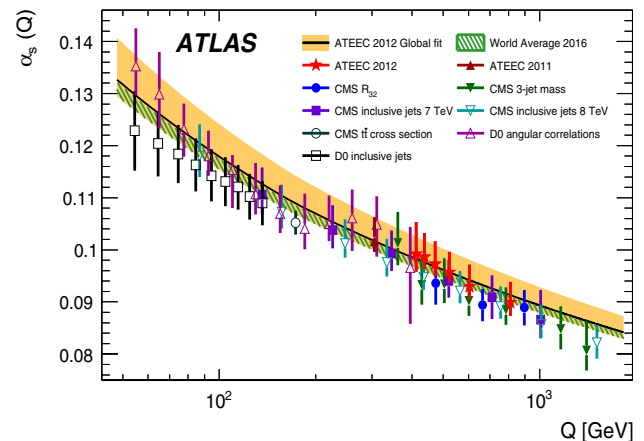


Fig. 11 Comparison of the values of $\alpha_s(Q)$ obtained from fits to the ATEEC functions at the energy scales given by $\langle H_{T2} \rangle / 2$ (red star points) with the uncertainty band from the global fit (orange full band) and the 2016 world average (green hatched band). Determinations from other experiments are also shown as data points. The error bars, as well as the orange full band, include all experimental and theoretical sources of uncertainty. The strong coupling constant is assumed to run according to the two-loop solution of the RGE

is smaller in ATEEC fits than in TEEC fits. The values of the χ^2 function at the minima show excellent agreement between the data and the pQCD predictions.

The final result for the ATEEC fit is

$$\alpha_s(m_Z) = 0.1196 \pm 0.0013 \text{ (exp.) } ^{+0.0061}_{-0.0013} \text{ (scale)} \\ \pm 0.0017 \text{ (PDF)} \pm 0.0004 \text{ (NP)}.$$

The values from Table 6 are compared with previous experimental results from Refs. [41, 76, 80–83, 85, 86] in Fig. 11, showing good compatibility, as well as with the value from the current world average [79].

12 Conclusion

The TEEC and ATEEC functions are measured in 20.2 fb^{-1} of pp collisions at a centre-of-mass energy $\sqrt{s} = 8 \text{ TeV}$ using the ATLAS detector at the LHC. The data, binned in six intervals of the sum of transverse momenta of the two leading jets, $H_{T2} = p_{T1} + p_{T2}$, are corrected for detec-

tor effects and compared to the predictions of perturbative QCD, corrected for hadronisation and multi-parton interaction effects. The results show that the data are compatible with the theoretical predictions, within the uncertainties.

The data are used to determine the strong coupling constant α_s and its evolution with the interaction scale $Q = (p_{T1} + p_{T2})/2$ by means of a χ^2 fit to the theoretical predictions for both TEEC and ATEEC in each energy bin. Additionally, global fits to the TEEC and ATEEC data are performed, leading to

$$\begin{aligned}\alpha_s(m_Z) &= 0.1162 \pm 0.0011 \text{ (exp.) }^{+0.0076}_{-0.0061} \text{ (scale)} \\ &\pm 0.0018 \text{ (PDF)} \pm 0.0003 \text{ (NP)}, \\ \alpha_s(m_Z) &= 0.1196 \pm 0.0013 \text{ (exp.) }^{+0.0061}_{-0.0013} \text{ (scale)} \\ &\pm 0.0017 \text{ (PDF)} \pm 0.0004 \text{ (NP)},\end{aligned}$$

respectively. Conservatively, the values obtained using the NNPDF 3.0 PDF set are chosen, as they provide the largest PDF uncertainty among the four PDF sets investigated. These two values are in good agreement with the determinations in previous experiments and with the current world average $\alpha_s(m_Z) = 0.1181 \pm 0.0011$. The correlation coefficient between the two determinations is $\rho = 0.60$.

The present results are limited by the theoretical scale uncertainties, which amount to 6% of the value of $\alpha_s(m_Z)$ in the case of the TEEC determination and to 4% in the case of the ATEEC. This uncertainty is expected to decrease as higher orders are calculated for the perturbative expansion.

Acknowledgements We thank CERN for the very successful operation of the LHC, as well as the support staff from our institutions without whom ATLAS could not be operated efficiently. We acknowledge the support of ANPCyT, Argentina; YerPhI, Armenia; ARC, Australia; BMWFW and FWF, Austria; ANAS, Azerbaijan; SSTC, Belarus; CNPq and FAPESP, Brazil; NSERC, NRC and CFI, Canada; CERN; CONICYT, Chile; CAS, MOST and NSFC, China; COLCIENCIAS, Colombia; MSMT CR, MPO CR and VSC CR, Czech Republic; DNRF and DNSRC, Denmark; IN2P3-CNRS, CEA-DRF/IRFU, France; SRNSF, Georgia; BMBF, HGF, and MPG, Germany; GSRT, Greece; RGC, Hong Kong SAR, China; ISF, I-CORE

and Benoziyo Center, Israel; INFN, Italy; MEXT and JSPS, Japan; CNRST, Morocco; NWO, Netherlands; RCN, Norway; MNiSW and NCN, Poland; FCT, Portugal; MNE/IFA, Romania; MES of Russia and NRC KI, Russian Federation; JINR; MESTD, Serbia; MSSR, Slovakia; ARRS and MIZŠ, Slovenia; DST/NRF, South Africa; MINECO, Spain; SRC and Wallenberg Foundation, Sweden; SERI, SNSF and Cantons of Bern and Geneva, Switzerland; MOST, Taiwan; TAEK, Turkey; STFC, United Kingdom; DOE and NSF, United States of America. In addition, individual groups and members have received support from BCKDF, the Canada Council, CANARIE, CRC, Compute Canada, FQRNT, and the Ontario Innovation Trust, Canada; EPLANET, ERC, ERDF, FP7, Horizon 2020 and Marie Skłodowska-Curie Actions, European Union; Investissements d'Avenir Labex and Idex, ANR, Région Auvergne and Fondation Partager le Savoir, France; DFG and AvH Foundation, Germany; Herakleitos, Thales and Aristeia programmes co-financed by EU-ESF and the Greek NSRF; BSF, GIF and Minerva, Israel; BRF, Norway; CERCA Programme Generalitat de Catalunya, Generalitat Valenciana, Spain; the Royal Society and Leverhulme Trust, United Kingdom. The crucial computing support from all WLCG partners is acknowledged gratefully, in particular from CERN, the ATLAS Tier-1 facilities at TRIUMF (Canada), NDGF (Denmark, Norway, Sweden), CC-IN2P3 (France), KIT/GridKA (Germany), INFN-CNAF (Italy), NL-T1 (Netherlands), PIC (Spain), ASGC (Taiwan), RAL (UK) and BNL (USA), the Tier-2 facilities worldwide and large non-WLCG resource providers. Major contributors of computing resources are listed in Ref. [87].

Open Access This article is distributed under the terms of the Creative Commons Attribution 4.0 International License (<http://creativecommons.org/licenses/by/4.0/>), which permits unrestricted use, distribution, and reproduction in any medium, provided you give appropriate credit to the original author(s) and the source, provide a link to the Creative Commons license, and indicate if changes were made.

Funded by SCOAP³.

Appendix

This appendix contains tables in which the measured values of $\alpha_s(m_Z)$ are extrapolated to different values of Q from the central results, given by the average p_T of the third jet, $\langle p_{T3} \rangle$, the average value of the three leading jets, $\langle (p_{T1} + p_{T2} + p_{T3}) \rangle / 3$ and the average value of the transverse momentum for each pair of jets (i, j) , $\langle (p_{T1} + p_{T2}) \rangle / 2$ (Tables 8, 9, 10, 11, 12, 13).

Table 8 Values of α_s , obtained from TEEC fits, evolved to the average value of the third-jet transverse momentum in each event, $\langle p_{T3} \rangle$ for each bin in H_{T2}

$\langle p_{T3} \rangle$ (GeV)	$\alpha_s(\langle p_{T3} \rangle)$ value (TEEC, NNPDF 3.0)
169	$0.1072 \pm 0.0017 \text{ (exp.) }^{+0.0067}_{-0.0019} \text{ (scale)} \pm 0.0011 \text{ (PDF)} \pm 0.0001 \text{ (NP)}$
174	$0.1074 \pm 0.0014 \text{ (exp.) }^{+0.0060}_{-0.0014} \text{ (scale)} \pm 0.0012 \text{ (PDF)} \pm 0.0002 \text{ (NP)}$
179	$0.1068 \pm 0.0014 \text{ (exp.) }^{+0.0064}_{-0.0019} \text{ (scale)} \pm 0.0012 \text{ (PDF)} \pm 0.0001 \text{ (NP)}$
186	$0.1052 \pm 0.0014 \text{ (exp.) }^{+0.0054}_{-0.0013} \text{ (scale)} \pm 0.0013 \text{ (PDF)} \pm 0.0001 \text{ (NP)}$
197	$0.1060 \pm 0.0014 \text{ (exp.) }^{+0.0065}_{-0.0018} \text{ (scale)} \pm 0.0014 \text{ (PDF)} \pm 0.0004 \text{ (NP)}$
215	$0.1052 \pm 0.0018 \text{ (exp.) }^{+0.0066}_{-0.0027} \text{ (scale)} \pm 0.0015 \text{ (PDF)} \pm 0.0003 \text{ (NP)}$

Table 9 Values of α_s , obtained from TEEC fits, evolved to the average value of the average transverse momentum of the three leading jets in each event, $\langle(p_{T1} + p_{T2} + p_{T3})/3\rangle$ for each bin in H_{T2}

$\langle H_{T3}/3 \rangle$ (GeV)	$\alpha_s(\langle H_{T3}/3 \rangle)$ value (TEEC, NNPDF 3.0)
289	0.1005 ± 0.0015 (exp.) $^{+0.0059}_{-0.0016}$ (scale) ± 0.0010 (PDF) ± 0.0001 (NP)
307	0.1004 ± 0.0013 (exp.) $^{+0.0052}_{-0.0012}$ (scale) ± 0.0010 (PDF) ± 0.0002 (NP)
332	0.0994 ± 0.0012 (exp.) $^{+0.0055}_{-0.0016}$ (scale) ± 0.0010 (PDF) ± 0.0001 (NP)
366	0.0973 ± 0.0012 (exp.) $^{+0.0046}_{-0.0011}$ (scale) ± 0.0011 (PDF) ± 0.0001 (NP)
423	0.0970 ± 0.0012 (exp.) $^{+0.0054}_{-0.0015}$ (scale) ± 0.0012 (PDF) ± 0.0003 (NP)
564	0.0943 ± 0.0014 (exp.) $^{+0.0053}_{-0.0022}$ (scale) ± 0.0012 (PDF) ± 0.0002 (NP)

Table 10 Values of α_s , obtained from TEEC fits, evolved to the average value of transverse momentum for every pair of jets in each event, $\langle(p_{Ti} + p_{Tj})/2\rangle$ for each bin in H_{T2}

$\langle H_{Tij}/2 \rangle$ (GeV)	$\alpha_s(\langle H_{Tij}/2 \rangle)$ value (TEEC, NNPDF 3.0)
366	0.0979 ± 0.0014 (exp.) $^{+0.0055}_{-0.0015}$ (scale) ± 0.0009 (PDF) ± 0.0001 (NP)
386	0.0978 ± 0.0012 (exp.) $^{+0.0049}_{-0.0012}$ (scale) ± 0.0010 (PDF) ± 0.0002 (NP)
413	0.0969 ± 0.0011 (exp.) $^{+0.0052}_{-0.0016}$ (scale) ± 0.0010 (PDF) ± 0.0001 (NP)
452	0.0951 ± 0.0011 (exp.) $^{+0.0044}_{-0.0011}$ (scale) ± 0.0011 (PDF) ± 0.0001 (NP)
515	0.0949 ± 0.0011 (exp.) $^{+0.0052}_{-0.0014}$ (scale) ± 0.0011 (PDF) ± 0.0003 (NP)
672	0.0925 ± 0.0014 (exp.) $^{+0.0051}_{-0.0021}$ (scale) ± 0.0012 (PDF) ± 0.0002 (NP)

Table 11 Values of α_s , obtained from ATEEC fits, evolved to the average value of the third-jet transverse momentum in each event, $\langle p_{T3} \rangle$ for each bin in H_{T2}

$\langle p_{T3} \rangle$ (GeV)	$\alpha_s(\langle p_{T3} \rangle)$ value (ATEEC, NNPDF 3.0)
169	0.1104 ± 0.0030 (exp.) $^{+0.0070}_{-0.0025}$ (scale) ± 0.0011 (PDF) ± 0.0003 (NP)
174	0.1101 ± 0.0022 (exp.) $^{+0.0052}_{-0.0011}$ (scale) ± 0.0012 (PDF) ± 0.0008 (NP)
179	0.1090 ± 0.0023 (exp.) $^{+0.0049}_{-0.0011}$ (scale) ± 0.0013 (PDF) ± 0.0002 (NP)
186	0.1079 ± 0.0021 (exp.) $^{+0.0044}_{-0.0008}$ (scale) ± 0.0014 (PDF) ± 0.0003 (NP)
197	0.1056 ± 0.0025 (exp.) $^{+0.0046}_{-0.0006}$ (scale) ± 0.0016 (PDF) ± 0.0004 (NP)
215	0.1041 ± 0.0029 (exp.) $^{+0.0042}_{-0.0007}$ (scale) ± 0.0017 (PDF) ± 0.0001 (NP)

Table 12 Values of α_s , obtained from ATEEC fits, evolved to the average value of the average transverse momentum of the three leading jets in each event, $\langle(p_{T1} + p_{T2} + p_{T3})/3\rangle$ for each bin in H_{T2}

$\langle H_{T3}/3 \rangle$ (GeV)	$\alpha_s(\langle H_{T3}/3 \rangle)$ value (ATEEC, NNPDF 3.0)
289	0.1033 ± 0.0026 (exp.) $^{+0.0061}_{-0.0022}$ (scale) ± 0.0009 (PDF) ± 0.0003 (NP)
307	0.1027 ± 0.0019 (exp.) $^{+0.0045}_{-0.0010}$ (scale) ± 0.0011 (PDF) ± 0.0007 (NP)
332	0.1013 ± 0.0019 (exp.) $^{+0.0042}_{-0.0009}$ (scale) ± 0.0011 (PDF) ± 0.0001 (NP)
366	0.0996 ± 0.0017 (exp.) $^{+0.0037}_{-0.0007}$ (scale) ± 0.0012 (PDF) ± 0.0003 (NP)
423	0.0966 ± 0.0021 (exp.) $^{+0.0038}_{-0.0005}$ (scale) ± 0.0013 (PDF) ± 0.0003 (NP)
564	0.0934 ± 0.0023 (exp.) $^{+0.0033}_{-0.0006}$ (scale) ± 0.0014 (PDF) ± 0.0001 (NP)

Table 13 Values of α_s , obtained from ATEEC fits, evolved to the average value of transverse momentum for every pair of jets in each event, $\langle(p_{Ti} + p_{Tj})/2\rangle$ for each bin in H_{T2}

$\langle H_{Tij}/2 \rangle$ (GeV)	$\alpha_s(\langle H_{Tij}/2 \rangle)$ value (ATEEC, NNPDF 3.0)
366	0.1005 ± 0.0025 (exp.) $^{+0.0058}_{-0.0021}$ (scale) ± 0.0009 (PDF) ± 0.0002 (NP)
386	0.1000 ± 0.0018 (exp.) $^{+0.0043}_{-0.0009}$ (scale) ± 0.0010 (PDF) ± 0.0007 (NP)
413	0.0987 ± 0.0018 (exp.) $^{+0.0040}_{-0.0009}$ (scale) ± 0.0010 (PDF) ± 0.0001 (NP)
452	0.0973 ± 0.0017 (exp.) $^{+0.0035}_{-0.0007}$ (scale) ± 0.0011 (PDF) ± 0.0003 (NP)
515	0.0946 ± 0.0020 (exp.) $^{+0.0037}_{-0.0005}$ (scale) ± 0.0013 (PDF) ± 0.0003 (NP)
672	0.0917 ± 0.0022 (exp.) $^{+0.0032}_{-0.0006}$ (scale) ± 0.0013 (PDF) ± 0.0001 (NP)

References

1. PLUTO Collaboration, Ch. Berger et al., Energy dependence of jet measures in e^+e^- annihilation. *Z. Phys. C* **12**, 297 (1982). <https://doi.org/10.1007/BF01557575>
2. TASSO Collaboration, W. Braunschweig et al., Global jet properties at 14–44 GeV center of mass energy in e^+e^- annihilation. *Z. Phys. C* **47**, 187 (1990). <https://doi.org/10.1007/BF01552339>
3. JADE Collaboration, S. Bethke et al., Determination of the strong coupling α_s from hadronic event shapes and NNLO QCD predictions using JADE data. *Eur. Phys. J. C* **64**, 351 (2009). <https://doi.org/10.1140/epjc/s10052-009-1149-1>. arXiv:0810.1389 [hep-ex]
4. OPAL Collaboration, G. Abbiendi et al., Determination of α_s using OPAL hadronic event shapes at $\sqrt{s} = 91$ –209 GeV and resummed NNLO calculations. *Eur. Phys. J. C* **71**, 1733 (2011). <https://doi.org/10.1140/epjc/s10052-011-1733-z>. arXiv:1101.1470 [hep-ex]
5. ALEPH Collaboration, A. Heister et al., Studies of QCD at e^+e^- centre of mass energies between 91 and 209 GeV. *Eur. Phys. J. C* **35**, 457 (2003). <https://doi.org/10.1140/epjc/s2004-01891-4>
6. DELPHI Collaboration, J. Abdallah et al., A study of the energy evolution of event shape distributions and their means with the DELPHI detector at LEP. *Eur. Phys. J. C* **29**, 285 (2003). <https://doi.org/10.1140/epjc/s2003-01198-0>. arXiv:hep-ex/0307048
7. L3 Collaboration, P. Achard et al., Determination of α_s from hadronic event shapes in e^+e^- annihilation at $192 < \sqrt{s} < 208$ GeV. *Phys. Lett. B* **536**, 217 (2002). [https://doi.org/10.1016/S0370-2693\(02\)01814-2](https://doi.org/10.1016/S0370-2693(02)01814-2). arXiv:hep-ex/0206052
8. ZEUS Collaboration, S. Chekanov et al., Measurement of event shapes in deep inelastic scattering at HERA. *Eur. Phys. J. C* **27**, 531 (2003). <https://doi.org/10.1140/epjc/s2003-01148-x>. arXiv:hep-ex/0211040
9. ZEUS Collaboration, S. Chekanov et al., Event shapes in deep inelastic scattering at HERA. *Nucl. Phys. B* **767**, 1 (2007). <https://doi.org/10.1016/j.nuclphysb.2006.05.016>. arXiv:hep-ex/0604032
10. H1 Collaboration, C. Adloff et al., Measurement of event shape variables in deep inelastic e^+e^- scattering. *Phys. Lett. B* **406**, 256 (1997). [https://doi.org/10.1016/S0370-2693\(97\)00754-5](https://doi.org/10.1016/S0370-2693(97)00754-5). arXiv:hep-ex/9706002
11. H1 Collaboration, C. Adloff et al., Investigation of power corrections to event shape variables measured in deep-inelastic scattering. *Eur. Phys. J. C* **14**, 255 (2000). <https://doi.org/10.1007/s100520000344>. arXiv:hep-ex/9912052
12. H1 Collaboration, H. Aktas et al., Measurement of event shape variables in deep-inelastic scattering at HERA. *Eur. Phys. J. C* **46**, 343 (2006). <https://doi.org/10.1140/epjc/s2006-02493-x>. arXiv:hep-ex/0512014
13. CDF Collaboration, T. Aaltonen et al., Measurement of event shapes in proton–antiproton collisions at center-of-mass energy 1.96 TeV. *Phys. Rev. D* **83**, 112007 (2011). <https://doi.org/10.1103/PhysRevD.83.112007>. arXiv:1103.5143 [hep-ex]
14. CMS Collaboration, First measurement of hadronic event shapes in pp collisions at $\sqrt{s} = 7$ TeV. *Phys. Lett. B* **699**, 48 (2011). <https://doi.org/10.1016/j.physletb.2011.03.060>. arXiv:1102.0068 [hep-ex]
15. ATLAS Collaboration, Measurement of event shapes at large momentum transfer with the ATLAS detector in pp collisions at $\sqrt{s} = 7$ TeV. *Eur. Phys. J. C* **72**, 2211 (2012). <https://doi.org/10.1140/epjc/s10052-012-2211-y>. arXiv:1206.2135 [hep-ex]
16. S. Brandt, C. Peyrou, R. Sosnowski, A. Wroblewski, The principal axis of jets—an attempt to analyse high-energy collisions as two-body processes. *Phys. Lett.* **12**, 57 (1964). [https://doi.org/10.1016/0031-9163\(64\)91176-X](https://doi.org/10.1016/0031-9163(64)91176-X)
17. J.D. Bjorken, S.J. Brodsky, Statistical model for electron–positron annihilation into hadrons. *Phys. Rev. D* **1**, 1416 (1970). <https://doi.org/10.1103/PhysRevD.1.1416>
18. C.L. Basham, L.S. Brown, S.D. Ellis, S.T. Love, Energy correlations in electron–positron annihilation: testing quantum chromodynamics. *Phys. Rev. Lett.* **41**, 1585 (1978). <https://doi.org/10.1103/PhysRevLett.41.1585>
19. PLUTO Collaboration, Ch. Berger et al., Energy–energy correlations in e^+e^- annihilation into hadrons. *Phys. Lett. B* **99**, 292 (1981). [https://doi.org/10.1016/0370-2693\(81\)91128-X](https://doi.org/10.1016/0370-2693(81)91128-X)
20. CELLO Collaboration, H.J. Behrend et al., On the model dependence of the determination of the strong coupling constant in second order QCD from e^+e^- annihilation into hadrons. *Phys. Lett. B* **138**, 311 (1984). [https://doi.org/10.1016/0370-2693\(84\)91667-8](https://doi.org/10.1016/0370-2693(84)91667-8)
21. JADE Collaboration, W. Bartel et al., Measurements of energy correlations in $e^+e^- \rightarrow$ hadrons. *Z. Phys. C* **25**, 231 (1984). <https://doi.org/10.1007/BF01547922>
22. TASSO Collaboration, W. Braunschweig et al., A study of energy–energy correlations between 12 and 46.8 GeV c.m. energies. *Z. Phys. C* **36**, 349 (1987). <https://doi.org/10.1007/BF01573928>
23. MARKJ Collaboration, B. Adeva et al., Model-independent second-order determination of the strong-coupling constant α_s . *Phys. Rev. Lett.* **50**, 2051 (1983). <https://doi.org/10.1103/PhysRevLett.50.2051>
24. MARKII Collaboration, D. Schlatter et al., Measurement of energy correlations in $e^+e^- \rightarrow$ hadrons. *Phys. Rev. Lett.* **49**, 521 (1982). <https://doi.org/10.1103/PhysRevLett.49.521>
25. MAC Collaboration, E. Fernández et al., Measurement of energy–energy correlations in $e^+e^- \rightarrow$ hadrons at $\sqrt{s} = 29$ GeV. *Phys. Rev. D* **31**, 2724 (1985). <https://doi.org/10.1103/PhysRevD.31.2724>
26. TOPAZ Collaboration, I. Adachi et al., Measurements of α_s in e^+e^- annihilation at $\sqrt{s} = 53.3$ GeV and 59.5 GeV. *Phys. Lett. B* **227**, 495 (1989). [https://doi.org/10.1016/0370-2693\(89\)90969-6](https://doi.org/10.1016/0370-2693(89)90969-6)
27. ALEPH Collaboration, D. Decamp et al., Measurement of α_s from the structure of particle clusters produced in hadronic Z decays. *Phys. Lett. B* **257**, 479 (1991). [https://doi.org/10.1016/0370-2693\(91\)91926-M](https://doi.org/10.1016/0370-2693(91)91926-M)
28. DELPHI Collaboration, P. Abreu et al., Energy–energy correlations in hadronic final states from Z^0 decays. *Phys. Lett. B* **252**, 149 (1990). [https://doi.org/10.1016/0370-2693\(90\)91097-U](https://doi.org/10.1016/0370-2693(90)91097-U)
29. OPAL Collaboration, M.Z. Akrawy et al., A measurement of energy correlations and a determination of $\alpha_s(M_{Z^0}^2)$ in e^+e^- annihilations at $\sqrt{s} = 91$ GeV. *Phys. Lett. B* **252**, 159 (1990). [https://doi.org/10.1016/0370-2693\(90\)91098-V](https://doi.org/10.1016/0370-2693(90)91098-V)
30. L3 Collaboration, B. Adeva et al., Determination of α_s from energy–energy correlations measured on the Z^0 resonance. *Phys. Lett. B* **257**, 469 (1991). [https://doi.org/10.1016/0370-2693\(91\)91925-L](https://doi.org/10.1016/0370-2693(91)91925-L)
31. SLD Collaboration, K. Abe et al., Measurement of $\alpha_s(M_Z^2)$ from hadronic event observables at the Z^0 resonance. *Phys. Rev. D* **51**, 962 (1995). <https://doi.org/10.1103/PhysRevD.51.962>
32. A. Ali, F. Barreiro, An $\mathcal{O}(\alpha_s)^2$ calculation of energy–energy correlation in e^+e^- annihilation and comparison with experimental data. *Phys. Lett. B* **118**, 155 (1982). [https://doi.org/10.1016/0370-2693\(82\)90621-9](https://doi.org/10.1016/0370-2693(82)90621-9)
33. A. Ali, F. Barreiro, Energy–energy correlations in e^+e^- annihilation. *Nucl. Phys. B* **236**, 269 (1984). [https://doi.org/10.1016/0550-3213\(84\)90536-4](https://doi.org/10.1016/0550-3213(84)90536-4)
34. D.G. Richards, W.J. Stirling, S.D. Ellis, Second order corrections to the energy–energy correlation function in quantum chromodynamics. *Phys. Lett. B* **119**, 193 (1982). [https://doi.org/10.1016/0370-2693\(82\)90275-1](https://doi.org/10.1016/0370-2693(82)90275-1)
35. E.W.N. Glover, M.R. Sutton, The energy–energy correlation function revisited. *Phys. Lett. B* **342**, 375 (1995). [https://doi.org/10.1016/0370-2693\(94\)01354-F](https://doi.org/10.1016/0370-2693(94)01354-F). arXiv:hep-ph/9410234
36. A. Ali, E. Pietarinen, W.J. Stirling, Transverse energy–energy correlations: a test of perturbative QCD for the proton–antiproton

- collider. Phys. Lett. B **141**, 447 (1984). [https://doi.org/10.1016/0370-2693\(84\)90283-1](https://doi.org/10.1016/0370-2693(84)90283-1)
37. A. Ali, F. Barreiro, J. Llorente, W. Wang, Transverse energy–energy correlations in next-to-leading order in α_s at the LHC. Phys. Rev. D **86**, 114017 (2012). <https://doi.org/10.1103/PhysRevD.86.114017>. [arXiv:1205.1689](https://arxiv.org/abs/1205.1689) [hep-ph]
 38. Z. Nagy, Three-jet cross-sections in hadron–hadron collisions at NLO. Phys. Rev. Lett. **88**, 122003 (2002). <https://doi.org/10.1103/PhysRevLett.88.122003>. [arXiv:hep-ph/0110315](https://arxiv.org/abs/hep-ph/0110315)
 39. Z. Nagy, Next-to-leading order calculation of three-jet observables in hadron–hadron collisions. Phys. Rev. D **68**, 094002 (2003). <https://doi.org/10.1103/PhysRevD.68.094002>. [arXiv:hep-ph/0307268](https://arxiv.org/abs/hep-ph/0307268)
 40. G. Altarelli, *The Development of Perturbative QCD* (World Scientific, Singapore, 1994). <https://doi.org/10.1142/9789814354141>
 41. ATLAS Collaboration, Measurement of transverse energy–energy correlations in multi-jet events in pp collisions at $\sqrt{s} = 7$ TeV using the ATLAS detector and determination of the strong coupling constant $\alpha_s(m_Z)$. Phys. Lett. B **750**, 427 (2015). <https://doi.org/10.1016/j.physletb.2015.09.050>. [arXiv:1508.01579](https://arxiv.org/abs/1508.01579) [hep-ex]
 42. D.E. Kaplan, M.D. Schwartz, Constraining light colored particles with event shapes. Phys. Rev. Lett. **101**, 022002 (2008). <https://doi.org/10.1103/PhysRevLett.101.022002>. [arXiv:0804.2477](https://arxiv.org/abs/0804.2477) [hep-ph]
 43. D. Becciolini et al., Constraining new coloured matter from the ratio of 3- to 2-jets cross sections at the LHC. Phys. Rev. D **91**, 015010 (2015). <https://doi.org/10.1103/PhysRevD.91.015010>. [arXiv:1403.7411](https://arxiv.org/abs/1403.7411) [hep-ph]
 44. ATLAS Collaboration, The ATLAS experiment at the CERN large hadron collider. JINST **3**, S08003 (2008). <https://doi.org/10.1088/1748-0221/3/08/S08003>
 45. ATLAS Collaboration, Performance of the ATLAS trigger system in 2010. Eur. Phys. J. C **72**, 1849 (2012). <https://doi.org/10.1140/epjc/s10052-011-1849-1>. [arXiv:1110.1530](https://arxiv.org/abs/1110.1530) [hep-ex]
 46. ATLAS Collaboration, The ATLAS simulation infrastructure. Eur. Phys. J. C **70**, 823 (2010). <https://doi.org/10.1140/epjc/s10052-010-1429-9>. [arXiv:1005.4568](https://arxiv.org/abs/1005.4568) [physics.ins-det]
 47. GEANT4 Collaboration, S. Agostinelli et al., Geant4—a simulation toolkit. Nucl. Instrum. Methods A **506**, 250–303 (2003). [https://doi.org/10.1016/S0168-9002\(03\)01368-8](https://doi.org/10.1016/S0168-9002(03)01368-8)
 48. T. Sjöstrand et al., High-energy-physics event generation with PYTHIA 6.1. Comput. Phys. Commun. **135**, 238 (2001). [https://doi.org/10.1016/S0010-4655\(00\)00236-8](https://doi.org/10.1016/S0010-4655(00)00236-8). [arXiv:hep-ph/0010017](https://arxiv.org/abs/hep-ph/0010017)
 49. H.L. Lai et al., New parton distributions for collider physics. Phys. Rev. D **82**, 074024 (2010). <https://doi.org/10.1103/PhysRevD.82.074024>. [arXiv:1007.2241](https://arxiv.org/abs/1007.2241) [hep-ph]
 50. ATLAS Collaboration, Summary of ATLAS Pythia 8 tunes ATL-PHYS-PUB-2012-003 (2012). <https://cds.cern.ch/record/1474107>
 51. B. Andersson, G. Gustafson, G. Ingelman, T. Sjöstrand, Parton fragmentation and string dynamics. Phys. Rep. **97**, 31 (1983). [https://doi.org/10.1016/0370-1573\(83\)90080-7](https://doi.org/10.1016/0370-1573(83)90080-7)
 52. M. Bahr et al., Herwig++ physics and manual. Eur. Phys. J. C **58**, 639 (2008). <https://doi.org/10.1140/epjc/s10052-008-0798-9>. [arXiv:0803.0883](https://arxiv.org/abs/0803.0883) [hep-ph]
 53. J. Pumplin et al., New generation of parton distributions with uncertainties from global QCD analysis. JHEP **0207**, 012 (2002). <https://doi.org/10.1088/1126-6708/2002/07/012>. [arXiv:hep-ph/0201195](https://arxiv.org/abs/hep-ph/0201195)
 54. S. Gieseke, C. Röhr, A. Sjödmok, Colour reconnections in Herwig++. Eur. Phys. J. C **72**, 2225 (2012). <https://doi.org/10.1140/epjc/s10052-012-2225-5>. [arXiv:1206.0041](https://arxiv.org/abs/1206.0041) [hep-ph]
 55. J.M. Butterworth, J.R. Forshaw, M.H. Seymour, Multiparton interactions in photoproduction at HERA. Z. Phys. C **72**, 637 (1996). <https://doi.org/10.1007/s002880050286>. [arXiv:hep-ph/9601371](https://arxiv.org/abs/hep-ph/9601371)
 56. T. Gleisberg et al., Event generation with SHERPA 1.1. JHEP **0902**, 007 (2008). <https://doi.org/10.1088/1126-6708/2009/02/007>. [arXiv:0811.4622](https://arxiv.org/abs/0811.4622)
 57. S. Catani, F. Krauss, R. Kuhn, B.R. Webber, QCD Matrix elements + parton showers. JHEP **0111**, 063 (2001). <https://doi.org/10.1088/1126-6708/2001/11/063>. [arXiv:hep-ph/0109231](https://arxiv.org/abs/hep-ph/0109231)
 58. M. Cacciari, G.P. Salam, G. Soyez, The anti- k_t jet clustering algorithm. JHEP **063**, 0804 (2008). <https://doi.org/10.1088/1126-6708/2008/04/063>. [arXiv:0802.1189](https://arxiv.org/abs/0802.1189) [hep-ph]
 59. M. Cacciari, G.P. Salam, G. Soyez, FastJet user manual. Eur. Phys. J. C **072**, 1896 (2012). <https://doi.org/10.1140/epjc/s10052-012-1896-2>. [arXiv:1111.6097](https://arxiv.org/abs/1111.6097) [hep-ph]
 60. W. Lampl, et al., Calorimeter clustering algorithms: description and performance ATLAS-LARG-PUB-2008-002 (2008). <http://cds.cern.ch/record/1099735>
 61. C. Issever, K. Borras, D. Wegener, An improved weighting algorithm to achieve software compensation in a fine grained LAr calorimeter. Nucl. Instrum. Methods A **545**, 803 (2005). <https://doi.org/10.1016/j.nima.2005.02.010>. [arXiv:physics/0408129](https://arxiv.org/abs/physics/0408129)
 62. ATLAS Collaboration, Local hadronic calibration ATL-LARG-PUB-2009-001-2 (2009). <http://cds.cern.ch/record/1112035>
 63. ATLAS Collaboration, Jet energy measurement and its systematic uncertainty in proton–proton collisions at $\sqrt{s} = 7$ TeV with the ATLAS detector. Eur. Phys. J. C **75**, 17 (2015). <https://doi.org/10.1140/epjc/s10052-014-3190-y>. [arXiv:1406.0076](https://arxiv.org/abs/1406.0076)
 64. ATLAS Collaboration, Characterisation and mitigation of beam-induced backgrounds observed in the ATLAS detector during the 2011 proton–proton run. JINST **8**, P07004 (2013). <https://doi.org/10.1088/1748-0221/8/07/P07004>. [arXiv:1303.0223](https://arxiv.org/abs/1303.0223) [hep-ex]
 65. ATLAS Collaboration, Measurement of dijet azimuthal decorrelations in pp collisions at $\sqrt{s} = 7$ TeV. Phys. Rev. Lett. **106**, 172002 (2011). <https://doi.org/10.1103/PhysRevLett.106.172002>. [arXiv:1102.2696](https://arxiv.org/abs/1102.2696) [hep-ex]
 66. ATLAS Collaboration, Measurements of jet vetoes and azimuthal decorrelations in dijet events produced in pp collisions at $\sqrt{s} = 7$ TeV using the ATLAS detector. Eur. Phys. J. C **74**, 3117 (2014). <https://doi.org/10.1140/epjc/s10052-014-3117-7>. [arXiv:1407.5756](https://arxiv.org/abs/1407.5756) [hep-ex]
 67. G. D'Agostini, A multidimensional unfolding method based on Bayes' theorem. Nucl. Instrum. Methods A **362**, 487 (1995). [https://doi.org/10.1016/0168-9002\(95\)00274-X](https://doi.org/10.1016/0168-9002(95)00274-X)
 68. T. Adye, Unfolding algorithms and tests using RooUnfold (2011). [arXiv:1105.1160](https://arxiv.org/abs/1105.1160) [physics.data-an]
 69. ATLAS Collaboration, Jet energy resolution in proton–proton collisions at $\sqrt{s} = 7$ TeV recorded in 2010 with the ATLAS detector. Eur. Phys. J. C **73**, 2306 (2013). <https://doi.org/10.1140/epjc/s10052-013-2306-0>. [arXiv:1210.6210](https://arxiv.org/abs/1210.6210) [hep-ex]
 70. L.A. Harland-Lang, A.D. Martin, P. Motylinski, R.S. Thorne, Parton distributions in the LHC era: MMHT 2014 PDFs. Eur. Phys. J. C **75**, 204 (2015). <https://doi.org/10.1140/epjc/s10052-015-3397-6>. [arXiv:1412.3989](https://arxiv.org/abs/1412.3989) [hep-ph]
 71. S. Dulat et al., New parton distribution functions from a global analysis of quantum chromodynamics. Phys. Rev. D **93**, 033006 (2016). <https://doi.org/10.1103/PhysRevD.93.033006>. [arXiv:1506.07443](https://arxiv.org/abs/1506.07443) [hep-ph]
 72. R.D. Ball et al., Parton distributions for the LHC Run II. JHEP **04**, 040 (2015). [https://doi.org/10.1007/JHEP04\(2015\)040](https://doi.org/10.1007/JHEP04(2015)040). [arXiv:1410.8849](https://arxiv.org/abs/1410.8849) [hep-ph]
 73. H1 and ZEUS Collaborations, F.D. Aaron et al., Combined measurement and QCD analysis of the inclusive ep scattering cross sections at HERA. JHEP **01**, 109 (2010). [https://doi.org/10.1007/JHEP01\(2010\)109](https://doi.org/10.1007/JHEP01(2010)109). [arXiv:0911.0884](https://arxiv.org/abs/0911.0884) [hep-ex]
 74. A. Buckley et al., LHAPDF6: parton density access in the LHC precision era. Eur. Phys. J. C **75**, 132 (2015). <https://doi.org/10.1140/epjc/s10052-015-3318-8>. [arXiv:1412.7420](https://arxiv.org/abs/1412.7420) [hep-ph]
 75. F. Maltoni, T. McElmurry, R. Putman, S. Willenbrock, Choosing the factorization scale in perturbative QCD (2007). [arXiv:hep-ph/0703156](https://arxiv.org/abs/hep-ph/0703156)

76. CMS Collaboration, Measurement of the ratio of the inclusive 3-jet cross section to the inclusive 2-jet cross section in pp collisions at $\sqrt{s} = 7$ TeV and first determination of the strong coupling constant in the TeV range. *Eur. Phys. J. C* **73**, 2604 (2013). <https://doi.org/10.1140/epjc/s10052-013-2604-6>. [arXiv:1304.7498](https://arxiv.org/abs/1304.7498) [hep-ex]
77. ATLAS Collaboration, Further ATLAS tunes of PYTHIA 6 and Pythia 8 ATL-PHYS-PUB-2011-014 (2011). <https://cds.cern.ch/record/1400677>
78. R. Corke, T. Sjöstrand, Interleaved parton showers and tuning prospects. *JHEP* **03**, 032 (2011). [https://doi.org/10.1007/JHEP03\(2011\)032](https://doi.org/10.1007/JHEP03(2011)032)
79. C. Patrignani et al. (Particle Data Group), Review of particle physics. *Chin. Phys. C* **40**, 100001 (2016). <https://doi.org/10.1088/1674-1137/40/10/100001>
80. CMS Collaboration, Measurement of the inclusive 3-jet production differential cross section in proton–proton collisions at 7 TeV and determination of the strong coupling constant in the TeV range. *Eur. Phys. J. C* **75**, 186 (2015). <https://doi.org/10.1140/epjc/s10052-015-3376-y>. [arXiv:1412.1633](https://arxiv.org/abs/1412.1633) [hep-ex]
81. CMS Collaboration, Constraints on parton distribution functions and extraction of the strong coupling constant from the inclusive jet cross section in pp collisions at $\sqrt{s} = 7$ TeV. *Eur. Phys. J. C* **75**, 288 (2015). <https://doi.org/10.1140/epjc/s10052-015-3499-1>. [arXiv:1410.6765](https://arxiv.org/abs/1410.6765) [hep-ex]
82. CMS Collaboration, Measurement and QCD analysis of double-differential inclusive jet cross-sections in pp collisions at $\sqrt{s} = 8$ TeV and ratios to 2.76 and 7 TeV. *JHEP* **1703**, 156 (2017). [https://doi.org/10.1007/JHEP03\(2017\)156](https://doi.org/10.1007/JHEP03(2017)156). [arXiv:1609.05331](https://arxiv.org/abs/1609.05331) [hep-ex]
83. CMS Collaboration, Determination of the top-quark pole mass and strong coupling constant from the $t\bar{t}$ production cross section in pp collisions at $\sqrt{s} = 7$ TeV. *Phys. Lett. B* **728**, 496 (2013). <https://doi.org/10.1016/j.physletb.2013.12.009>. <https://doi.org/10.1016/j.physletb.2014.08.040>. [arXiv:1307.1907](https://arxiv.org/abs/1307.1907) [hep-ex]
84. B. Malaescu, P. Starovoitov, Evaluation of the strong coupling constant α_s using the ATLAS inclusive jet cross-section data. *Eur. Phys. J. C* **72**, 2041 (2012). <https://doi.org/10.1140/epjc/s10052-012-2041-y>. [arXiv:1203.5416](https://arxiv.org/abs/1203.5416) [hep-ph]
85. D0 Collaboration, V.M. Abazov et al., Measurement of angular correlations of jets at $\sqrt{s} = 1.96$ TeV and determination of the strong coupling at high momentum transfers. *Phys. Lett. B* **718**, 56 (2012). <https://doi.org/10.1016/j.physletb.2012.10.003>. [arXiv:1207.4957](https://arxiv.org/abs/1207.4957) [hep-ex]
86. D0 Collaboration, V.M. Abazov et al., Determination of the strong coupling constant from the inclusive jet cross section in $p\bar{p}$ collisions at $\sqrt{s} = 1.96$ TeV. *Phys. Rev. D* **80**, 111107 (2009). <https://doi.org/10.1103/PhysRevD.80.111107>. [arXiv:0911.2710](https://arxiv.org/abs/0911.2710) [hep-ex]
87. ATLAS Collaboration, ATL-GEN-PUB-2016-002 ATLAS Computing Acknowledgements 2016–2017. <https://cds.cern.ch/record/2202407>

ATLAS Collaboration

M. Aaboud^{137d}, G. Aad⁸⁸, B. Abbott¹¹⁵, J. Abdallah⁸, O. Abdinov^{12,*}, B. Abeloos¹¹⁹, S. H. Abidi¹⁶¹, O. S. AbouZeid¹³⁹, N. L. Abraham¹⁵¹, H. Abramowicz¹⁵⁵, H. Abreu¹⁵⁴, R. Abreu¹¹⁸, Y. Abulaiti^{148a,148b}, B. S. Acharya^{167a,167b,a}, S. Adachi¹⁵⁷, L. Adamczyk^{41a}, J. Adelman¹¹⁰, M. Adersberger¹⁰², T. Adye¹³³, A. A. Affolder¹³⁹, T. Agatonovic-Jovin¹⁴, C. Agheorghiesei^{28c}, J. A. Aguilar-Saavedra^{128a,128f}, S. P. Ahlen²⁴, F. Ahmadov^{68,b}, G. Aielli^{135a,135b}, S. Akatsuka⁷¹, H. Akerstedt^{148a,148b}, T. P. A. Åkesson⁸⁴, E. Akilli⁵², A. V. Akimov⁹⁸, G. L. Alberghi^{22a,22b}, J. Albert¹⁷², P. Albicocco⁵⁰, M. J. Alconada Verzini⁷⁴, M. Aleksa³², I. N. Aleksandrov⁶⁸, C. Alexa^{28b}, G. Alexander¹⁵⁵, T. Alexopoulos¹⁰, M. Alhroob¹¹⁵, B. Ali¹³⁰, M. Aliev^{76a,76b}, G. Alimonti^{94a}, J. Alison³³, S. P. Alkire³⁸, B. M. M. Allbrooke¹⁵¹, B. W. Allen¹¹⁸, P. P. Allport¹⁹, A. Aloisio^{106a,106b}, A. Alonso³⁹, F. Alonso⁷⁴, C. Alpigiani¹⁴⁰, A. A. Alshehri⁵⁶, M. I. Alstaty⁸⁸, B. Alvarez Gonzalez³², D. Álvarez Piqueras¹⁷⁰, M. G. Alviggi^{106a,106b}, B. T. Amadio¹⁶, Y. Amaral Coutinho^{26a}, C. Amelung²⁵, D. Amidei⁹², S. P. Amor Dos Santos^{128a,128c}, A. Amorim^{128a,128b}, S. Amoroso³², G. Amundsen²⁵, C. Anastopoulos¹⁴¹, L. S. Ancu⁵², N. Andari¹⁹, T. Andeen¹¹, C. F. Anders^{60b}, J. K. Anders⁷⁷, K. J. Anderson³³, A. Andreazza^{94a,94b}, V. Andrei^{60a}, S. Angelidakis⁹, I. Angelozzi¹⁰⁹, A. Angerami³⁸, A. V. Anisenkov^{111,c}, N. Anjos¹³, A. Annovi^{126a,126b}, C. Antel^{60a}, M. Antonelli⁵⁰, A. Antonov^{100,*}, D. J. Antrim¹⁶⁶, F. Anulli^{134a}, M. Aoki⁶⁹, L. Aperio Bella³², G. Arabidze⁹³, Y. Arai⁶⁹, J. P. Araque^{128a}, V. Araujo Ferraz^{26a}, A. T. H. Arce⁴⁸, R. E. Ardell⁸⁰, F. A. Arduh⁷⁴, J-F. Arguin⁹⁷, S. Argyropoulos⁶⁶, M. Arik^{20a}, A. J. Armbruster³², L. J. Armitage⁷⁹, O. Arnaez¹⁶¹, H. Arnold⁵¹, M. Arratia³⁰, O. Arslan²³, A. Artamonov⁹⁹, G. Artoni¹²², S. Artz⁸⁶, S. Asai¹⁵⁷, N. Asbah⁴⁵, A. Ashkenazi¹⁵⁵, L. Asquith¹⁵¹, K. Assamagan²⁷, R. Astalos^{146a}, M. Atkinson¹⁶⁹, N. B. Atlay¹⁴³, K. Augsten¹³⁰, G. Avolio³², B. Axen¹⁶, M. K. Ayoub¹¹⁹, G. Azuelos^{97,d}, A. E. Baas^{60a}, M. J. Baca¹⁹, H. Bachacou¹³⁸, K. Bachas^{76a,76b}, M. Backes¹²², M. Backhaus³², P. Bagnaia^{134a,134b}, H. Bahrasemani¹⁴⁴, J. T. Baines¹³³, M. Bajic³⁹, O. K. Baker¹⁷⁹, E. M. Baldwin^{111,c}, P. Balek¹⁷⁵, F. Balli¹³⁸, W. K. Balunas¹²⁴, E. Banas⁴², Sw. Banerjee^{176,e}, A. A. E. Bannoura¹⁷⁸, L. Barak³², E. L. Barberio⁹¹, D. Barberis^{53a,53b}, M. Barbero⁸⁸, T. Barillari¹⁰³, M-S. Barisits³², J. T. Barkeloo¹¹⁸, T. Barklow¹⁴⁵, N. Barlow³⁰, S. L. Barnes^{36c}, B. M. Barnett¹³³, R. M. Barnett¹⁶, Z. Barnovska-Blenessy^{36a}, A. Baroncelli^{136a}, G. Barone²⁵, A. J. Barr¹²², L. Barranco Navarro¹⁷⁰, F. Barreiro⁸⁵, J. Barreiro Guimarães da Costa^{35a}, R. Bartoldus¹⁴⁵, A. E. Barton⁷⁵, P. Bartos^{146a}, A. Basalaev¹²⁵, A. Bassalat^{119,f}, R. L. Bates⁵⁶, S. J. Batista¹⁶¹, J. R. Batley³⁰, M. Battaglia¹³⁹, M. Bause^{134a,134b}, F. Bauer¹³⁸, H. S. Bawa^{145,g}, J. B. Beacham¹¹³, M. D. Beattie⁷⁵, T. Beau⁸³, P. H. Beauchemin¹⁶⁵, P. Bechtel²³, H. P. Beck^{18,h}, K. Becker¹²², M. Becker⁸⁶, M. Beckingham¹⁷³, C. Becot¹¹², A. J. Beddall^{20d}, A. Beddall^{20b}, V. A. Bednyakov⁶⁸, M. Bedognetti¹⁰⁹, C. P. Bee¹⁵⁰, T. A. Beermann³², M. Begalli^{26a}, M. Begel²⁷, J. K. Behr⁴⁵,

- A. S. Bell⁸¹, G. Bella¹⁵⁵, L. Bellagamba^{22a}, A. Bellerive³¹, M. Bellomo¹⁵⁴, K. Belotskiy¹⁰⁰, O. Beltramello³², N. L. Belyaev¹⁰⁰, O. Benary^{155,*}, D. Bencheikroun^{137a}, M. Bender¹⁰², K. Bendtz^{148a,148b}, N. Benekos¹⁰, Y. Benhammou¹⁵⁵, E. Benhar Noccioli¹⁷⁹, J. Benitez⁶⁶, D. P. Benjamin⁴⁸, M. Benoit⁵², J. R. Bensinger²⁵, S. Bentvelsen¹⁰⁹, L. Beresford¹²², M. Beretta⁵⁰, D. Berge¹⁰⁹, E. Bergeaas Kuutmann¹⁶⁸, N. Berger⁵, J. Beringer¹⁶, S. Berlendis⁵⁸, N. R. Bernard⁸⁹, G. Bernardi⁸³, C. Bernius¹⁴⁵, F. U. Bernlochner²³, T. Berry⁸⁰, P. Berta¹³¹, C. Bertella^{35a}, G. Bertoli^{148a,148b}, F. Bertolucci^{126a,126b}, I. A. Bertram⁷⁵, C. Bertsche⁴⁵, D. Bertsche¹¹⁵, G. J. Besjes³⁹, O. Bessidskaia Bylund^{148a,148b}, M. Bessner⁴⁵, N. Besson¹³⁸, C. Betancourt⁵¹, A. Bethani⁸⁷, S. Bethke¹⁰³, A. J. Bevan⁷⁹, J. Beyer¹⁰³, R. M. Bianchi¹²⁷, O. Biebel¹⁰², D. Biedermann¹⁷, R. Bielski⁸⁷, N. V. Biesuz^{126a,126b}, M. Biglietti^{136a}, J. Bilbao De Mendizabal⁵², T. R. V. Billoud⁹⁷, H. Bilokon⁵⁰, M. Bindi⁵⁷, A. Bingul^{20b}, C. Bini^{134a,134b}, S. Biondi^{22a,22b}, T. Bisanz⁵⁷, C. Bittrich⁴⁷, D. M. Bjergaard⁴⁸, C. W. Black¹⁵², J. E. Black¹⁴⁵, K. M. Black²⁴, R. E. Blair⁶, T. Blazek^{146a}, I. Bloch⁴⁵, C. Blocker²⁵, A. Blue⁵⁶, W. Blum^{86,*}, U. Blumenschein⁷⁹, S. Blunier^{34a}, G. J. Bobbink¹⁰⁹, V. S. Bobrovnikov^{111,c}, S. S. Bocchetta⁸⁴, A. Bocci⁴⁸, C. Bock¹⁰², M. Boehler⁵¹, D. Boerner¹⁷⁸, D. Bogavac¹⁰², A. G. Bogdanchikov¹¹¹, C. Bohm^{148a}, V. Boisvert⁸⁰, P. Bokan^{168,i}, T. Bold^{41a}, A. S. Boldyrev¹⁰¹, A. E. Bolz^{60b}, M. Bomben⁸³, M. Bona⁷⁹, M. Boonekamp¹³⁸, A. Borisov¹³², G. Borissov⁷⁵, J. Bortfeldt², D. Bortoletto¹²², V. Bortolotto^{62a,62b,62c}, D. Boscherini^{22a}, M. Bosman¹³, J. D. Bossio Sola²⁹, J. Boudreau¹²⁷, J. Bouffard², E. V. Bouhova-Thacker⁷⁵, D. Boumedienne³⁷, C. Bourdarios¹¹⁹, S. K. Boutle⁵⁶, A. Boveia¹¹³, J. Boyd³², I. R. Boyko⁶⁸, J. Bracinik¹⁹, A. Brandt⁸, G. Brandt⁵⁷, O. Brandt^{60a}, U. Bratzler¹⁵⁸, B. Brau⁸⁹, J. E. Brau¹¹⁸, W. D. Breaden Madden⁵⁶, K. Brendlinger⁴⁵, A. J. Brennan⁹¹, L. Brenner¹⁰⁹, R. Brenner¹⁶⁸, S. Bressler¹⁷⁵, D. L. Briglin¹⁹, T. M. Bristow⁴⁹, D. Britton⁵⁶, D. Britzger⁴⁵, F. M. Brochu³⁰, I. Brock²³, R. Brock⁹³, G. Brooijmans³⁸, T. Brooks⁸⁰, W. K. Brooks^{34b}, J. Brosamer¹⁶, E. Brost¹¹⁰, J. H. Broughton¹⁹, P. A. Bruckman de Renstrom⁴², D. Bruncko^{146b}, A. Bruni^{22a}, G. Bruni^{22a}, L. S. Bruni¹⁰⁹, B. H. Brunt³⁰, M. Bruschi^{22a}, N. Bruscino²³, P. Bryant³³, L. Bryngemark⁴⁵, T. Buane¹⁵, Q. Buat¹⁴⁴, P. Buchholz¹⁴³, A. G. Buckley⁵⁶, I. A. Budagov⁶⁸, F. Buehrer⁵¹, M. K. Bugge¹²¹, O. Bulekov¹⁰⁰, D. Bullock⁸, T. J. Burch¹¹⁰, S. Burdin⁷⁷, C. D. Burgard⁵¹, A. M. Burger⁵, B. Burghgrave¹¹⁰, K. Burka⁴², S. Burke¹³³, I. Burmeister⁴⁶, J. T. P. Burr¹²², E. Busato³⁷, D. Büscher⁵¹, V. Büscher⁸⁶, P. Bussey⁵⁶, J. M. Butler²⁴, C. M. Buttar⁵⁶, J. M. Butterworth⁸¹, P. Butti³², W. Buttinger²⁷, A. Buzatu^{35c}, A. R. Buzykaev^{111,c}, S. Cabrera Urbán¹⁷⁰, D. Caforio¹³⁰, V. M. Cairo^{40a,40b}, O. Cakir^{4a}, N. Calace⁵², P. Calafiura¹⁶, A. Calandri⁸⁸, G. Calderini⁸³, P. Calfayan⁶⁴, G. Callea^{40a,40b}, L. P. Caloba^{26a}, S. Calvente Lopez⁸⁵, D. Calvet³⁷, S. Calvet³⁷, T. P. Calvet⁸⁸, R. Camacho Toro³³, S. Camarda³², P. Camarri^{135a,135b}, D. Cameron¹²¹, R. Caminal Armadans¹⁶⁹, C. Camincher⁵⁸, S. Campana³², M. Campanelli⁸¹, A. Camplani^{94a,94b}, A. Campoverde¹⁴³, V. Canale^{106a,106b}, M. Cano Bret^{36c}, J. Cantero¹¹⁶, T. Cao¹⁵⁵, M. D. M. Capeans Garrido³², I. Caprini^{28b}, M. Caprini^{28b}, M. Capua^{40a,40b}, R. M. Carbone³⁸, R. Cardarelli^{135a}, F. Cardillo⁵¹, I. Carli¹³¹, T. Carli³², G. Carlino^{106a}, B. T. Carlson¹²⁷, L. Carminati^{94a,94b}, R. M. D. Carney^{148a,148b}, S. Caron¹⁰⁸, E. Carquin^{34b}, S. Carrá^{94a,94b}, G. D. Carrillo-Montoya³², J. Carvalho^{128a,128c}, D. Casadei¹⁹, M. P. Casado^{13,j}, M. Casolino¹³, D. W. Casper¹⁶⁶, R. Castelijns¹⁰⁹, V. Castillo Gimenez¹⁷⁰, N. F. Castro^{128a,k}, A. Catinaccio³², J. R. Catmore¹²¹, A. Cattai³², J. Caudron²³, V. Cavaliere¹⁶⁹, E. Cavallaro¹³, D. Cavalli^{94a}, M. Cavalli-Sforza¹³, V. Cavasinni^{126a,126b}, E. Celebi^{20a}, F. Ceradini^{136a,136b}, L. Cerda Alberich¹⁷⁰, A. S. Cerqueira^{26b}, A. Cerri¹⁵¹, L. Cerrito^{135a,135b}, F. Cerutti¹⁶, A. Cervelli¹⁸, S. A. Cetin^{20c}, A. Chafaq^{137a}, D. Chakraborty¹¹⁰, S. K. Chan⁵⁹, W. S. Chan¹⁰⁹, Y. L. Chan^{62a}, P. Chang¹⁶⁹, J. D. Chapman³⁰, D. G. Charlton¹⁹, C. C. Chau¹⁶¹, C. A. Chavez Barajas¹⁵¹, S. Che¹¹³, S. Cheatham^{167a,167c}, A. Chegwidden⁹³, S. Chekanov⁶, S. V. Chekulaev^{163a}, G. A. Chelkov^{68,l}, M. A. Chelstowska³², C. Chen⁶⁷, H. Chen²⁷, S. Chen^{35b}, S. Chen¹⁵⁷, X. Chen^{35c,m}, Y. Chen⁷⁰, H. C. Cheng⁹², H. J. Cheng^{35a}, A. Cheplakov⁶⁸, E. Cheremushkina¹³², R. Cherkaoui El Moursli^{137e}, V. Chernyatin^{27,*}, E. Cheu⁷, K. Cheung⁶³, L. Chevalier¹³⁸, V. Chiarella⁵⁰, G. Chiarelli^{126a,126b}, G. Chiodini^{76a}, A. S. Chisholm³², A. Chitan^{28b}, Y. H. Chiu¹⁷², M. V. Chizhov⁶⁸, K. Choi⁶⁴, A. R. Chomont³⁷, S. Chouridou¹⁵⁶, V. Christodoulou⁸¹, D. Chromek-Burckhart³², M. C. Chu^{62a}, J. Chudoba¹²⁹, A. J. Chuinard⁹⁰, J. J. Chwastowski⁴², L. Chytka¹¹⁷, A. K. Ciftci^{4a}, D. Cinca⁴⁶, V. Cindro⁷⁸, I. A. Cioara²³, C. Ciocca^{22a,22b}, A. Ciochio¹⁶, F. Ciotto^{106a,106b}, Z. H. Citron¹⁷⁵, M. Citterio^{94a}, M. Ciubancan^{28b}, A. Clark⁵², B. L. Clark⁵⁹, M. R. Clark³⁸, P. J. Clark⁴⁹, R. N. Clarke¹⁶, C. Clement^{148a,148b}, Y. Coadou⁸⁸, M. Cobal^{167a,167c}, A. Coccaro⁵², J. Cochran⁶⁷, L. Colasurdo¹⁰⁸, B. Cole³⁸, A. P. Colijn¹⁰⁹, J. Collot⁵⁸, T. Colombo¹⁶⁶, P. Conde Muino^{128a,128b}, E. Coniavitis⁵¹, S. H. Connell^{147b}, I. A. Connelly⁸⁷, S. Constantinescu^{28b}, G. Conti³², F. Conventi^{106a,n}, M. Cooke¹⁶, A. M. Cooper-Sarkar¹²², F. Cormier¹⁷¹, K. J. R. Cormier¹⁶¹, M. Corradi^{134a,134b}, F. Corriveau^{90,o}, A. Cortes-Gonzalez³², G. Cortiana¹⁰³, G. Costa^{94a}, M. J. Costa¹⁷⁰, D. Costanzo¹⁴¹, G. Cottin³⁰, G. Cowan⁸⁰, B. E. Cox⁸⁷, K. Cranmer¹¹², S. J. Crawley⁵⁶, R. A. Creager¹²⁴, G. Cree³¹, S. Crépe-Renaudin⁵⁸, F. Crescioli⁸³, W. A. Cribbs^{148a,148b}, M. Cristinziani²³, V. Croft¹⁰⁸, G. Crosetti^{40a,40b}, A. Cueto⁸⁵, T. Cuhadar Donszelmann¹⁴¹

- A. R. Cukierman¹⁴⁵, J. Cummings¹⁷⁹, M. Curatolo⁵⁰, J. Cúth⁸⁶, H. Czirr¹⁴³, P. Czodrowski³², G. D'amen^{22a,22b}, S. D'Auria⁵⁶, L. D'eraimo⁸³, M. D'Onofrio⁷⁷, M. J. Da Cunha Sargedas De Sousa^{128a,128b}, C. Da Via⁸⁷, W. Dabrowski^{41a}, T. Dado^{146a}, T. Dai⁹², O. Dale¹⁵, F. Dallaire⁹⁷, C. Dallapiccola⁸⁹, M. Dam³⁹, J. R. Dandoy¹²⁴, M. F. Daneri²⁹, N. P. Dang¹⁷⁶, A. C. Daniells¹⁹, N. S. Dann⁸⁷, M. Danninger¹⁷¹, M. Dano Hoffmann¹³⁸, V. Dao¹⁵⁰, G. Darbo^{53a}, S. Darmora⁸, J. Dassoulas³, A. Dattagupta¹¹⁸, T. Daubney⁴⁵, W. Davey²³, C. David⁴⁵, T. Davidek¹³¹, M. Davies¹⁵⁵, D. R. Davis⁴⁸, P. Davison⁸¹, E. Dawe⁹¹, I. Dawson¹⁴¹, K. De⁸, R. de Asmundis^{106a}, A. De Benedetti¹¹⁵, S. De Castro^{22a,22b}, S. De Cecco⁸³, N. De Groot¹⁰⁸, P. de Jong¹⁰⁹, H. De la Torre⁹³, F. De Lorenzi⁶⁷, A. De Maria⁵⁷, D. De Pedis^{134a}, A. De Salvo^{134a}, U. De Sanctis^{135a,135b}, A. De Santo¹⁵¹, K. De Vasconcelos Corga⁸⁸, J. B. De Vivie De Regie¹¹⁹, W. J. Dearnaley⁷⁵, R. Debbe²⁷, C. Debenedetti¹³⁹, D. V. Dedovich⁶⁸, N. Dehghanian³, I. Deigaard¹⁰⁹, M. Del Gaudio^{40a,40b}, J. Del Peso⁸⁵, T. Del Prete^{126a,126b}, D. Delgove¹¹⁹, F. Deliot¹³⁸, C. M. Delitzsch⁵², A. Dell'Acqua³², L. Dell'Asta²⁴, M. Dell'Orso^{126a,126b}, M. Della Pietra^{106a,106b}, D. della Volpe⁵², M. Delmastro⁵, C. Delporte¹¹⁹, P. A. Delsart⁵⁸, D. A. DeMarco¹⁶¹, S. Demers¹⁷⁹, M. Demichev⁶⁸, A. Demilly⁸³, S. P. Denisov¹³², D. Denysiuk¹³⁸, D. Derendarz⁴², J. E. Derkaoui^{137d}, F. Derue⁸³, P. Dervan⁷⁷, K. Desch²³, C. Deterre⁴⁵, K. Dette⁴⁶, M. R. Devesa²⁹, P. O. Deviveiros³², A. Dewhurst¹³³, S. Dhaliwal²⁵, F. A. Di Bello⁵², A. Di Ciaccio^{135a,135b}, L. Di Ciaccio⁵, W. K. Di Clemente¹²⁴, C. Di Donato^{106a,106b}, A. Di Girolamo³², B. Di Girolamo³², B. Di Micco^{136a,136b}, R. Di Nardo³², K. F. Di Petrillo⁵⁹, A. Di Simone⁵¹, R. Di Sipio¹⁶¹, D. Di Valentino³¹, C. Diaconu⁸⁸, M. Diamond¹⁶¹, F. A. Dias³⁹, M. A. Diaz^{34a}, E. B. Diehl⁹², J. Dietrich¹⁷, S. Díez Cornell⁴⁵, A. Dimitrievska¹⁴, J. Dingfelder²³, P. Dita^{28b}, S. Dita^{28b}, F. Dittus³², F. Djama⁸⁸, T. Djobava^{54b}, J. I. Djuvsland^{60a}, M. A. B. do Vale^{26c}, D. Dobos³², M. Dobre^{28b}, C. Doglioni⁸⁴, J. Dolejsi¹³¹, Z. Dolezal¹³¹, M. Donadelli^{26d}, S. Donati^{126a,126b}, P. Dondero^{123a,123b}, J. Donini³⁷, J. Dopke¹³³, A. Doria^{106a}, M. T. Dova⁷⁴, A. T. Doyle⁵⁶, E. Drechsler⁵⁷, M. Dris¹⁰, Y. Du^{36b}, J. Duarte-Camperros¹⁵⁵, A. Dubreuil⁵², E. Duchovni¹⁷⁵, G. Duckeck¹⁰², A. Ducourthial⁸³, O. A. Ducu^{97p}, D. Duda¹⁰⁹, A. Dudarev³², A. Chr. Dudder⁸⁶, E. M. Duffield¹⁶, L. Duflo¹¹⁹, M. Dührssen³², M. Dumancic¹⁷⁵, A. E. Dumitriu^{28b}, A. K. Duncan⁵⁶, M. Dunford^{60a}, H. Duran Yildiz^{4a}, M. Düren⁵⁵, A. Durglishvili^{54b}, D. Duschinger⁴⁷, B. Dutta⁴⁵, M. Dyndal⁴⁵, B. S. Dziedzic⁴², C. Eckardt⁴⁵, K. M. Ecker¹⁰³, R. C. Edgar⁹², T. Eifert³², G. Eigen¹⁵, K. Einsweiler¹⁶, T. Ekelof¹⁶⁸, M. El Kacimi^{137c}, R. El Kosseifi⁸⁸, V. Ellajosyula⁸⁸, M. Ellert¹⁶⁸, S. Elles⁵, F. Ellinghaus¹⁷⁸, A. A. Elliot¹⁷², N. Ellis³², J. Elmsheuser²⁷, M. Elsing³², D. Emeliyanov¹³³, Y. Enari¹⁵⁷, O. C. Endner⁸⁶, J. S. Ennis¹⁷³, J. Erdmann⁴⁶, A. Ereditato¹⁸, G. Ernis¹⁷⁸, M. Ernst²⁷, S. Errede¹⁶⁹, M. Escalier¹¹⁹, C. Escobar¹⁷⁰, B. Esposito⁵⁰, O. Estrada Pastor¹⁷⁰, A. I. Etiennevre¹³⁸, E. Etzion¹⁵⁵, H. Evans⁶⁴, A. Ezhilov¹²⁵, M. Ezzi^{137e}, F. Fabbri^{22a,22b}, L. Fabbri^{22a,22b}, V. Fabiani¹⁰⁸, G. Facini³³, R. M. Fakhruddinov¹³², S. Falciano^{134a}, R. J. Falla⁸¹, J. Faltova³², Y. Fang^{35a}, M. Fanti^{94a,94b}, A. Farbin⁸, A. Farilla^{136a}, C. Farina¹²⁷, E. M. Farina^{123a,123b}, T. Farooque⁹³, S. Farrell¹⁶, S. M. Farrington¹⁷³, P. Farthouat³², F. Fassi^{137e}, P. Fassnacht³², D. Fassoulitis⁹, M. Faucci Giannelli⁸⁰, A. Favareto^{53a,53b}, W. J. Fawcett¹²², L. Fayard¹¹⁹, O. L. Fedin^{125q}, W. Fedorko¹⁷¹, S. Feigl¹²¹, L. Feligioni⁸⁸, C. Feng^{36b}, E. J. Feng³², H. Feng⁹², M. J. Fenton⁵⁶, A. B. Fenyuk¹³², L. Feremenga⁸, P. Fernandez Martinez¹⁷⁰, S. Fernandez Perez¹³, J. Ferrando⁴⁵, A. Ferrari¹⁶⁸, P. Ferrari¹⁰⁹, R. Ferrari^{123a}, D. E. Ferreira de Lima^{60b}, A. Ferrer¹⁷⁰, D. Ferrere⁵², C. Ferretti⁹², F. Fiedler⁸⁶, A. Filipčič⁷⁸, M. Filipuzzi⁴⁵, F. Filthaut¹⁰⁸, M. Fincke-Keeler¹⁷², K. D. Finelli¹⁵², M. C. N. Fiolhais^{128a,128c,r}, L. Fiorini¹⁷⁰, A. Fischer², C. Fischer¹³, J. Fischer¹⁷⁸, W. C. Fisher⁹³, N. Flaschel⁴⁵, I. Fleck¹⁴³, P. Fleischmann⁹², R. R. M. Fletcher¹²⁴, T. Flick¹⁷⁸, B. M. Flierl¹⁰², L. R. Flores Castillo^{62a}, M. J. Flowerdew¹⁰³, G. T. Forcolin⁸⁷, A. Formica¹³⁸, F. A. Förster¹³, A. Forti⁸⁷, A. G. Foster¹⁹, D. Fournier¹¹⁹, H. Fox⁷⁵, S. Fracchia¹⁴¹, P. Francavilla⁸³, M. Franchini^{22a,22b}, S. Franchino^{60a}, D. Francis³², L. Franconi¹²¹, M. Franklin⁵⁹, M. Frate¹⁶⁶, M. Fraternali^{123a,123b}, D. Freeborn⁸¹, S. M. Fressard-Batraneanu³², B. Freund⁹⁷, D. Froidevaux³², J. A. Frost¹²², C. Fukunaga¹⁵⁸, T. Fusayasu¹⁰⁴, J. Fuster¹⁷⁰, C. Gabaldon⁵⁸, O. Gabizon¹⁵⁴, A. Gabrielli^{22a,22b}, A. Gabrielli¹⁶, G. P. Gach^{41a}, S. Gadatsch³², S. Gadomski⁸⁰, G. Gagliardi^{53a,53b}, L. G. Gagnon⁹⁷, C. Galea¹⁰⁸, B. Galhardo^{128a,128c}, E. J. Gallas¹²², B. J. Gallop¹³³, P. Gallus¹³⁰, G. Galster³⁹, K. K. Gan¹¹³, S. Ganguly³⁷, Y. Gao⁷⁷, Y. S. Gao^{145g}, F. M. Garay Walls⁴⁹, C. García¹⁷⁰, J. E. García Navarro¹⁷⁰, J. A. García Pascual^{35a}, M. Garcia-Sciveres¹⁶, R. W. Gardner³³, N. Garelli¹⁴⁵, V. Garonne¹²¹, A. Gascon Bravo⁴⁵, K. Gasnikova⁴⁵, C. Gatti⁵⁰, A. Gaudiello^{53a,53b}, G. Gaudio^{123a}, I. L. Gavrilenko⁹⁸, C. Gay¹⁷¹, G. Gaycken²³, E. N. Gazis¹⁰, C. N. P. Gee¹³³, J. Geisen⁵⁷, M. Geisen⁸⁶, M. P. Geisler^{60a}, K. Gellerstedt^{148a,148b}, C. Gemme^{53a}, M. H. Genest⁵⁸, C. Geng⁹², S. Gentile^{134a,134b}, C. Gentsos¹⁵⁶, S. George⁸⁰, D. Gerbaudo¹³, A. Gershon¹⁵⁵, G. Geßner⁴⁶, S. Ghasemi¹⁴³, M. Ghneimat²³, B. Giacobbe^{22a}, S. Giagu^{134a,134b}, P. Giannetti^{126a,126b}, S. M. Gibson⁸⁰, M. Gignac¹⁷¹, M. Gilchriese¹⁶, D. Gillberg³¹, G. Gilles¹⁷⁸, D. M. Gingrich^{3,d}, N. Giokaris^{9,*}, M. P. Giordani^{167a,167c}, F. M. Giorgi^{22a}, P. F. Giraud¹³⁸, P. Giromini⁵⁹, D. Giugni^{94a}, F. Giuli¹²², C. Giuliani¹⁰³, M. Giulini^{60b}, B. K. Gjølsten¹²¹

- S. Gkaitatzis¹⁵⁶, I. Gkialas^{9,s}, E. L. Gkoukousis¹³⁹, P. Gkoutoumis¹⁰, L. K. Gladilin¹⁰¹, C. Glasman⁸⁵, J. Glatzer¹³, P. C. F. Glaysher⁴⁵, A. Glazov⁴⁵, M. Goblirsch-Kolb²⁵, J. Godlewski⁴², S. Goldfarb⁹¹, T. Golling⁵², D. Golubkov¹³², A. Gomes^{128a,128b,128d}, R. Gonçalo^{128a}, R. Gonçalves Gama^{26a}, J. Gonçalves Pinto Firmino Da Costa¹³⁸, G. Gonella⁵¹, L. Gonella¹⁹, A. Gongadze⁶⁸, S. González de la Hoz¹⁷⁰, S. Gonzalez-Sevilla⁵², L. Goossens³², P. A. Gorbounov⁹⁹, H. A. Gordon²⁷, I. Gorelov¹⁰⁷, B. Gorini³², E. Gorini^{76a,76b}, A. Gorišek⁷⁸, A. T. Goshaw⁴⁸, C. Gössling⁴⁶, M. I. Gostkin⁶⁸, C. A. Gottardo²³, C. R. Goudet¹¹⁹, D. Goujdami^{137c}, A. G. Goussiou¹⁴⁰, N. Govender^{147b,t}, E. Gozani¹⁵⁴, L. Graber⁵⁷, I. Grabowska-Bold^{41a}, P. O. J. Gradin¹⁶⁸, J. Gramling¹⁶⁶, E. Gramstad¹²¹, S. Grancagnolo¹⁷, V. Gratchev¹²⁵, P. M. Gravila^{28f}, C. Gray⁵⁶, H. M. Gray¹⁶, Z. D. Greenwood^{82,u}, C. Greife²³, K. Gregersen⁸¹, I. M. Gregor⁴⁵, P. Grenier¹⁴⁵, K. Grevtsov⁵, J. Griffiths⁸, A. A. Grillo¹³⁹, K. Grimm⁷⁵, S. Grinstein^{13,v}, Ph. Gris³⁷, J.-F. Grivaz¹¹⁹, S. Groh⁸⁶, E. Gross¹⁷⁵, J. Grosse-Knetter⁵⁷, G. C. Grossi⁸², Z. J. Grout⁸¹, A. Grummer¹⁰⁷, L. Guan⁹², W. Guan¹⁷⁶, J. Guenther⁶⁵, F. Guescini^{163a}, D. Guest¹⁶⁶, O. Gueta¹⁵⁵, B. Gui¹¹³, E. Guido^{53a,53b}, T. Guillemain⁵, S. Guindon², U. Gul⁵⁶, C. Gumpert³², J. Guo^{36c}, W. Guo⁹², Y. Guo^{36a}, R. Gupta⁴³, S. Gupta¹²², G. Gustavino^{134a,134b}, P. Gutierrez¹¹⁵, N. G. Gutierrez Ortiz⁸¹, C. Gutsche⁸¹, C. Guyot¹³⁸, M. P. Guzik^{41a}, C. Gwenlan¹²², C. B. Gwilliam⁷⁷, A. Haas¹¹², C. Haber¹⁶, H. K. Hadavand⁸, N. Haddad^{137e}, A. Hader⁸⁸, S. Hageböck²³, M. Hagihara¹⁶⁴, H. Hakobyan^{180,*}, M. Haleem⁴⁵, J. Haley¹¹⁶, G. Halladjian⁹³, G. D. Hallowell⁸⁸, K. Hamacher¹⁷⁸, P. Hamal¹¹⁷, K. Hamano¹⁷², A. Hamilton^{147a}, G. N. Hamity¹⁴¹, P. G. Hamnett⁴⁵, L. Han³⁹, S. Han^{35a}, K. Hanagaki^{69,w}, K. Hanawa¹⁵⁷, M. Hance¹³⁹, B. Haney¹²⁴, P. Hanke^{60a}, J. B. Hansen³⁹, J. D. Hansen³⁹, M. C. Hansen²³, P. H. Hansen³⁹, K. Hara¹⁶⁴, A. S. Hard¹⁷⁶, T. Harenberg¹⁷⁸, F. Hariri¹¹⁹, S. Harkusha⁹⁵, R. D. Harrington⁴⁹, P. F. Harrison¹⁷³, N. M. Hartmann¹⁰², M. Hasegawa⁷⁰, Y. Hasegawa¹⁴², A. Hasib⁴⁹, S. Hassani¹³⁸, S. Haug¹⁸, R. Hauser⁹³, L. Hauswald⁴⁷, L. B. Havener³⁸, M. Havranek¹³⁰, C. M. Hawkes¹⁹, R. J. Hawkins³², D. Hayakawa¹⁵⁹, D. Hayden⁹³, C. P. Hays¹²², J. M. Hays⁷⁹, H. S. Hayward⁷⁷, S. J. Haywood¹³³, S. J. Head¹⁹, T. Heck⁸⁶, V. Hedberg⁸⁴, L. Heelan⁸, K. K. Heidegger⁵¹, S. Heim⁴⁵, T. Heim¹⁶, B. Heinemann^{45,x}, J. J. Heinrich¹⁰², L. Heinrich¹¹², C. Heinz⁵⁵, J. Hejbal¹²⁹, L. Helary³², A. Held¹⁷¹, S. Hellman^{148a,148b}, C. Helsens³², R. C. W. Henderson⁷⁵, Y. Heng¹⁷⁶, S. Henkelmann¹⁷¹, A. M. Henriques Correia³², S. Henrot-Versille¹¹⁹, G. H. Herbert¹⁷, H. Herde²⁵, V. Herget¹⁷⁷, Y. Hernández Jiménez^{147c}, H. Herr⁸⁶, G. Herten⁵¹, R. Hertenberger¹⁰², L. Hervas³², T. C. Herwig¹²⁴, G. G. Hesketh⁸¹, N. P. Hessey^{163a}, J. W. Hetherly⁴³, S. Higashino⁶⁹, E. Higón-Rodríguez¹⁷⁰, E. Hill¹⁷², J. C. Hill³⁰, K. H. Hiller⁴⁵, S. J. Hillier¹⁹, M. Hils⁴⁷, I. Hinchliffe¹⁶, M. Hirose⁵¹, D. Hirschbuehl¹⁷⁸, B. Hiti⁷⁸, O. Hladik¹²⁹, X. Hoad⁴⁹, J. Hobbs¹⁵⁰, N. Hod^{163a}, M. C. Hodgkinson¹⁴¹, P. Hodgson¹⁴¹, A. Hoecker³², M. R. Hoferkamp¹⁰⁷, F. Hoening¹⁰², D. Hohn²³, T. R. Holmes³³, M. Homann⁴⁶, S. Honda¹⁶⁴, T. Honda⁶⁹, T. M. Hong¹²⁷, B. H. Hooberman¹⁶⁹, W. H. Hopkins¹¹⁸, Y. Horii¹⁰⁵, A. J. Horton¹⁴⁴, J.-Y. Hostachy⁵⁸, S. Hou¹⁵³, A. Hoummada^{137a}, J. Howarth⁸⁷, J. Hoya⁷⁴, M. Hrabovsky¹¹⁷, J. Hrdinka³², I. Hristova¹⁷, J. Hrivnac¹¹⁹, T. Hryn'ova⁵, A. Hrynevich⁹⁶, P. J. Hsu⁶³, S.-C. Hsu¹⁴⁰, Q. Hu^{36a}, S. Hu^{36c}, Y. Huang^{35a}, Z. Hubacek¹³⁰, F. Hubaut⁸⁸, F. Huegging²³, T. B. Huffman¹²², E. W. Hughes³⁸, G. Hughes⁷⁵, M. Huhtinen³², P. Huo¹⁵⁰, N. Huseynov^{68,b}, J. Huston⁹³, J. Huth⁵⁹, G. Iacobucci⁵², G. Iakovidis²⁷, I. Ibragimov¹⁴³, L. Iconomidou-Fayard¹¹⁹, Z. Idrissi^{137e}, P. Iengo³², O. Igonkina^{109,y}, T. Iizawa¹⁷⁴, Y. Ikegami⁶⁹, M. Ikeno⁶⁹, Y. Ilchenko^{11,z}, D. Iliadis¹⁵⁶, N. Ilic¹⁴⁵, G. Introzzi^{123a,123b}, P. Ioannou^{9,*}, M. Iodice^{136a}, K. Iordanidou³⁸, V. Ippolito⁵⁹, M. F. Isacson¹⁶⁸, N. Ishijima¹²⁰, M. Ishino¹⁵⁷, M. Ishitsuka¹⁵⁹, C. Issever¹²², S. Istin^{20a}, F. Ito¹⁶⁴, J. M. Iturbe Ponce⁸⁷, R. Iuppa^{162a,162b}, H. Iwasaki⁶⁹, J. M. Izen⁴⁴, V. Izzo^{106a}, S. Jabbar³, P. Jackson¹, R. M. Jacobs²³, V. Jain², K. B. Jakobi⁸⁶, K. Jakobs⁵¹, S. Jakobsen⁶⁵, T. Jakoubek¹²⁹, D. O. Jamin¹¹⁶, D. K. Jana⁸², R. Jansky⁵², J. Janssen²³, M. Janus⁵⁷, P. A. Janus^{41a}, G. Jarlskog⁸⁴, N. Javadov^{68,b}, T. Javůrek⁵¹, M. Javurkova⁵¹, F. Jeanneau¹³⁸, L. Jeanty¹⁶, J. Jejelava^{54a,aa}, A. Jelinskas¹⁷³, P. Jenni^{51,ab}, C. Jeske¹⁷³, S. Jézéquel⁵, H. Ji¹⁷⁶, J. Jia¹⁵⁰, H. Jiang⁶⁷, Y. Jiang^{36a}, Z. Jiang¹⁴⁵, S. Jiggins⁸¹, J. Jimenez Pena¹⁷⁰, S. Jin^{35a}, A. Jinaru^{28b}, O. Jinnouchi¹⁵⁹, H. Jivan^{147c}, P. Johansson¹⁴¹, K. A. Johns⁷, C. A. Johnson⁶⁴, W. J. Johnson¹⁴⁰, K. Jon-And^{148a,148b}, R. W. L. Jones⁷⁵, S. D. Jones¹⁵¹, S. Jones⁷, T. J. Jones⁷⁷, J. Jongmanns^{60a}, P. M. Jorge^{128a,128b}, J. Jovicevic^{163a}, X. Ju¹⁷⁶, A. Juste Rozas^{13,v}, M. K. Köhler¹⁷⁵, A. Kaczmarska⁴², M. Kado¹¹⁹, H. Kagan¹¹³, M. Kagan¹⁴⁵, S. J. Kahn⁸⁸, T. Kaji¹⁷⁴, E. Kajomovitz⁴⁸, C. W. Kalderon⁸⁴, A. Kaluza⁸⁶, S. Kama⁴³, A. Kamenshchikov¹³², N. Kanaya¹⁵⁷, L. Kanjir⁷⁸, V. A. Kantserov¹⁰⁰, J. Kanzaki⁶⁹, B. Kaplan¹¹², L. S. Kaplan¹⁷⁶, D. Kar^{147c}, K. Karakostas¹⁰, N. Karastathis¹⁰, M. J. Kareem⁵⁷, E. Karentzos¹⁰, S. N. Karpov⁶⁸, Z. M. Karpova⁶⁸, K. Karthik¹¹², V. Kartvelishvili⁷⁵, A. N. Karyukhin¹³², K. Kasahara¹⁶⁴, L. Kashif¹⁷⁶, R. D. Kass¹¹³, A. Kastanas¹⁴⁹, Y. Kataoka¹⁵⁷, C. Kato¹⁵⁷, A. Katre⁵², J. Katzy⁴⁵, K. Kawade⁷⁰, K. Kawagoe⁷³, T. Kawamoto¹⁵⁷, G. Kawamura⁵⁷, E. F. Kay⁷⁷, V. F. Kazanin^{111,c}, R. Keeler¹⁷², R. Kehoe⁴³, J. S. Keller³¹, J. J. Kempster⁸⁰, J. Kendrick¹⁹, H. Keoshkerian¹⁶¹, O. Kepka¹²⁹, B. P. Kerševan⁷⁸, S. Kersten¹⁷⁸, R. A. Keyes⁹⁰, M. Khader¹⁶⁹, F. Khalil-zada¹², A. Khanov¹¹⁶, A. G. Kharlamov^{111,c}, T. Kharlamova^{111,c}

- A. Khodinov¹⁶⁰, T. J. Khoo⁵², V. Khovanskiy^{99,*}, E. Khramov⁶⁸, J. Khubua^{54b,ac}, S. Kido⁷⁰, C. R. Kilby⁸⁰, H. Y. Kim⁸, S. H. Kim¹⁶⁴, Y. K. Kim³³, N. Kimura¹⁵⁶, O. M. Kind¹⁷, B. T. King⁷⁷, D. Kirchmeier⁴⁷, J. Kirk¹³³, A. E. Kiryunin¹⁰³, T. Kishimoto¹⁵⁷, D. Kisielska^{41a}, V. Kitali⁴⁵, K. Kiuchi¹⁶⁴, O. Kivernyk⁵, E. Kladiva^{146b}, T. Klapdor-Kleingrothaus⁵¹, M. H. Klein³⁸, M. Klein⁷⁷, U. Klein⁷⁷, K. Kleinknecht⁸⁶, P. Klimek¹¹⁰, A. Klimentov²⁷, R. Klingenberg⁴⁶, T. Klingl²³, T. Klioutchnikova³², E.-E. Kluge^{60a}, P. Kluit¹⁰⁹, S. Kluth¹⁰³, E. Kneringer⁶⁵, E. B. F. G. Knoops⁸⁸, A. Knue¹⁰³, A. Kobayashi¹⁵⁷, D. Kobayashi¹⁵⁹, T. Kobayashi¹⁵⁷, M. Kobel⁴⁷, M. Kocian¹⁴⁵, P. Kodys¹³¹, T. Koffas³¹, E. Koffeman¹⁰⁹, N. M. Köhler¹⁰³, T. Koi¹⁴⁵, M. Kolb^{60b}, I. Koletsou⁵, A. A. Komar^{98,*}, Y. Komori¹⁵⁷, T. Kondo⁶⁹, N. Kondrashova^{36c}, K. Köneke⁵¹, A. C. König¹⁰⁸, T. Kono^{69,ad}, R. Konoplich^{112,ae}, N. Konstantinidis⁸¹, R. Kopeliansky⁶⁴, S. Koperny^{41a}, A. K. Kopp⁵¹, K. Korcyl⁴², K. Kordas¹⁵⁶, A. Korn⁸¹, A. A. Korol^{111,c}, I. Korolkov¹³, E. V. Korolkova¹⁴¹, O. Kortner¹⁰³, S. Kortner¹⁰³, T. Kosek¹³¹, V. V. Kostyukhin²³, A. Kotwal⁴⁸, A. Koulouris¹⁰, A. Kourkoulis-Charalampidi^{123a,123b}, C. Kourkoulis⁹, E. Kourlitis¹⁴¹, V. Kouskoura²⁷, A. B. Kowalewska⁴², R. Kowalewski¹⁷², T. Z. Kowalski^{41a}, C. Kozakai¹⁵⁷, W. Kozanecki¹³⁸, A. S. Kozhin¹³², V. A. Kramarenko¹⁰¹, G. Kramberger⁷⁸, D. Krasnopevtsev¹⁰⁰, M. W. Krasny⁸³, A. Krasznahorkay³², D. Krauss¹⁰³, J. A. Kremer^{41a}, J. Kretschmar⁷⁷, K. Kreutzfeldt⁵⁵, P. Krieger¹⁶¹, K. Krizka³³, K. Kroeninger⁴⁶, H. Kroha¹⁰³, J. Kroll¹²⁹, J. Kroll¹²⁴, J. Kroseberg²³, J. Krstic¹⁴, U. Kruchonak⁶⁸, H. Krüger²³, N. Krumnack⁶⁷, M. C. Kruse⁴⁸, T. Kubota⁹¹, H. Kucuk⁸¹, S. Kuday^{4b}, J. T. Kuechler¹⁷⁸, S. Kuehn³², A. Kugel^{60a}, F. Kuger¹⁷⁷, T. Kuhl⁴⁵, V. Kukhtin⁶⁸, R. Kukla⁸⁸, Y. Kulchitsky⁹⁵, S. Kuleshov^{34b}, Y. P. Kulinich¹⁶⁹, M. Kuna^{134a,134b}, T. Kunigo⁷¹, A. Kupco¹²⁹, T. Kupfer⁴⁶, O. Kuprash¹⁵⁵, H. Kurashige⁷⁰, L. L. Kurchaninov^{163a}, Y. A. Kurochkin⁹⁵, M. G. Kurth^{35a}, V. Kus¹²⁹, E. S. Kuwertz¹⁷², M. Kuze¹⁵⁹, J. Kvita¹¹⁷, T. Kwan¹⁷², D. Kyriazopoulos¹⁴¹, A. La Rosa¹⁰³, J. L. La Rosa Navarro^{26d}, L. La Rotonda^{40a,40b}, F. La Ruffa^{40a,40b}, C. Lacasta¹⁷⁰, F. Lacava^{134a,134b}, J. Lacey⁴⁵, H. Lacker¹⁷, D. Lacour⁸³, E. Ladygin⁶⁸, R. Lafaye⁵, B. Laforge⁸³, T. Lagouri¹⁷⁹, S. Lai⁵⁷, S. Lammers⁶⁴, W. Lampl⁷, E. Lançon²⁷, U. Landgraf⁵¹, M. P. J. Landon⁷⁹, M. C. Lanfermann⁵², V. S. Lang^{60a}, J. C. Lange¹³, R. J. Langenberg³², A. J. Lankford¹⁶⁶, F. Lanni²⁷, K. Lantzsch²³, A. Lanza^{123a}, A. Lapertosa^{53a,53b}, S. Laplace⁸³, J. F. Laporte¹³⁸, T. Lari^{94a}, F. Lasagni Manghi^{22a,22b}, M. Lassnig³², P. Laurelli⁵⁰, W. Lavrijsen¹⁶, A. T. Law¹³⁹, P. Laycock⁷⁷, T. Lazovich⁵⁹, M. Lazzaroni^{94a,94b}, B. Le⁹¹, O. Le Dortz⁸³, E. Le Guirriec⁸⁸, E. P. Le Quilleuc¹³⁸, M. LeBlanc¹⁷², T. LeCompte⁶, F. Ledroit-Guillon⁵⁸, C. A. Lee²⁷, G. R. Lee^{133,af}, S. C. Lee¹⁵³, L. Lee⁵⁹, B. Lefebvre⁹⁰, G. Lefebvre⁸³, M. Lefebvre¹⁷², F. Legger¹⁰², C. Leggett¹⁶, A. Lehan⁷⁷, G. Lehmann Miotto³², X. Lei⁷, W. A. Leight⁴⁵, M. A. L. Leite^{26d}, R. Leitner¹³¹, D. Lellouch¹⁷⁵, B. Lemmer⁵⁷, K. J. C. Leney⁸¹, T. Lenz²³, B. Lenzi³², R. Leone⁷, S. Leone^{126a,126b}, C. Leonidopoulos⁴⁹, G. Lerner¹⁵¹, C. Leroy⁹⁷, A. A. J. Lesage¹³⁸, C. G. Lester³⁰, M. Levchenko¹²⁵, J. Levêque⁵, D. Levin⁹², L. J. Levinson¹⁷⁵, M. Levy¹⁹, D. Lewis⁷⁹, B. Li^{36a,ag}, Changqiao Li^{36a}, H. Li¹⁵⁰, L. Li^{36c}, Q. Li^{35a}, S. Li⁴⁸, X. Li^{36c}, Y. Li¹⁴³, Z. Liang^{35a}, B. Liberti^{135a}, A. Liblong¹⁶¹, K. Lie^{62c}, J. Liebal²³, W. Liebig¹⁵, A. Limosani¹⁵², S. C. Lin¹⁸², T. H. Lin⁸⁶, B. E. Lindquist¹⁵⁰, A. E. Lioni⁵², E. Lipeles¹²⁴, A. Lipniacka¹⁵, M. Lisovyi^{60b}, T. M. Liss^{169,ah}, A. Lister¹⁷¹, A. M. Litke¹³⁹, B. Liu^{153,ai}, H. Liu⁹², H. Liu²⁷, J. K. K. Liu¹²², J. Liu^{36b}, J. B. Liu^{36a}, K. Liu⁸⁸, L. Liu¹⁶⁹, M. Liu^{36a}, Y. L. Liu^{36a}, Y. Liu^{36a}, M. Livan^{123a,123b}, A. Lleres⁵⁸, J. Llorente Merino^{35a}, S. L. Lloyd⁷⁹, C. Y. Lo^{62b}, F. Lo Sterzo¹⁵³, E. M. Lobodzinska⁴⁵, P. Loch⁷, F. K. Loebinger⁸⁷, A. Loesle⁵¹, K. M. Loew²⁵, A. Loginov^{179,*}, T. Lohse¹⁷, K. Lohwasser¹⁴¹, M. Lokajicek¹²⁹, B. A. Long²⁴, J. D. Long¹⁶⁹, R. E. Long⁷⁵, L. Longo^{76a,76b}, K. A. Looper¹¹³, J. A. Lopez^{34b}, D. Lopez Mateos⁵⁹, I. Lopez Paz¹³, A. Lopez Solis⁸³, J. Lorenz¹⁰², N. Lorenzo Martinez⁵, M. Losada²¹, P. J. Lösel¹⁰², X. Lou^{35a}, A. Lounis¹¹⁹, J. Love⁶, P. A. Love⁷⁵, H. Lu^{62a}, N. Lu⁹², Y. J. Lu⁶³, H. J. Lubatti¹⁴⁰, C. Luci^{134a,134b}, A. Lucotte⁵⁸, C. Luedtke⁵¹, F. Luehring⁶⁴, W. Lukas⁶⁵, L. Luminari^{134a}, O. Lundberg^{148a,148b}, B. Lund-Jensen¹⁴⁹, P. M. Luzi⁸³, D. Lynn²⁷, R. Lysak¹²⁹, E. Lytken⁸⁴, F. Lyu^{35a}, V. Lyubushkin⁶⁸, H. Ma²⁷, L. L. Ma^{36b}, Y. Ma^{36b}, G. Maccarrone⁵⁰, A. Macchiolo¹⁰³, C. M. Macdonald¹⁴¹, B. Maček⁷⁸, J. Machado Miguens^{124,128b}, D. Madaffari¹⁷⁰, R. Madar³⁷, W. F. Mader⁴⁷, A. Madsen⁴⁵, J. Maeda⁷⁰, S. Maeland¹⁵, T. Maeno²⁷, A. S. Maevskiy¹⁰¹, E. Magradze⁵⁷, J. Mahlstedt¹⁰⁹, C. Maiani¹¹⁹, C. Maidantchik^{26a}, A. A. Maier¹⁰³, T. Maier¹⁰², A. Maio^{128a,128b,128d}, O. Majersky^{146a}, S. Majewski¹¹⁸, Y. Makida⁶⁹, N. Makovec¹¹⁹, B. Malaescu⁸³, Pa. Malecki⁴², V. P. Maleev¹²⁵, F. Malek⁵⁸, U. Mallik⁶⁶, D. Malon⁶, C. Malone³⁰, S. Maltezos¹⁰, S. Malyukov³², J. Mamuzic¹⁷⁰, G. Mancini⁵⁰, L. Mandelli^{94a}, I. Mandić⁷⁸, J. Maneira^{128a,128b}, L. Manhaes de Andrade Filho^{26b}, J. Manjarres Ramos⁴⁷, K. H. Mankinen⁸⁴, A. Mann¹⁰², A. Manousos³², B. Mansoulie¹³⁸, J. D. Mansour^{35a}, R. Mantifel⁹⁰, M. Mantoani⁵⁷, S. Manzoni^{94a,94b}, L. Mapelli³², G. Marceca²⁹, L. March⁵², L. Marchese¹²², G. Marchiori⁸³, M. Marcisovsky¹²⁹, M. Marjanovic³⁷, D. E. Marley⁹², F. Marroquim^{26a}, S. P. Marsden⁸⁷, Z. Marshall¹⁶, M. U. F. Martensson¹⁶⁸, S. Marti-Garcia¹⁷⁰, C. B. Martin¹¹³, T. A. Martin¹⁷³, V. J. Martin⁴⁹, B. Martin dit Latour¹⁵, M. Martinez^{13,v}, V. I. Martinez Outschoorn¹⁶⁹, S. Martin-Haugh¹³³, V. S. Martoiu^{28b}, A. C. Martyniuk⁸¹, A. Marzin³², L. Masetti⁸⁶, T. Mashimo¹⁵⁷, R. Mashinistov⁹⁸,

- J. Masik⁸⁷, A. L. Maslennikov^{111,c}, L. Massa^{135a,135b}, P. Mastrandrea⁵, A. Mastroberardino^{40a,40b}, T. Masubuchi¹⁵⁷, P. Mättig¹⁷⁸, J. Maurer^{28b}, S. J. Maxfield⁷⁷, D. A. Maximov^{111,c}, R. Mazini¹⁵³, I. Maznas¹⁵⁶, S. M. Mazza^{94a,94b}, N.C. McFadden¹⁰⁷, G. Mc Goldrick¹⁶¹, S. P. Mc Kee⁹², A. McCarn⁹², R. L. McCarthy¹⁵⁰, T. G. McCarthy¹⁰³, L. I. McClymont⁸¹, E. F. McDonald⁹¹, J. A. Mcfayden⁸¹, G. Mchedlidze⁵⁷, S. J. McMahon¹³³, P. C. McNamara⁹¹, R. A. McPherson^{172,o}, S. Meehan¹⁴⁰, T. J. Megy⁵¹, S. Mehlhase¹⁰², A. Mehta⁷⁷, T. Meideck⁵⁸, K. Meier^{60a}, B. Meirose⁴⁴, D. Melini^{170,aj}, B. R. Mellado Garcia^{147c}, J. D. Mellenthin⁵⁷, M. Melo^{146a}, F. Meloni¹⁸, S. B. Menary⁸⁷, L. Meng⁷⁷, X. T. Meng⁹², A. Mengarelli^{22a,22b}, S. Menke¹⁰³, E. Meoni^{40a,40b}, S. Mergelmeyer¹⁷, P. Mermod⁵², L. Merola^{106a,106b}, C. Meroni^{94a}, F. S. Merritt³³, A. Messina^{134a,134b}, J. Metcalfe⁶, A. S. Mete¹⁶⁶, C. Meyer¹²⁴, J.-P. Meyer¹³⁸, J. Meyer¹⁰⁹, H. Meyer Zu Theenhausen^{60a}, F. Miano¹⁵¹, R. P. Middleton¹³³, S. Miglioranza^{53a,53b}, L. Mijović⁴⁹, G. Mikenberg¹⁷⁵, M. Mikestikova¹²⁹, M. Mikuz⁷⁸, M. Milesi⁹¹, A. Milic¹⁶¹, D. W. Miller³³, C. Mills⁴⁹, A. Milov¹⁷⁵, D. A. Milstead^{148a,148b}, A. A. Minaenko¹³², Y. Minami¹⁵⁷, I. A. Minashvili⁶⁸, A. I. Mincer¹¹², B. Mindur^{41a}, M. Mineev⁶⁸, Y. Minegishi¹⁵⁷, Y. Ming¹⁷⁶, L. M. Mir¹³, K. P. Mistry¹²⁴, T. Mitani¹⁷⁴, J. Mitrevski¹⁰², V. A. Mitsou¹⁷⁰, A. Miucci¹⁸, P. S. Miyagawa¹⁴¹, A. Mizukami⁶⁹, J. U. Mjörnmark⁸⁴, T. Mkrtchyan¹⁸⁰, M. Mlynarikova¹³¹, T. Moa^{148a,148b}, K. Mochizuki⁹⁷, P. Mogg⁵¹, S. Mohapatra³⁸, S. Molander^{148a,148b}, R. Moles-Valls³², R. Monden⁷¹, M. C. Mondragon⁹³, K. Möning⁴⁵, J. Monk³⁹, E. Monnier⁸⁸, A. Montalbano¹⁵⁰, J. Montejo Berlingen³², F. Monticelli⁷⁴, S. Monzani^{94a,94b}, R. W. Moore³, N. Morange¹¹⁹, D. Moreno²¹, M. Moreno Llacer³², P. Morettini^{53a}, S. Morgenstern³², D. Mori¹⁴⁴, T. Mori¹⁵⁷, M. Morii⁵⁹, M. Morinaga¹⁵⁷, V. Morisbak¹²¹, A. K. Morley¹⁵², G. Mornacchi³², J. D. Morris⁷⁹, L. Morvaj¹⁵⁰, P. Moschovakos¹⁰, M. Mosidze^{54b}, H. J. Moss¹⁴¹, J. Moss^{145,ak}, K. Motohashi¹⁵⁹, R. Mount¹⁴⁵, E. Mountricha²⁷, E. J. W. Moyse⁸⁹, S. Muanza⁸⁸, R. D. Mudd¹⁹, F. Mueller¹⁰³, J. Mueller¹²⁷, R. S. P. Mueller¹⁰², D. Muenstermann⁷⁵, P. Mullen⁵⁶, G. A. Mullier¹⁸, F. J. Munoz Sanchez⁸⁷, W. J. Murray^{173,133}, H. Musheghyan³², M. Muškinja⁷⁸, A. G. Myagkov^{132,al}, M. Myska¹³⁰, B. P. Nachman¹⁶, O. Nackenhorst⁵², K. Nagai¹²², R. Nagai^{69,ad}, K. Nagano⁶⁹, Y. Nagasaka⁶¹, K. Nagata¹⁶⁴, M. Nagel⁵¹, E. Nagy⁸⁸, A. M. Nairz³², Y. Nakahama¹⁰⁵, K. Nakamura⁶⁹, T. Nakamura¹⁵⁷, I. Nakano¹¹⁴, R. F. Naranjo Garcia⁴⁵, R. Narayan¹¹, D. I. Narrias Villar^{60a}, I. Naryshkin¹²⁵, T. Naumann⁴⁵, G. Navarro²¹, R. Nayyar⁷, H. A. Neal⁹², P. Yu. Nechaeva⁹⁸, T. J. Neep¹³⁸, A. Negri^{123a,123b}, M. Negrini^{22a}, S. Nektarijevic¹⁰⁸, C. Nellist¹¹⁹, A. Nelson¹⁶⁶, M. E. Nelson¹²², S. Nemecek¹²⁹, P. Nemethy¹¹², M. Nessi^{32,am}, M. S. Neubauer¹⁶⁹, M. Neumann¹⁷⁸, P. R. Newman¹⁹, T. Y. Ng^{62c}, T. Nguyen Manh⁹⁷, R. B. Nickerson¹²², R. Nicolaidou¹³⁸, J. Nielsen¹³⁹, V. Nikolaenko^{132,al}, I. Nikolic-Audit⁸³, K. Nikolopoulos¹⁹, J. K. Nilsen¹²¹, P. Nilsson²⁷, Y. Ninomiya¹⁵⁷, A. Nisati^{134a}, N. Nishu^{35c}, R. Nisius¹⁰³, I. Nitsche⁴⁶, T. Nitta¹⁷⁴, T. Nobe¹⁵⁷, Y. Noguchi⁷¹, M. Nomachi¹²⁰, I. Nomidis³¹, M. A. Nomura²⁷, T. Nooney⁷⁹, M. Nordberg³², N. Norjoharuddeen¹²², O. Novgorodova⁴⁷, S. Nowak¹⁰³, M. Nozaki⁶⁹, L. Nozka¹¹⁷, K. Ntekas¹⁶⁶, E. Nurse⁸¹, F. Nuti⁹¹, K. O'connor²⁵, D. C. O'Neil¹⁴⁴, A. A. O'Rourke⁴⁵, V. O'Shea⁵⁶, F. G. Oakham^{31,d}, H. Oberlack¹⁰³, T. Obermann²³, J. Ocariz⁸³, A. Ochi⁷⁰, I. Ochoa³⁸, J. P. Ochoa-Ricoux^{34a}, S. Oda⁷³, S. Odaka⁶⁹, H. Ogren⁶⁴, A. Oh⁸⁷, S. H. Oh⁴⁸, C. C. Ohm¹⁶, H. Ohman¹⁶⁸, H. Oide^{53a,53b}, H. Okawa¹⁶⁴, Y. Okumura¹⁵⁷, T. Okuyama⁶⁹, A. Olariu^{28b}, L. F. Oleiro Seabra^{128a}, S. A. Olivares Pino⁴⁹, D. Oliveira Damazio²⁷, A. Olszewski⁴², J. Olszowska⁴², A. Onofre^{128a,128e}, K. Onogi¹⁰⁵, P. U. E. Onyisi^{11,z}, M. J. Oreglia³³, Y. Oren¹⁵⁵, D. Orestano^{136a,136b}, N. Orlando^{62b}, R. S. Orr¹⁶¹, B. Osculati^{53a,53b,*}, R. Ospanov^{36a}, G. Otero y Garzon²⁹, H. Otono⁷³, M. Ouchrif^{137d}, F. Ould-Saada¹²¹, A. Ouraou¹³⁸, K. P. Oussoren¹⁰⁹, Q. Ouyang^{35a}, M. Owen⁵⁶, R. E. Owen¹⁹, V. E. Ozcan^{20a}, N. Ozturk⁸, K. Pachal¹⁴⁴, A. Pacheco Pages¹³, L. Pacheco Rodriguez¹³⁸, C. Padilla Aranda¹³, S. Pagan Griso¹⁶, M. Paganini¹⁷⁹, F. Paige²⁷, G. Palacino⁶⁴, S. Palazzo^{40a,40b}, S. Palestini³², M. Palka^{41b}, D. Pallin³⁷, E. St. Panagiotopoulou¹⁰, I. Panagoulas¹⁰, C. E. Pandini⁸³, J. G. Panduro Vazquez⁸⁰, P. Pani³², S. Panitkin²⁷, D. Pantea^{28b}, L. Paolozzi⁵², Th. D. Papadopoulou¹⁰, K. Papageorgiou^{9,s}, A. Paramonov⁶, D. Paredes Hernandez¹⁷⁹, A. J. Parker⁷⁵, M. A. Parker³⁰, K. A. Parker⁴⁵, F. Parodi^{53a,53b}, J. A. Parsons³⁸, U. Parzefall⁵¹, V. R. Pascuzzi¹⁶¹, J. M. Pasner¹³⁹, E. Pasqualucci^{134a}, S. Passaggio^{53a}, Fr. Pastore⁸⁰, S. Patariaia⁸⁶, J. R. Pater⁸⁷, T. Pauly³², B. Pearson¹⁰³, S. Pedraza Lopez¹⁷⁰, R. Pedro^{128a,128b}, S. V. Peleganchuk^{111,c}, O. Penc¹²⁹, C. Peng^{35a}, H. Peng^{36a}, J. Penwell⁶⁴, B. S. Peralva^{26b}, M. M. Perego¹³⁸, D. V. Perepelitsa²⁷, F. Peri¹⁷, L. Perini^{94a,94b}, H. Pernegger³², S. Perrella^{106a,106b}, R. Peschke⁴⁵, V. D. Peshekhonov^{68,*}, K. Peters⁴⁵, R. F. Y. Peters⁸⁷, B. A. Petersen³², T. C. Petersen³⁹, E. Petit⁵⁸, A. Petridis¹, C. Petridou¹⁵⁶, P. Petroff¹¹⁹, E. Petrolo^{134a}, M. Petrov¹²², F. Petrucci^{136a,136b}, N. E. Pettersson⁸⁹, A. Peyaud¹³⁸, R. Pezoa^{34b}, F. H. Phillips⁹³, P. W. Phillips¹³³, G. Piacquadio¹⁵⁰, E. Pianori¹⁷³, A. Picazio⁸⁹, E. Piccaro⁷⁹, M. A. Pickering¹²², R. Piegai²⁹, J. E. Pilcher³³, A. D. Pilkington⁸⁷, A. W. J. Pin⁸⁷, M. Pinamonti^{135a,135b}, J. L. Pinfold³, H. Pirumov⁴⁵, M. Pitt¹⁷⁵, L. Plazak^{146a}, M.-A. Pleier²⁷, V. Pleskot⁸⁶, E. Plotnikova⁶⁸, D. Pluth⁶⁷, P. Podberezko¹¹¹, R. Poettgen^{148a,148b}, R. Poggi^{123a,123b}, L. Poggioli¹¹⁹, D. Pohl²³, G. Polesello^{123a}, A. Poley⁴⁵, A. Policicchio^{40a,40b}, R. Polifka³², A. Polini^{22a}, C. S. Pollard⁵⁶, V. Polychronakos²⁷

- K. Pommès³², D. Ponomarenko¹⁰⁰, L. Pontecorvo^{134a}, B. G. Pope⁹³, G. A. Popeneciu^{28d}, A. Poppleton³², S. Pospisil¹³⁰, K. Potamianos¹⁶, I. N. Potrap⁶⁸, C. J. Potter³⁰, G. Poulard³², T. Poulsen⁸⁴, J. Poveda³², M. E. Pozo Astigarraga³², P. Pralavorio⁸⁸, A. Pranko¹⁶, S. Prell⁶⁷, D. Price⁸⁷, L. E. Price⁶, M. Primavera^{76a}, S. Prince⁹⁰, N. Proklova¹⁰⁰, K. Prokofiev^{62c}, F. Prokoshin^{34b}, S. Protopopescu²⁷, J. Proudfoot⁶, M. Przybycien^{41a}, A. Puri¹⁶⁹, P. Puzo¹¹⁹, J. Qian⁹², G. Qin⁵⁶, Y. Qin⁸⁷, A. Quadt⁵⁷, M. Queitsch-Maitland⁴⁵, D. Quilty⁵⁶, S. Raddum¹²¹, V. Radeka²⁷, V. Radescu¹²², S. K. Radhakrishnan¹⁵⁰, P. Radloff¹¹⁸, P. Rados⁹¹, F. Ragusa^{94a,94b}, G. Rahal¹⁸¹, J. A. Raine⁸⁷, S. Rajagopalan²⁷, C. Rangel-Smith¹⁶⁸, T. Rashid¹¹⁹, S. Raspopov⁵, M. G. Ratti^{94a,94b}, D. M. Rauch⁴⁵, F. Rauscher¹⁰², S. Rave⁸⁶, I. Ravinovich¹⁷⁵, J. H. Rawling⁸⁷, M. Raymond³², A. L. Read¹²¹, N. P. Readioff⁵⁸, M. Reale^{76a,76b}, D. M. Rebuffi^{123a,123b}, A. Redelbach¹⁷⁷, G. Redlinger²⁷, R. Reece¹³⁹, R. G. Reed^{147c}, K. Reeves⁴⁴, L. Rehnisch¹⁷, J. Reichert¹²⁴, A. Reiss⁸⁶, C. Rembser³², H. Ren^{35a}, M. Rescigno^{134a}, S. Resconi^{94a}, E. D. Resseguie¹²⁴, S. Rettie¹⁷¹, E. Reynolds¹⁹, O. L. Rezanova^{111c}, P. Reznicek¹³¹, R. Rezvani⁹⁷, R. Richter¹⁰³, S. Richter⁸¹, E. Richter-Was^{41b}, O. Ricken²³, M. Ridel⁸³, P. Rieck¹⁰³, C. J. Riegel¹⁷⁸, J. Rieger⁵⁷, O. Rifki¹¹⁵, M. Rijssenbeek¹⁵⁰, A. Rimoldi^{123a,123b}, M. Rimoldi¹⁸, L. Rinaldi^{22a}, G. Ripellino¹⁴⁹, B. Ristić³², E. Ritsch³², I. Riu¹³, F. Rizatdinova¹¹⁶, E. Rizvi⁷⁹, C. Rizzi¹³, R. T. Roberts⁸⁷, S. H. Robertson^{90o}, A. Robichaud-Veronneau⁹⁰, D. Robinson³⁰, J. E. M. Robinson⁴⁵, A. Robson⁵⁶, E. Rocco⁸⁶, C. Roda^{126a,126b}, Y. Rodina^{88,an}, S. Rodriguez Bosca¹⁷⁰, A. Rodriguez Perez¹³, D. Rodriguez Rodriguez¹⁷⁰, S. Roe³², C. S. Rogan⁵⁹, O. Røhne¹²¹, J. Roloff⁵⁹, A. Romaniouk¹⁰⁰, M. Romano^{22a,22b}, S. M. Romano Saez³⁷, E. Romero Adam¹⁷⁰, N. Rompotis⁷⁷, M. Ronzani⁵¹, L. Roos⁸³, S. Rosati^{134a}, K. Rosbach⁵¹, P. Rose¹³⁹, N.-A. Rosien⁵⁷, E. Rossi^{106a,106b}, L. P. Rossi^{53a}, J. H. N. Rosten³⁰, R. Rosten¹⁴⁰, M. Rotaru^{28b}, I. Roth¹⁷⁵, J. Rothberg¹⁴⁰, D. Rousseau¹¹⁹, A. Rozanov⁸⁸, Y. Rozen¹⁵⁴, X. Ruan^{147c}, F. Rubbo¹⁴⁵, F. Rühr⁵¹, A. Ruiz-Martinez³¹, Z. Rurikova⁵¹, N. A. Rusakovich⁶⁸, H. L. Russell⁹⁰, J. P. Rutherford⁷, N. Ruthmann³², Y. F. Ryabov¹²⁵, M. Rybar¹⁶⁹, G. Rybkin¹¹⁹, S. Ryu⁶, A. Ryzhov¹³², G. F. Rzehorz⁵⁷, A. F. Saavedra¹⁵², G. Sabato¹⁰⁹, S. Sacerdoti²⁹, H.F.-W. Sadrozinski¹³⁹, R. Sadykov⁶⁸, F. Safai Tehrani^{134a}, P. Saha¹¹⁰, M. Sahinsoy^{60a}, M. Saimpert⁴⁵, M. Saito¹⁵⁷, T. Saito¹⁵⁷, H. Sakamoto¹⁵⁷, Y. Sakurai¹⁷⁴, G. Salamanna^{136a,136b}, J. E. Salazar Loyola^{34b}, D. Salek¹⁰⁹, P. H. Sales De Bruin¹⁶⁸, D. Salihagic¹⁰³, A. Salnikov¹⁴⁵, J. Salt¹⁷⁰, D. Salvatore^{40a,40b}, F. Salvatore¹⁵¹, A. Salvucci^{62a,62b,62c}, A. Salzburger³², D. Sammel⁵¹, D. Sampsonidis¹⁵⁶, D. Sampsonidou¹⁵⁶, J. Sánchez¹⁷⁰, V. Sanchez Martinez¹⁷⁰, A. Sanchez Pineda^{167a,167c}, H. Sandaker¹²¹, R. L. Sandbach⁷⁹, C. O. Sander⁴⁵, M. Sandhoff¹⁷⁸, C. Sandoval²¹, D. P. C. Sankey¹³³, M. Sannino^{53a,53b}, Y. Sano¹⁰⁵, A. Sansoni⁵⁰, C. Santoni³⁷, R. Santonicio^{135a,135b}, H. Santos^{128a}, I. Santoyo Castillo¹⁵¹, A. Sapronov⁶⁸, J. G. Saraiva^{128a,128d}, B. Sarrazin²³, O. Sasaki⁶⁹, K. Sato¹⁶⁴, E. Sauvan⁵, G. Savage⁸⁰, P. Savard^{161d}, N. Savic¹⁰³, C. Sawyer¹³³, L. Sawyer^{82u}, J. Saxon³³, C. Sbarra^{22a}, A. Sbrizzi^{22a,22b}, T. Scanlon⁸¹, D. A. Scannicchio¹⁶⁶, M. Scarcella¹⁵², V. Scarfone^{40a,40b}, J. Schaarschmidt¹⁴⁰, P. Schacht¹⁰³, B. M. Schachtner¹⁰², D. Schaefer³², L. Schaefer¹²⁴, R. Schaefer⁴⁵, J. Schaeffer⁸⁶, S. Schaepe²³, S. Schaetzel^{60b}, U. Schäfer⁸⁶, A. C. Schaffer¹¹⁹, D. Schaile¹⁰², R. D. Schamberger¹⁵⁰, V. Scharf^{60a}, V. A. Schegelsky¹²⁵, D. Scheirich¹³¹, M. Schernau¹⁶⁶, C. Schiavi^{53a,53b}, S. Schier¹³⁹, L. K. Schildgen²³, C. Schillo⁵¹, M. Schioppa^{40a,40b}, S. Schlenker³², K. R. Schmidt-Sommerfeld¹⁰³, K. Schmieden³², C. Schmitt⁸⁶, S. Schmitt⁴⁵, S. Schmitz⁸⁶, U. Schnoor⁵¹, L. Schoeffel¹³⁸, A. Schoening^{60b}, B. D. Schoenrock⁹³, E. Schopf²³, M. Schott⁸⁶, J. F. P. Schouwenberg¹⁰⁸, J. Schovancova³², S. Schramm⁵², N. Schuh⁸⁶, A. Schulte⁸⁶, M. J. Schultens²³, H.-C. Schultz-Coulon^{60a}, H. Schulz¹⁷, M. Schumacher⁵¹, B. A. Schumm¹³⁹, Ph. Schune¹³⁸, A. Schwartzman¹⁴⁵, T. A. Schwarz⁹², H. Schweiger⁸⁷, Ph. Schwemling¹³⁸, R. Schwienhorst⁹³, J. Schwindling¹³⁸, A. Sciandra²³, G. Sciolla²⁵, M. Scornajenghi^{40a,40b}, F. Scuri^{126a,126b}, F. Scutti⁹¹, J. Searcy⁹², P. Seema²³, S. C. Seidel¹⁰⁷, A. Seiden¹³⁹, J. M. Seixas^{26a}, G. Sekhniaidze^{106a}, K. Sekhon⁹², S. J. Sekula⁴³, N. Semprini-Cesari^{22a,22b}, S. Senkin³⁷, C. Serfon¹²¹, L. Serin¹¹⁹, L. Serkin^{167a,167b}, M. Sessa^{136a,136b}, R. Seuster¹⁷², H. Severini¹¹⁵, T. Sfiligoj⁷⁸, F. Sforza³², A. Sfyrila⁵², E. Shabalina⁵⁷, N. W. Shaikh^{148a,148b}, L. Y. Shan^{35a}, R. Shang¹⁶⁹, J. T. Shank²⁴, M. Shapiro¹⁶, P. B. Shatalov⁹⁹, K. Shaw^{167a,167b}, S. M. Shaw⁸⁷, A. Shcherbakova^{148a,148b}, C. Y. Shehu¹⁵¹, Y. Shen¹¹⁵, N. Sherafati³¹, P. Sherwood⁸¹, L. Shi^{153,ao}, S. Shimizu⁷⁰, C. O. Shimmin¹⁷⁹, M. Shimojima¹⁰⁴, I. P. J. Shipsey¹²², S. Shirabe⁷³, M. Shiyakova^{68,ap}, J. Shlomi¹⁷⁵, A. Shmeleva⁹⁸, D. Shoaleh Saadi⁹⁷, M. J. Shochet³³, S. Shojaii^{94a}, D. R. Shope¹¹⁵, S. Shrestha¹¹³, E. Shulga¹⁰⁰, M. A. Shupe⁷, P. Sicho¹²⁹, A. M. Sickles¹⁶⁹, P. E. Sidebo¹⁴⁹, E. Sideras Haddad^{147c}, O. Sidiropoulou¹⁷⁷, A. Sidoti^{22a,22b}, F. Siegert⁴⁷, Dj. Sijacki¹⁴, J. Silva^{128a,128d}, S. B. Silverstein^{148a}, V. Simak¹³⁰, Lj. Simic¹⁴, S. Simion¹¹⁹, E. Simioni⁸⁶, B. Simmons⁸¹, M. Simon⁸⁶, P. Sinervo¹⁶¹, N. B. Sinev¹¹⁸, M. Sioli^{22a,22b}, G. Siragusa¹⁷⁷, I. Siral⁹², S. Yu. Sivoklokov¹⁰¹, J. Sjölin^{148a,148b}, M. B. Skinner⁷⁵, P. Skubic¹¹⁵, M. Slater¹⁹, T. Slavicek¹³⁰, M. Slawinska⁴², K. Sliwa¹⁶⁵, R. Slovak¹³¹, V. Smakhtin¹⁷⁵, B. H. Smart⁵, J. Smiesko^{146a}, N. Smirnov¹⁰⁰, S. Yu. Smirnov¹⁰⁰, Y. Smirnov¹⁰⁰, L. N. Smirnova^{101,aq}, O. Smirnova⁸⁴, J. W. Smith⁵⁷, M. N. K. Smith³⁸, R. W. Smith³⁸, M. Smizanska⁷⁵, K. Smolek¹³⁰

- A. A. Snesarev⁹⁸, I. M. Snyder¹¹⁸, S. Snyder²⁷, R. Sobie^{172,o}, F. Socher⁴⁷, A. Soffer¹⁵⁵, D. A. Soh¹⁵³, G. Sokhrannyi⁷⁸, C. A. Solans Sanchez³², M. Solar¹³⁰, E. Yu. Soldatov¹⁰⁰, U. Soldevila¹⁷⁰, A. A. Solodkov¹³², A. Soloshenko⁶⁸, O. V. Solovyanov¹³², V. Solovyev¹²⁵, P. Sommer⁵¹, H. Son¹⁶⁵, A. Sopczak¹³⁰, D. Sosa^{60b}, C. L. Sotiropoulou^{126a,126b}, R. Soualah^{167a,167c}, A. M. Soukharev^{111,c}, D. South⁴⁵, B. C. Sowden⁸⁰, S. Spagnolo^{76a,76b}, M. Spalla^{126a,126b}, M. Spangenberg¹⁷³, F. Spano⁸⁰, D. Sperlich¹⁷, F. Spettel¹⁰³, T. M. Spieker^{60a}, R. Spighi^{22a}, G. Spigo³², L. A. Spiller⁹¹, M. Spousta¹³¹, R. D. St. Denis^{56,*}, A. Stabile^{94a}, R. Stamen^{60a}, S. Stamm¹⁷, E. Stanecka⁴², R. W. Stanek⁶, C. Stanescu¹²⁹, M. M. Stanitzki⁴⁵, B. S. Stapf¹⁰⁹, S. Stapnes¹²¹, E. A. Starchenko¹³², G. H. Stark³³, J. Stark⁵⁸, S. H. Stark³⁹, P. Staroba¹²⁹, P. Starovoitov^{60a}, S. Stärz³², R. Staszewski⁴², P. Steinberg²⁷, B. Stelzer¹⁴⁴, H. J. Stelzer³², O. Stelzer-Chilton^{163a}, H. Stenzel⁵⁵, G. A. Stewart⁵⁶, M. C. Stockton¹¹⁸, M. Stoebe⁹⁰, G. Stoica^{28b}, P. Stolte⁵⁷, S. Stonjek¹⁰³, A. R. Stradling⁸, A. Straessner⁴⁷, M. E. Stramaglia¹⁸, J. Strandberg¹⁴⁹, S. Strandberg^{148a,148b}, M. Strauss¹¹⁵, P. Strizenec^{146b}, R. Ströhmer¹⁷⁷, D. M. Strom¹¹⁸, R. Stroynowski⁴³, A. Strubig¹⁰⁸, S. A. Stucci²⁷, B. Stugu¹⁵, N. A. Styles⁴⁵, D. Su¹⁴⁵, J. Su¹²⁷, S. Suchek^{60a}, Y. Sugaya¹²⁰, M. Suk¹³⁰, V. V. Sulin⁹⁸, DMS Sultan^{162a,162b}, S. Sultansoy^{4c}, T. Sumida⁷¹, S. Sun⁵⁹, X. Sun³, K. Suruliz¹⁵¹, C. J. E. Suster¹⁵², M. R. Sutton¹⁵¹, S. Suzuki⁶⁹, M. Svatos¹²⁹, M. Swiatkowski³³, S. P. Swift², I. Sykora^{146a}, T. Sykora¹³¹, D. Ta⁵¹, K. Tackmann⁴⁵, J. Taenzer¹⁵⁵, A. Taffard¹⁶⁶, R. Tafirout^{163a}, N. Taiblum¹⁵⁵, H. Takai²⁷, R. Takashima⁷², E. H. Takasugi¹⁰³, T. Takeshita¹⁴², Y. Takubo⁶⁹, M. Talby⁸⁸, A. A. Talyshiev^{111,c}, J. Tanaka¹⁵⁷, M. Tanaka¹⁵⁹, R. Tanaka¹¹⁹, S. Tanaka⁶⁹, R. Tanioka⁷⁰, B. B. Tannenwald¹¹³, S. Tapia Araya^{34b}, S. Tapprogge⁸⁶, S. Tarem¹⁵⁴, G. F. Tartarelli^{94a}, P. Tas¹³¹, M. Tasevsky¹²⁹, T. Tashiro⁷¹, E. Tassi^{163b}, A. Tavares Delgado^{128a,128b}, Y. Tayalati^{137e}, A. C. Taylor¹⁰⁷, G. N. Taylor⁹¹, P. T. E. Taylor⁹¹, W. Taylor^{163b}, P. Teixeira-Dias⁸⁰, D. Temple¹⁴⁴, H. Ten Kate³², P. K. Teng¹⁵³, J. J. Teoh¹²⁰, F. Tepel¹⁷⁸, S. Terada⁶⁹, K. Terashi¹⁵⁷, J. Terron⁸⁵, S. Terzo¹³, M. Testa⁵⁰, R. J. Teuscher^{161,o}, T. Theveneaux-Pelzer⁸⁸, J. P. Thomas¹⁹, J. Thomas-Wilsker⁸⁰, P. D. Thompson¹⁹, A. S. Thompson⁵⁶, L. A. Thomsen¹⁷⁹, E. Thomson¹²⁴, M. J. Tibbetts¹⁶, R. E. Ticse Torres⁸⁸, V. O. Tikhomirov^{98,ar}, Yu. A. Tikhonov^{111,c}, S. Timoshenko¹⁰⁰, P. Tipton¹⁷⁹, S. Tisserant⁸⁸, K. Todome¹⁵⁹, S. Todorova-Nova⁵, S. Todt⁴⁷, J. Tojo⁷³, S. Tokár^{146a}, K. Tokushuku⁶⁹, E. Tolley⁵⁹, L. Tomlinson⁸⁷, M. Tomoto¹⁰⁵, L. Tompkins^{145,as}, K. Toms¹⁰⁷, B. Tong⁵⁹, P. Tornambe⁵¹, E. Torrence¹¹⁸, H. Torres¹⁴⁴, E. Torró Pastor¹⁴⁰, J. Toth^{88,at}, F. Touchard⁸⁸, D. R. Tovey¹⁴¹, C. J. Treado¹¹², T. Trefzger¹⁷⁷, F. Tresoldi¹⁵¹, A. Tricoli²⁷, I. M. Trigger^{163a}, S. Trincaz-Duvoid⁸³, M. F. Tripiana¹³, W. Trischuk¹⁶¹, B. Trocme⁵⁸, A. Trofymov⁴⁵, C. Troncon^{94a}, M. Trotter-McDonald¹⁶, M. Trovatielli¹⁷², L. Truong^{167a,167c}, M. Trzebinski⁴², A. Trzupek⁴², K. W. Tsang^{62a}, J. C. L. Tseng¹²², P. V. Tsiarshka⁹⁵, G. Tsipolitis¹⁰, N. Tsirintanis⁹, S. Tsiskaridze¹³, V. Tsiskaridze⁵¹, E. G. Tskhadadze^{54a}, K. M. Tsui^{62a}, I. I. Tsukerman⁹⁹, V. Tsulaia¹⁶, S. Tsuno⁶⁹, D. Tsybychev¹⁵⁰, Y. Tu^{62b}, A. Tudorache^{28b}, V. Tudorache^{28b}, T. T. Tulbure^{28a}, A. N. Tuna⁵⁹, S. A. Tuppuri^{22a,22b}, S. Turchikhin⁶⁸, D. Turgeman¹⁷⁵, I. Turk Cakir^{4b,au}, R. Turra^{94a}, P. M. Tuts³⁸, G. Uchielli^{22a,22b}, I. Ueda⁶⁹, M. Ughetto^{148a,148b}, F. Ukegawa¹⁶⁴, G. Unal³², A. Undrus²⁷, G. Unel¹⁶⁶, F. C. Ungaro⁹¹, Y. Unno⁶⁹, C. Unverdorben¹⁰², J. Urban^{146b}, P. Urquijo⁹¹, P. Urrejola⁸⁶, G. Usai⁸, J. Usui⁶⁹, L. Vacavant⁸⁸, V. Vacek¹³⁰, B. Vachon⁹⁰, A. Vaidya⁸¹, C. Valderanis¹⁰², E. Valdes Santurio^{148a,148b}, S. Valentini^{22a,22b}, A. Valero¹⁷⁰, L. Valéry¹³, S. Valkar¹³¹, A. Vallier⁵, J. A. Valls Ferrer¹⁷⁰, W. Van Den Wollenberg¹⁰⁹, H. van der Graaf¹⁰⁹, P. van Gemmeren⁶, J. Van Nieuwkoop¹⁴⁴, I. van Vulpen¹⁰⁹, M. C. van Woerden¹⁰⁹, M. Vanadia^{135a,135b}, W. Vandelli³², A. Vaniachine¹⁶⁰, P. Vankov¹⁰⁹, G. Vardanyan¹⁸⁰, R. Vari^{134a}, E. W. Varnes⁷, C. Varni^{53a,53b}, T. Varol⁴³, D. Varouchas¹¹⁹, A. Vartapetian⁸, K. E. Varvell¹⁵², J. G. Vasquez¹⁷⁹, G. A. Vasquez^{34b}, F. Vazeille³⁷, T. Vazquez Schroeder⁹⁰, J. Veatch⁵⁷, V. Veeraraghavan⁷, L. M. Veloce¹⁶¹, F. Veloso^{128a,128c}, S. Veneziano^{134a}, A. Ventura^{76a,76b}, M. Venturi¹⁷², N. Venturi³², A. Venturini²⁵, V. Vercesi^{123a}, M. Verducci^{136a,136b}, W. Verkerke¹⁰⁹, A. T. Vermeulen¹⁰⁹, J. C. Vermeulen¹⁰⁹, M. C. Vetterli^{144,d}, N. Viaux Maira^{34b}, O. Viazlo⁸⁴, I. Vichou^{169,*}, T. Vickey¹⁴¹, O. E. Vickey Boeriu¹⁴¹, G. H. A. Viehhauser¹²², S. Viel¹⁶, L. Vigani¹²², M. Villa^{22a,22b}, M. Villaplana Perez^{94a,94b}, E. Vilucchi⁵⁰, M. G. Vincet³¹, V. B. Vinogradov⁶⁸, A. Vishwakarma⁴⁵, C. Vittori^{22a,22b}, I. Vivarelli¹⁵¹, S. Vlachos¹⁰, M. Vogel¹⁷⁸, P. Vokac¹³⁰, G. Volpi^{126a,126b}, H. von der Schmitt¹⁰³, E. von Toerne²³, V. Vorobel¹³¹, K. Vorobev¹⁰⁰, M. Vos¹⁷⁰, R. Voss³², J. H. Vosseveld⁷⁷, N. Vranjes¹⁴, M. Vranjes Milosavljevic¹⁴, V. Vrba¹³⁰, M. Vreeswijk¹⁰⁹, R. Vuillermet³², I. Vukotic³³, P. Wagner²³, W. Wagner¹⁷⁸, J. Wagner-Kuhr¹⁰², H. Wahlberg⁷⁴, S. Wahrenand⁴⁷, J. Wakabayashi¹⁰⁵, J. Walder⁷⁵, R. Walker¹⁰², W. Walkowiak¹⁴³, V. Wallangen^{148a,148b}, C. Wang^{35b}, C. Wang^{36b,av}, F. Wang¹⁷⁶, H. Wang¹⁶, H. Wang³, J. Wang⁴⁵, J. Wang¹⁵², Q. Wang¹¹⁵, R. Wang⁶, S. M. Wang¹⁵³, T. Wang³⁸, W. Wang^{153,aw}, W. Wang^{36a}, Z. Wang^{36c}, C. Wanotayaroj¹¹⁸, A. Warburton⁹⁰, C. P. Ward³⁰, D. R. Wardrope⁸¹, A. Washbrook⁴⁹, P. M. Watkins¹⁹, A. T. Watson¹⁹, M. F. Watson¹⁹, G. Watts¹⁴⁰, S. Watts⁸⁷, B. M. Waugh⁸¹, A. F. Webb¹¹, S. Webb⁸⁶, M. S. Weber¹⁸, S. W. Weber¹⁷⁷, S. A. Weber³¹, J. S. Webster¹⁹, A. R. Weidberg¹²², B. Weinert⁶⁴, J. Weingarten⁵⁷, M. Weirich⁸⁶, C. Weiser⁵¹, H. Weits¹⁰⁹, P. S. Wells³², T. Wenaus²⁷, T. Wengler³², S. Wenig³², N. Wermes²³

M. D. Werner⁶⁷, P. Werner³², M. Wessels^{60a}, K. Whalen¹¹⁸, N. L. Whallon¹⁴⁰, A. M. Wharton⁷⁵, A. S. White⁹², A. White⁸, M. J. White¹, R. White^{34b}, D. Whiteson¹⁶⁶, B. W. Whitmore⁷⁵, F. J. Wickens¹³³, W. Wiedenmann¹⁷⁶, M. Wielers¹³³, C. Wiglesworth³⁹, L. A. M. Wiik-Fuchs²³, A. Wildauer¹⁰³, F. Wilk⁸⁷, H. G. Wilkens³², H. H. Williams¹²⁴, S. Williams¹⁰⁹, C. Willis⁹³, S. Willocq⁸⁹, J. A. Wilson¹⁹, I. Wingerter-Seez⁵, E. Winkels¹⁵¹, F. Winklmeier¹¹⁸, O. J. Winston¹⁵¹, B. T. Winter²³, M. Wittgen¹⁴⁵, M. Wobisch^{82,u}, T. M. H. Wolf¹⁰⁹, R. Wolff⁸⁸, M. W. Wolter⁴², H. Wolters^{128a,128c}, V. W. S. Wong¹⁷¹, S. D. Worm¹⁹, B. K. Wosiek⁴², J. Wotschack³², K. W. Wozniak⁴², M. Wu³³, S. L. Wu¹⁷⁶, X. Wu⁵², Y. Wu⁹², T. R. Wyatt⁸⁷, B. M. Wynne⁴⁹, S. Xella³⁹, Z. Xi⁹², L. Xia^{35c}, D. Xu^{35a}, L. Xu²⁷, T. Xu¹³⁸, B. Yabsley¹⁵², S. Yacoub^{147a}, D. Yamaguchi¹⁵⁹, Y. Yamaguchi¹²⁰, A. Yamamoto⁶⁹, S. Yamamoto¹⁵⁷, T. Yamanaka¹⁵⁷, M. Yamatani¹⁵⁷, K. Yamauchi¹⁰⁵, Y. Yamazaki⁷⁰, Z. Yan²⁴, H. Yang^{36c}, H. Yang¹⁶, Y. Yang¹⁵³, Z. Yang¹⁵, W.-M. Yao¹⁶, Y. C. Yap⁸³, Y. Yasu⁶⁹, E. Yatsenko⁵, K. H. Yau Wong²³, J. Ye⁴³, S. Ye²⁷, I. Yeletsikh⁶⁸, E. Yigitbasi²⁴, E. Yildirim⁸⁶, K. Yorita¹⁷⁴, K. Yoshihara¹²⁴, C. Young¹⁴⁵, C. J. S. Young³², J. Yu⁸, J. Yu⁶⁷, S. P. Y. Yuen²³, I. Yusuff^{30,ax}, B. Zabinski⁴², G. Zacharis¹⁰, R. Zaidan¹³, A. M. Zaitsev^{132,al}, N. Zakharuk⁴⁵, J. Zalieckas¹⁵, A. Zaman¹⁵⁰, S. Zambito⁵⁹, D. Zanzi⁹¹, C. Zeitnitz¹⁷⁸, G. Zemaityte¹²², A. Zemla^{41a}, J. C. Zeng¹⁶⁹, Q. Zeng¹⁴⁵, O. Zenin¹³², T. Ženiš^{146a}, D. Zerwas¹¹⁹, D. Zhang⁹², F. Zhang¹⁷⁶, G. Zhang^{36a,ay}, H. Zhang^{35b}, J. Zhang⁶, L. Zhang⁵¹, L. Zhang^{36a}, M. Zhang¹⁶⁹, P. Zhang^{35b}, R. Zhang²³, R. Zhang^{36a,av}, X. Zhang^{36b}, Y. Zhang^{35a}, Z. Zhang¹¹⁹, X. Zhao⁴³, Y. Zhao^{36b,az}, Z. Zhao^{36a}, A. Zhemchugov⁶⁸, B. Zhou⁹², C. Zhou¹⁷⁶, L. Zhou⁴³, M. Zhou^{35a}, M. Zhou¹⁵⁰, N. Zhou^{35c}, C. G. Zhu^{36b}, H. Zhu^{35a}, J. Zhu⁹², Y. Zhu^{36a}, X. Zhuang^{35a}, K. Zhukov⁹⁸, A. Zibell¹⁷⁷, D. Zieminska⁶⁴, N. I. Zimine⁶⁸, C. Zimmermann⁸⁶, S. Zimmermann⁵¹, Z. Zinonos¹⁰³, M. Zinser⁸⁶, M. Ziolkowski¹⁴³, L. Živković¹⁴, G. Zobernig¹⁷⁶, A. Zoccoli^{22a,22b}, R. Zou³³, M. zur Nedden¹⁷, L. Zwalinski³²

¹ Department of Physics, University of Adelaide, Adelaide, Australia

² Physics Department, SUNY Albany, Albany, NY, USA

³ Department of Physics, University of Alberta, Edmonton, AB, Canada

⁴ (a) Department of Physics, Ankara University, Ankara, Turkey; (b) Istanbul Aydin University, Istanbul, Turkey; (c) Division of Physics, TOBB University of Economics and Technology, Ankara, Turkey

⁵ LAPP, CNRS/IN2P3 and Université Savoie Mont Blanc, Annecy-le-Vieux, France

⁶ High Energy Physics Division, Argonne National Laboratory, Argonne, IL, USA

⁷ Department of Physics, University of Arizona, Tucson, AZ, USA

⁸ Department of Physics, The University of Texas at Arlington, Arlington, TX, USA

⁹ Physics Department, National and Kapodistrian University of Athens, Athens, Greece

¹⁰ Physics Department, National Technical University of Athens, Zografou, Greece

¹¹ Department of Physics, The University of Texas at Austin, Austin, TX, USA

¹² Institute of Physics, Azerbaijan Academy of Sciences, Baku, Azerbaijan

¹³ Institut de Física d'Altes Energies (IFAE), The Barcelona Institute of Science and Technology, Barcelona, Spain

¹⁴ Institute of Physics, University of Belgrade, Belgrade, Serbia

¹⁵ Department for Physics and Technology, University of Bergen, Bergen, Norway

¹⁶ Physics Division, Lawrence Berkeley National Laboratory, University of California, Berkeley, CA, USA

¹⁷ Department of Physics, Humboldt University, Berlin, Germany

¹⁸ Albert Einstein Center for Fundamental Physics, Laboratory for High Energy Physics, University of Bern, Bern, Switzerland

¹⁹ School of Physics and Astronomy, University of Birmingham, Birmingham, UK

²⁰ (a) Department of Physics, Bogazici University, Istanbul, Turkey; (b) Department of Physics Engineering, Gaziantep University, Gaziantep, Turkey; (c) Faculty of Engineering and Natural Sciences, Istanbul Bilgi University, Istanbul, Turkey; (d) Faculty of Engineering and Natural Sciences, Bahcesehir University, Istanbul, Turkey

²¹ Centro de Investigaciones, Universidad Antonio Narino, Bogotá, Colombia

²² (a) INFN Sezione di Bologna, Bologna, Italy; (b) Dipartimento di Fisica e Astronomia, Università di Bologna, Bologna, Italy

²³ Physikalisches Institut, University of Bonn, Bonn, Germany

²⁴ Department of Physics, Boston University, Boston, MA, USA

²⁵ Department of Physics, Brandeis University, Waltham, MA, USA

- 26 (a) Universidade Federal do Rio De Janeiro COPPE/EE/IF, Rio de Janeiro, Brazil; (b) Electrical Circuits Department, Federal University of Juiz de Fora (UFJF), Juiz de Fora, Brazil; (c) Federal University of Sao Joao del Rei (UFSJ), Sao Joao del Rei, Brazil; (d) Instituto de Fisica, Universidade de Sao Paulo, São Paulo, Brazil
- 27 Physics Department, Brookhaven National Laboratory, Upton, NY, USA
- 28 (a) Transilvania University of Brasov, Brasov, Romania; (b) Horia Hulubei National Institute of Physics and Nuclear Engineering, Bucharest, Romania; (c) Department of Physics, Alexandru Ioan Cuza University of Iasi, Iasi, Romania; (d) Physics Department, National Institute for Research and Development of Isotopic and Molecular Technologies, Cluj-Napoca, Romania; (e) University Politehnica Bucharest, Bucharest, Romania; (f) West University in Timisoara, Timisoara, Romania
- 29 Departamento de Física, Universidad de Buenos Aires, Buenos Aires, Argentina
- 30 Cavendish Laboratory, University of Cambridge, Cambridge, UK
- 31 Department of Physics, Carleton University, Ottawa, ON, Canada
- 32 CERN, Geneva, Switzerland
- 33 Enrico Fermi Institute, University of Chicago, Chicago, IL, USA
- 34 (a) Departamento de Física, Pontificia Universidad Católica de Chile, Santiago, Chile; (b) Departamento de Física, Universidad Técnica Federico Santa María, Valparaíso, Chile
- 35 (a) Institute of High Energy Physics, Chinese Academy of Sciences, Beijing, China; (b) Department of Physics, Nanjing University, Nanjing, Jiangsu, China; (c) Physics Department, Tsinghua University, Beijing 100084, China
- 36 (a) Department of Modern Physics and State Key Laboratory of Particle Detection and Electronics, University of Science and Technology of China, Hefei, Anhui, China; (b) School of Physics, Shandong University, Jinan, Shandong, China; (c) Department of Physics and Astronomy, Key Laboratory for Particle Physics, Astrophysics and Cosmology, Ministry of Education, Shanghai Key Laboratory for Particle Physics and Cosmology, Shanghai Jiao Tong University, Shanghai (also at PKU-CHEP), Shanghai, China
- 37 Université Clermont Auvergne, CNRS/IN2P3, LPC, Clermont-Ferrand, France
- 38 Nevis Laboratory, Columbia University, Irvington, NY, USA
- 39 Niels Bohr Institute, University of Copenhagen, Copenhagen, Denmark
- 40 (a) INFN Gruppo Collegato di Cosenza, Laboratori Nazionali di Frascati, Frascati, Italy; (b) Dipartimento di Fisica, Università della Calabria, Rende, Italy
- 41 (a) Faculty of Physics and Applied Computer Science, AGH University of Science and Technology, Kraków, Poland; (b) Marian Smoluchowski Institute of Physics, Jagiellonian University, Kraków, Poland
- 42 Institute of Nuclear Physics, Polish Academy of Sciences, Kraków, Poland
- 43 Physics Department, Southern Methodist University, Dallas, TX, USA
- 44 Physics Department, University of Texas at Dallas, Richardson, TX, USA
- 45 DESY, Hamburg and Zeuthen, Germany
- 46 Lehrstuhl für Experimentelle Physik IV, Technische Universität Dortmund, Dortmund, Germany
- 47 Institut für Kern- und Teilchenphysik, Technische Universität Dresden, Dresden, Germany
- 48 Department of Physics, Duke University, Durham, NC, USA
- 49 SUPA-School of Physics and Astronomy, University of Edinburgh, Edinburgh, UK
- 50 INFN e Laboratori Nazionali di Frascati, Frascati, Italy
- 51 Fakultät für Mathematik und Physik, Albert-Ludwigs-Universität, Freiburg, Germany
- 52 Departement de Physique Nucleaire et Corpusculaire, Université de Genève, Geneva, Switzerland
- 53 (a) INFN Sezione di Genova, Genoa, Italy; (b) Dipartimento di Fisica, Università di Genova, Genoa, Italy
- 54 (a) E. Andronikashvili Institute of Physics, Iv. Javakhishvili Tbilisi State University, Tbilisi, Georgia; (b) High Energy Physics Institute, Tbilisi State University, Tbilisi, Georgia
- 55 II Physikalisches Institut, Justus-Liebig-Universität Giessen, Giessen, Germany
- 56 SUPA-School of Physics and Astronomy, University of Glasgow, Glasgow, UK
- 57 II Physikalisches Institut, Georg-August-Universität, Göttingen, Germany
- 58 Laboratoire de Physique Subatomique et de Cosmologie, Université Grenoble-Alpes, CNRS/IN2P3, Grenoble, France
- 59 Laboratory for Particle Physics and Cosmology, Harvard University, Cambridge, MA, USA

- ⁶⁰ (a) Kirchhoff-Institut für Physik, Ruprecht-Karls-Universität Heidelberg, Heidelberg, Germany; (b) Physikalisches Institut, Ruprecht-Karls-Universität Heidelberg, Heidelberg, Germany
- ⁶¹ Faculty of Applied Information Science, Hiroshima Institute of Technology, Hiroshima, Japan
- ⁶² (a) Department of Physics, The Chinese University of Hong Kong, Shatin, NT, Hong Kong; (b) Department of Physics, The University of Hong Kong, Hong Kong, China; (c) Department of Physics, Institute for Advanced Study, The Hong Kong University of Science and Technology, Clear Water Bay, Kowloon, Hong Kong, China
- ⁶³ Department of Physics, National Tsing Hua University, Taiwan, Taiwan
- ⁶⁴ Department of Physics, Indiana University, Bloomington, IN, USA
- ⁶⁵ Institut für Astro- und Teilchenphysik, Leopold-Franzens-Universität, Innsbruck, Austria
- ⁶⁶ University of Iowa, Iowa City, IA, USA
- ⁶⁷ Department of Physics and Astronomy, Iowa State University, Ames, IA, USA
- ⁶⁸ Joint Institute for Nuclear Research, JINR Dubna, Dubna, Russia
- ⁶⁹ KEK, High Energy Accelerator Research Organization, Tsukuba, Japan
- ⁷⁰ Graduate School of Science, Kobe University, Kobe, Japan
- ⁷¹ Faculty of Science, Kyoto University, Kyoto, Japan
- ⁷² Kyoto University of Education, Kyoto, Japan
- ⁷³ Research Center for Advanced Particle Physics and Department of Physics, Kyushu University, Fukuoka, Japan
- ⁷⁴ Instituto de Física La Plata, Universidad Nacional de La Plata and CONICET, La Plata, Argentina
- ⁷⁵ Physics Department, Lancaster University, Lancaster, UK
- ⁷⁶ (a) INFN Sezione di Lecce, Lecce, Italy; (b) Dipartimento di Matematica e Fisica, Università del Salento, Lecce, Italy
- ⁷⁷ Oliver Lodge Laboratory, University of Liverpool, Liverpool, UK
- ⁷⁸ Department of Experimental Particle Physics, Jožef Stefan Institute and Department of Physics, University of Ljubljana, Ljubljana, Slovenia
- ⁷⁹ School of Physics and Astronomy, Queen Mary University of London, London, UK
- ⁸⁰ Department of Physics, Royal Holloway University of London, Surrey, UK
- ⁸¹ Department of Physics and Astronomy, University College London, London, UK
- ⁸² Louisiana Tech University, Ruston, LA, USA
- ⁸³ Laboratoire de Physique Nucléaire et de Hautes Energies, UPMC and Université Paris-Diderot and CNRS/IN2P3, Paris, France
- ⁸⁴ Fysiska institutionen, Lunds universitet, Lund, Sweden
- ⁸⁵ Departamento de Física Teórica C-15, Universidad Autónoma de Madrid, Madrid, Spain
- ⁸⁶ Institut für Physik, Universität Mainz, Mainz, Germany
- ⁸⁷ School of Physics and Astronomy, University of Manchester, Manchester, UK
- ⁸⁸ CPPM, Aix-Marseille Université and CNRS/IN2P3, Marseille, France
- ⁸⁹ Department of Physics, University of Massachusetts, Amherst, MA, USA
- ⁹⁰ Department of Physics, McGill University, Montreal, QC, Canada
- ⁹¹ School of Physics, University of Melbourne, Victoria, Australia
- ⁹² Department of Physics, The University of Michigan, Ann Arbor, MI, USA
- ⁹³ Department of Physics and Astronomy, Michigan State University, East Lansing, MI, USA
- ⁹⁴ (a) INFN Sezione di Milano, Milan, Italy; (b) Dipartimento di Fisica, Università di Milano, Milan, Italy
- ⁹⁵ B.I. Stepanov Institute of Physics, National Academy of Sciences of Belarus, Minsk, Republic of Belarus
- ⁹⁶ Research Institute for Nuclear Problems of Byelorussian State University, Minsk, Republic of Belarus
- ⁹⁷ Group of Particle Physics, University of Montreal, Montreal, QC, Canada
- ⁹⁸ P.N. Lebedev Physical Institute of the Russian Academy of Sciences, Moscow, Russia
- ⁹⁹ Institute for Theoretical and Experimental Physics (ITEP), Moscow, Russia
- ¹⁰⁰ National Research Nuclear University MEPhI, Moscow, Russia
- ¹⁰¹ D.V. Skobeltsyn Institute of Nuclear Physics, M.V. Lomonosov Moscow State University, Moscow, Russia
- ¹⁰² Fakultät für Physik, Ludwig-Maximilians-Universität München, Munich, Germany
- ¹⁰³ Max-Planck-Institut für Physik (Werner-Heisenberg-Institut), Munich, Germany
- ¹⁰⁴ Nagasaki Institute of Applied Science, Nagasaki, Japan
- ¹⁰⁵ Graduate School of Science and Kobayashi-Maskawa Institute, Nagoya University, Nagoya, Japan
- ¹⁰⁶ (a) INFN Sezione di Napoli, Naples, Italy; (b) Dipartimento di Fisica, Università di Napoli, Naples, Italy

- 107 Department of Physics and Astronomy, University of New Mexico, Albuquerque, NM, USA
- 108 Institute for Mathematics, Astrophysics and Particle Physics, Radboud University Nijmegen/Nikhef, Nijmegen, The Netherlands
- 109 Nikhef National Institute for Subatomic Physics, University of Amsterdam, Amsterdam, The Netherlands
- 110 Department of Physics, Northern Illinois University, DeKalb, IL, USA
- 111 Budker Institute of Nuclear Physics, SB RAS, Novosibirsk, Russia
- 112 Department of Physics, New York University, New York, NY, USA
- 113 Ohio State University, Columbus, OH, USA
- 114 Faculty of Science, Okayama University, Okayama, Japan
- 115 Homer L. Dodge Department of Physics and Astronomy, University of Oklahoma, Norman, OK, USA
- 116 Department of Physics, Oklahoma State University, Stillwater, OK, USA
- 117 Palacký University, RCPTM, Olomouc, Czech Republic
- 118 Center for High Energy Physics, University of Oregon, Eugene, OR, USA
- 119 LAL, Univ. Paris-Sud, CNRS/IN2P3, Université Paris-Saclay, Orsay, France
- 120 Graduate School of Science, Osaka University, Osaka, Japan
- 121 Department of Physics, University of Oslo, Oslo, Norway
- 122 Department of Physics, Oxford University, Oxford, UK
- 123 ^(a)INFN Sezione di Pavia, Pavia, Italy; ^(b)Dipartimento di Fisica, Università di Pavia, Pavia, Italy
- 124 Department of Physics, University of Pennsylvania, Philadelphia, PA, USA
- 125 National Research Centre “Kurchatov Institute” B.P. Konstantinov Petersburg Nuclear Physics Institute, St. Petersburg, Russia
- 126 ^(a)INFN Sezione di Pisa, Pisa, Italy; ^(b)Dipartimento di Fisica E. Fermi, Università di Pisa, Pisa, Italy
- 127 Department of Physics and Astronomy, University of Pittsburgh, Pittsburgh, PA, USA
- 128 ^(a)Laboratório de Instrumentação e Física Experimental de Partículas-LIP, Lisbon, Portugal; ^(b)Faculdade de Ciências, Universidade de Lisboa, Lisbon, Portugal; ^(c)Department of Physics, University of Coimbra, Coimbra, Portugal; ^(d)Centro de Física Nuclear da Universidade de Lisboa, Lisbon, Portugal; ^(e)Departamento de Física, Universidade do Minho, Braga, Portugal; ^(f)Departamento de Física Teórica y del Cosmos and CAFPE, Universidad de Granada, Granada, Spain; ^(g)Dep Física and CEFITEC of Faculdade de Ciências e Tecnologia, Universidade Nova de Lisboa, Caparica, Portugal
- 129 Institute of Physics, Academy of Sciences of the Czech Republic, Prague, Czech Republic
- 130 Czech Technical University in Prague, Prague, Czech Republic
- 131 Faculty of Mathematics and Physics, Charles University, Prague, Czech Republic
- 132 State Research Center Institute for High Energy Physics (Protvino), NRC KI, Protvino, Russia
- 133 Particle Physics Department, Rutherford Appleton Laboratory, Didcot, UK
- 134 ^(a)INFN Sezione di Roma, Rome, Italy; ^(b)Dipartimento di Fisica, Sapienza Università di Roma, Rome, Italy
- 135 ^(a)INFN Sezione di Roma Tor Vergata, Rome, Italy; ^(b)Dipartimento di Fisica, Università di Roma Tor Vergata, Rome, Italy
- 136 ^(a)INFN Sezione di Roma Tre, Rome, Italy; ^(b)Dipartimento di Matematica e Fisica, Università Roma Tre, Rome, Italy
- 137 ^(a)Faculté des Sciences Ain Chock, Réseau Universitaire de Physique des Hautes Energies-Université Hassan II, Casablanca, Morocco; ^(b)Centre National de l’Energie des Sciences Techniques Nucleaires, Rabat, Morocco; ^(c)Faculté des Sciences Semlalia, Université Cadi Ayyad, LPHEA-Marrakech, Marrakech, Morocco; ^(d)Faculté des Sciences, Université Mohamed Premier and LPTPM, Oujda, Morocco; ^(e)Faculté des Sciences, Université Mohammed V, Rabat, Morocco
- 138 DSM/IRFU (Institut de Recherches sur les Lois Fondamentales de l’Univers), CEA Saclay (Commissariat à l’Energie Atomique et aux Energies Alternatives), Gif-sur-Yvette, France
- 139 Santa Cruz Institute for Particle Physics, University of California Santa Cruz, Santa Cruz, CA, USA
- 140 Department of Physics, University of Washington, Seattle, WA, USA
- 141 Department of Physics and Astronomy, University of Sheffield, Sheffield, UK
- 142 Department of Physics, Shinshu University, Nagano, Japan
- 143 Department Physik, Universität Siegen, Siegen, Germany
- 144 Department of Physics, Simon Fraser University, Burnaby, BC, Canada

- 145 SLAC National Accelerator Laboratory, Stanford, CA, USA
- 146 ^(a) Faculty of Mathematics, Physics and Informatics, Comenius University, Bratislava, Slovak Republic; ^(b) Department of Subnuclear Physics, Institute of Experimental Physics of the Slovak Academy of Sciences, Kosice, Slovak Republic
- 147 ^(a) Department of Physics, University of Cape Town, Cape Town, South Africa; ^(b) Department of Physics, University of Johannesburg, Johannesburg, South Africa; ^(c) School of Physics, University of the Witwatersrand, Johannesburg, South Africa
- 148 ^(a) Department of Physics, Stockholm University, Stockholm, Sweden; ^(b) The Oskar Klein Centre, Stockholm, Sweden
- 149 Physics Department, Royal Institute of Technology, Stockholm, Sweden
- 150 Departments of Physics and Astronomy and Chemistry, Stony Brook University, Stony Brook, NY, USA
- 151 Department of Physics and Astronomy, University of Sussex, Brighton, UK
- 152 School of Physics, University of Sydney, Sydney, Australia
- 153 Institute of Physics, Academia Sinica, Taipei, Taiwan
- 154 Department of Physics, Technion: Israel Institute of Technology, Haifa, Israel
- 155 Raymond and Beverly Sackler School of Physics and Astronomy, Tel Aviv University, Tel Aviv, Israel
- 156 Department of Physics, Aristotle University of Thessaloniki, Thessaloniki, Greece
- 157 International Center for Elementary Particle Physics and Department of Physics, The University of Tokyo, Tokyo, Japan
- 158 Graduate School of Science and Technology, Tokyo Metropolitan University, Tokyo, Japan
- 159 Department of Physics, Tokyo Institute of Technology, Tokyo, Japan
- 160 Tomsk State University, Tomsk, Russia
- 161 Department of Physics, University of Toronto, Toronto, ON, Canada
- 162 ^(a) INFN-TIFPA, Trento, Italy; ^(b) University of Trento, Trento, Italy
- 163 ^(a) TRIUMF, Vancouver, BC, Canada; ^(b) Department of Physics and Astronomy, York University, Toronto, ON, Canada
- 164 Faculty of Pure and Applied Sciences, and Center for Integrated Research in Fundamental Science and Engineering, University of Tsukuba, Tsukuba, Japan
- 165 Department of Physics and Astronomy, Tufts University, Medford, MA, USA
- 166 Department of Physics and Astronomy, University of California Irvine, Irvine, CA, USA
- 167 ^(a) INFN Gruppo Collegato di Udine, Sezione di Trieste, Udine, Italy; ^(b) ICTP, Trieste, Italy; ^(c) Dipartimento di Chimica, Fisica e Ambiente, Università di Udine, Udine, Italy
- 168 Department of Physics and Astronomy, University of Uppsala, Uppsala, Sweden
- 169 Department of Physics, University of Illinois, Urbana, IL, USA
- 170 Instituto de Física Corpuscular (IFIC), Centro Mixto Universidad de Valencia - CSIC, Valencia, Spain
- 171 Department of Physics, University of British Columbia, Vancouver, BC, Canada
- 172 Department of Physics and Astronomy, University of Victoria, Victoria, BC, Canada
- 173 Department of Physics, University of Warwick, Coventry, UK
- 174 Waseda University, Tokyo, Japan
- 175 Department of Particle Physics, The Weizmann Institute of Science, Rehovot, Israel
- 176 Department of Physics, University of Wisconsin, Madison, WI, USA
- 177 Fakultät für Physik und Astronomie, Julius-Maximilians-Universität, Würzburg, Germany
- 178 Fakultät für Mathematik und Naturwissenschaften, Fachgruppe Physik, Bergische Universität Wuppertal, Wuppertal, Germany
- 179 Department of Physics, Yale University, New Haven, CT, USA
- 180 Yerevan Physics Institute, Yerevan, Armenia
- 181 Centre de Calcul de l'Institut National de Physique Nucléaire et de Physique des Particules (IN2P3), Villeurbanne, France
- 182 Academia Sinica Grid Computing, Institute of Physics, Academia Sinica, Taipei, Taiwan
- ^a Also at Department of Physics, King's College London, London, UK
- ^b Also at Institute of Physics, Azerbaijan Academy of Sciences, Baku, Azerbaijan
- ^c Also at Novosibirsk State University, Novosibirsk, Russia
- ^d Also at TRIUMF, Vancouver, BC, Canada
- ^e Also at Department of Physics and Astronomy, University of Louisville, Louisville, KY, USA
- ^f Also at Physics Department, An-Najah National University, Nablus, Palestine

- ^g Also at Department of Physics, California State University, Fresno, CA, USA
- ^h Also at Department of Physics, University of Fribourg, Fribourg, Switzerland
- ⁱ Also at II Physikalisches Institut, Georg-August-Universität, Göttingen, Germany
- ^j Also at Departament de Física de la Universitat Autònoma de Barcelona, Barcelona, Spain
- ^k Also at Departamento de Física e Astronomia, Faculdade de Ciências, Universidade do Porto, Porto, Portugal
- ^l Also at Tomsk State University, Tomsk, Russia
- ^m Also at The Collaborative Innovation Center of Quantum Matter (CICQM), Beijing, China
- ⁿ Also at Università di Napoli Parthenope, Napoli, Italy
- ^o Also at Institute of Particle Physics (IPP), Canada
- ^p Also at Horia Hulubei National Institute of Physics and Nuclear Engineering, Bucharest, Romania
- ^q Also at Department of Physics, St. Petersburg State Polytechnical University, St. Petersburg, Russia
- ^r Also at Borough of Manhattan Community College, City University of New York, New York, USA
- ^s Also at Department of Financial and Management Engineering, University of the Aegean, Chios, Greece
- ^t Also at Centre for High Performance Computing, CSIR Campus, Rosebank, Cape Town, South Africa
- ^u Also at Louisiana Tech University, Ruston, LA, USA
- ^v Also at Institutio Catalana de Recerca i Estudis Avancats, ICREA, Barcelona, Spain
- ^w Also at Graduate School of Science, Osaka University, Osaka, Japan
- ^x Also at Fakultät für Mathematik und Physik, Albert-Ludwigs-Universität, Freiburg, Germany
- ^y Also at Institute for Mathematics, Astrophysics and Particle Physics, Radboud University Nijmegen/Nikhef, Nijmegen, The Netherlands
- ^z Also at Department of Physics, The University of Texas at Austin, Austin, TX, USA
- ^{aa} Also at Institute of Theoretical Physics, Ilia State University, Tbilisi, Georgia
- ^{ab} Also at CERN, Geneva, Switzerland
- ^{ac} Also at Georgian Technical University (GTU), Tbilisi, Georgia
- ^{ad} Also at Ochadai Academic Production, Ochanomizu University, Tokyo, Japan
- ^{ae} Also at Manhattan College, New York, NY, USA
- ^{af} Also at Departamento de Física, Pontificia Universidad Católica de Chile, Santiago, Chile
- ^{ag} Also at Department of Physics, The University of Michigan, Ann Arbor MI, United States of America
- ^{ah} Also at The City College of New York, New York NY, United States of America
- ^{ai} Also at School of Physics, Shandong University, Shandong, China
- ^{aj} Also at Departamento de Física Teórica y del Cosmos and CAFPE, Universidad de Granada, Granada, Spain
- ^{ak} Also at Department of Physics, California State University, Sacramento, CA, USA
- ^{al} Also at Moscow Institute of Physics and Technology State University, Dolgoprudny, Russia
- ^{am} Also at Departement de Physique Nucleaire et Corpusculaire, Université de Genève, Geneva, Switzerland
- ^{an} Also at Institut de Física d'Altes Energies (IFAE), The Barcelona Institute of Science and Technology, Barcelona, Spain
- ^{ao} Also at School of Physics, Sun Yat-sen University, Guangzhou, China
- ^{ap} Also at Institute for Nuclear Research and Nuclear Energy (INRNE) of the Bulgarian Academy of Sciences, Sofia, Bulgaria
- ^{aq} Also at Faculty of Physics, M.V. Lomonosov Moscow State University, Moscow, Russia
- ^{ar} Also at National Research Nuclear University MEPhI, Moscow, Russia
- ^{as} Also at Department of Physics, Stanford University, Stanford, CA, USA
- ^{at} Also at Institute for Particle and Nuclear Physics, Wigner Research Centre for Physics, Budapest, Hungary
- ^{au} Also at Faculty of Engineering, Giresun University, Giresun, Turkey
- ^{av} Also at CPPM, Aix-Marseille Université and CNRS/IN2P3, Marseille, France
- ^{aw} Also at Department of Physics, Nanjing University, Jiangsu, China
- ^{ax} Also at Department of Physics, University of Malaya, Kuala Lumpur, Malaysia
- ^{ay} Also at Institute of Physics, Academia Sinica, Taipei, Taiwan
- ^{az} Also at LAL, Univ. Paris-Sud, CNRS/IN2P3, Université Paris-Saclay, Orsay, France
- *Deceased